INFORMATION TO USERS

This reproduction was made from a copy of a document sent to us for microfilming. While the most advanced technology has been used to photograph and reproduce this document, the quality of the reproduction is heavily dependent upon the quality of the material submitted.

The following explanation of techniques is provided to help clarify markings or notations which may appear on this reproduction.

1. The sign or "target" for pages apparently lacking from the document photographed is "Missing Page(s)". If it was possible to obtain the missing page(s) or section, they are spliced into the film along with adjacent pages. This may have necessitated cutting through an image and duplicating adjacent pages to assure complete continuity.

2. When an image on the film is obliterated with a round black mark, it is an indication of either blurred copy because of movement during exposure, duplicate copy, or copyrighted materials that should not have been filmed. For blurred pages, a good image of the page can be found in the adjacent frame. If copyrighted materials were deleted, a target note will appear listing the pages in the adjacent frame.

3. When a map, drawing or chart, etc., is part of the material being photographed, a definite method of "sectioning" the material has been followed. It is customary to begin filming at the upper left hand corner of a large sheet and to continue from left to right in equal sections with small overlaps. If necessary, sectioning is continued again—beginning below the first row and continuing on until complete.

4. For illustrations that cannot be satisfactorily reproduced by xerographic means, photographic prints can be purchased at additional cost and inserted into your xerographic copy. These prints are available upon request from the Dissertations Customer Services Department.

5. Some pages in any document may have indistinct print. In all cases the best available copy has been filmed.

University Microfilms International
300 N. Zeeb Road
Ann Arbor, MI 48106

Downloaded from SHAREOK. Persistent Handle URL: https://hdl.handle.net/11244/5279

8425532

Abrahamson, Julie Kristine

AN INVESTIGATION OF PROTEIN-NUCLEIC ACID INTERACTIONS: THE AFFINITY OF AMINOACYL-TRANSFER-RNA FOR ELONGATION FACTOR TU

The University of Oklahoma PH.D. 1984

University
Microfilms
International 300 N. Zeeb Road, Ann Arbor, MI 48106

THE UNIVERSITY OF OKLAHOMA

GRADUATE COLLEGE

AN INVESTIGATION OF PROTEIN-NUCLEIC ACID INTERACTIONS: THE AFFINITY OF AMINOACYL-TRANSFER RNA FOR ELONGATION FACTOR Tu

A DISSERTATION

SUBMITTED TO THE GRADUATE FACULTY

in partial fulfillment of the requirements for the

degree of

Doctor of Philosophy

By

JULIE KRISTINE ABRAHAMSON

Norman, Oklahoma

1984

AN INVESTIGATION OF PROTEIN-NUCLEIC ACID INTERACTIONS:

THE AFFINITY OF AMINOACYL-TRANSFER RNA

FOR ELONGATION FACTOR Tu

A DISSERTATION

APPROVED FOR THE DEPARTMENT OF CHEMISTRY

By

Arthur E. Johnson

William A. Gilbert

David M. Crothers

Ridd W. Taft

Eddie Cartledge

ACKNOWLEDGEMENTS

I wish to extend my deep appreciation to the many individuals with whom I have worked and who were of great value to me in completing this dissertation. In particular, I thank Dr. Thomas M. Laue for assistance with the data analysis using nonlinear least squares on the IBM. I am also most grateful to Dr. David L. Miller for kindly providing the EF-Tu used in this research, and to the Graduate College of the University of Oklahoma for funds to purchase tRNA for this project.

A very special thank you goes to my husband, Harmon, and to my parents, for their understanding and tolerance of my pressures during my years as a graduate student.

I am fortunate to have had the opportunity to work with Dr. Arthur E. Johnson as a mentor and friend. Words cannot adequately express my gratitude for his insight, patience, encouragement, and humor, all of which have been an abundant resource for me. As he will continue to be an inspiration to his students, I can hope only to share with others his enthusiasm for research.

DEDICATION

This dissertation is dedicated to my husband, Harmon, without whose constant confidence and support I could not have persisted to reach this goal.

TABLE OF CONTENTS

Page

LIST OF TABLES vii

LIST OF ILLUSTRATIONS viii

ABSTRACT x

Chapter

I. INTRODUCTION 1

II. MATERIALS AND METHODS 23

Solvent Systems 23

Transfer RNA 24

EF-Tu 26

Protection and Deacylation Assays 28

Fluorescence Measurements 29

Titration Procedures 31

Ionic Strength Dependence of K_d 33

Determination of K_d Values for Fluorescent aa-tRNAs 34

Competition Experiments 37

Determination of K_d Values for Unmodified Nonfluorescent aa-tRNAs . . 39

Titration of $tRNA^{Phe}$-F^8 with EF-Tu*GTP . 42

III. RESULTS 43

Fluorescence-detected Ternary Complex Formation 43

Titration of Fluorescent-labeled aa-tRNA with EF-Tu*GTP 47

TABLE OF CONTENTS (CONT.)

Calculation of K_d for Fluorescent-labeled Aminoacyl-tRNAs 52

Nonlinear Least Squares Analysis of Titration Data 56

Ionic Strength Effects 61

Temperature Dependence of K_d 67

Determination of K_d Values for Unmodified Non-fluorescent Aminoacyl-tRNAs 67

Titration of Ternary Complex with Unacylated tRNA 78

Determination of K_d for Unacylated tRNA . 84

Determination of K_d for $tRNA^{Phe}$-F^8 . . . 85

Characterization of the Fluorescein-modified $tRNA_1^{Val}$ 88

Activity of EF-Tu 88

Factors Influencing the Fluorescence of the Probe 89

Experimental Considerations 92

IV. DISCUSSION 95

LITERATURE CITED 110

APPENDIX A 115

APPENDIX B 122

APPENDIX C 126

APPENDIX D 129

APPENDIX E 144

LIST OF TABLES

TABLE Page

I. Deacylation Rate Constants for Aminoacyl-tRNAs 38

II. Association of Fluorescent-Labeled aa-tRNA with EF-Tu*GTP 46

III. Association of Unmodified aa-tRNA with EF-Tu*GTP 71

IV. Comparision of Reported K_d Values for Aminoacyl-tRNAs 96

V. Thermodynamic Parameters Describing RNA-Protein Interactions 105

LIST OF ILLUSTRATIONS

FIGURE Page

1. Transmission of Genetic Information 3
2. Elongation Cycle of Protein Synthesis 6
3. Three-dimensional Representation of EF-Tu . . 10
4. Two- and Three-dimensional Representations of tRNA Structure 13
5. Fluorescein-modified $tRNA^{Phe}$ 21
6. Fluorescence Change Upon Ternary Complex Formation 45
7. EF-Tu*GTP Dependence of Phe-$tRNA^{Phe}$-F^8 Fluorescence Intensity 49
8. Two-log Range of EF-Tu Concentration for Fluorescence Change 51
9. Scatchard Analysis of Binding Data 55
10. Residuals as a Function of Tt and F/Fo for Titration of Phe-$tRNA^{Phe}$-F^8 with EF-Tu*GTP 58
11. Residuals as a Function of Tt and F/Fo Without Correction for Deacylation 60
12. Ionic Strength Dependence of the Ternary Complex Dissociation Constant 63
13. Protection of the Aminoacyl Bond by EF-Tu*GTP in the Presence of 1 M KCl 66
14. Titration of Phe-$tRNA^{Phe}$-F^8 with EF-Tu*GTP in the Presence or Absence of Competing Phe-$tRNA^{Phe}$ 70

LIST OF ILLUSTRATIONS (CONT.)

FIGURE Page

15. Asymmetry of Confidence Intervals for Competition Experiments 74

16. Titration of Phe-tRNA^{Phe}-F^{8}*EF-Tu*GTP with Aminoacylated or Unacylated tRNA . . . 77

17. Titration of Phe-tRNA^{Phe}-F^{8} with Unacylated tRNA in the Presence and Absence of EF-Tu*GTP. 81

18. Titration of Phe-tRNA^{Phe}-F^{8}*EF-Tu*GTP with Poly(rU) or Poly(rA) 83

19. Titration of tRNA^{Phe}-F^{8} with EF-Tu*GTP 87

ABSTRACT

I have investigated the formation of the aa-tRNA*EF-Tu*GTP ternary complex spectroscopically by monitoring a fluorescence change which accompanies the association of EF-Tu*GTP with Phe-tRNA^{Phe}-F^{8}, a functionally active analog of Phe-tRNA^{Phe} with a fluorescein moiety covalently attached to the s^{4}U-8 base. Using this approach, the protein-nucleic acid interaction could be examined directly and at equilibrium. The fluorescence emission intensity of each Phe-tRNA^{Phe}-F^{8} increased by 36-55% upon association with EF-Tu*GTP, depending on the solvent conditions. Thus, when Phe-tRNA^{Phe}-F^{8} was titrated with EF-Tu*GTP, the extent of ternary complex formation was determined from the increase in emission intensity. A nonlinear least squares analysis of the titration data yielded a dissociation constant of 0.85 nM for the ternary complex in 50 mM Hepes (pH 7.6), 10 mM $MgCl_2$, 50 mM NH_4Cl, at 6 ^{o}C. The ΔH^{o} of this interaction, determined by the temperature dependence of K_d, was -16 kcal/mol; the ΔS^{o} was therefore -16 cal mol^{-1} deg^{-1} at 6 ^{o}C in this buffer. In a more physiological polycation-containing solvent (polymix), the K_d was 4.7 nM. The ionic strength dependence of ternary complex formation showed that a minimum of two salt bridges and a substantial non-electrostatic contribution are involved in the binding of aa-tRNA to EF-Tu.

The affinities of unmodified tRNAs for EF-Tu*GTP were determined by their abilities to compete with the fluorescent aa-tRNA for binding to the protein. As expected, titrations using two different fluorescent aa-tRNAs, Phe-tRNA^{Phe}-F^{8} and Val-tRNA$_1^{Val}$-F^{8}, gave similar values for the

K_d of the E. coli Phe-$tRNA^{Phe}$ ternary complex. In polymix, the K_d values for yeast Phe-$tRNA^{Phe}$, E. coli Phe-$tRNA^{Phe}$ and E. coli Lys-$tRNA^{Lys}$ are 0.72, 1.16, and 7.7 nM, respectively. As expected the K_d value for fMet-$tRNA_f^{Met}$ for EF-Tu*GTP in polymix was shown to be much higher (2×10^{-7} M) than for the elongator tRNAs. Unacylated tRNA was found to have a weak affinity for EF-Tu*GTP also, with an approximate K_d of 10^{-5} M.

The affinity of EF-Tu*GTP for aa-tRNA is much higher than necessary to obtain ternary complex formation in the cell, and this suggests that the very tight association between the protein and the aa-tRNA is required to take full advantage of the discriminatory mechanisms of the ribosomal complex, thereby reducing translational errors.

AN INVESTIGATION OF PROTEIN-NUCLEIC ACID INTERACTIONS: THE AFFINITY OF AMINOACYL-TRANSFER RNA FOR ELONGATION FACTOR Tu

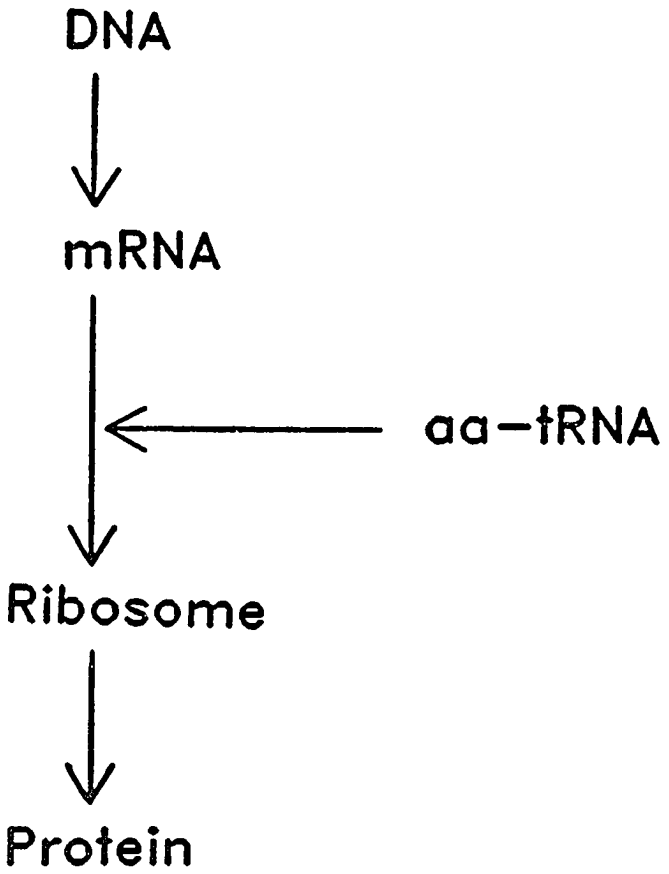
CHAPTER I

INTRODUCTION

The transmission of genetic information from chromosomes to proteins is accomplished by a complex and precise series of interactions between macromolecules. The information in the deoxyribonucleic acid (DNA) of the chromosomes is transcribed into a messenger ribonucleic acid (mRNA) molecule (Figure 1). The sequence of bases in the DNA dictates the mRNA sequence by base pairing interactions. The mRNA is translated into a protein product at the ribosome, the site for protein synthesis. The order of the amino acids in the protein polymer is determined by the sequence of bases in the mRNA. The amino acids are brought to the ribosomal complex covalently attached to a carrier macromolecule, the transfer RNA (tRNA), as an aminoacyl-tRNA (aa-tRNA). The result of this process is an efficient and accurate transmission of genetic information from the chromosome to a protein product.

Three phases of the synthesis of a linear protein polymer can be distinguished: initiation, elongation, and termination. (For reviews

Figure 1: The transmission of genetic information to proteins. The synthesis of a protein results from the transcription of the genetic information in the DNA into a mRNA and the translation of the mRNA at the ribosome into a protein, requiring the aid of the carrier molecule, aa-tRNA.

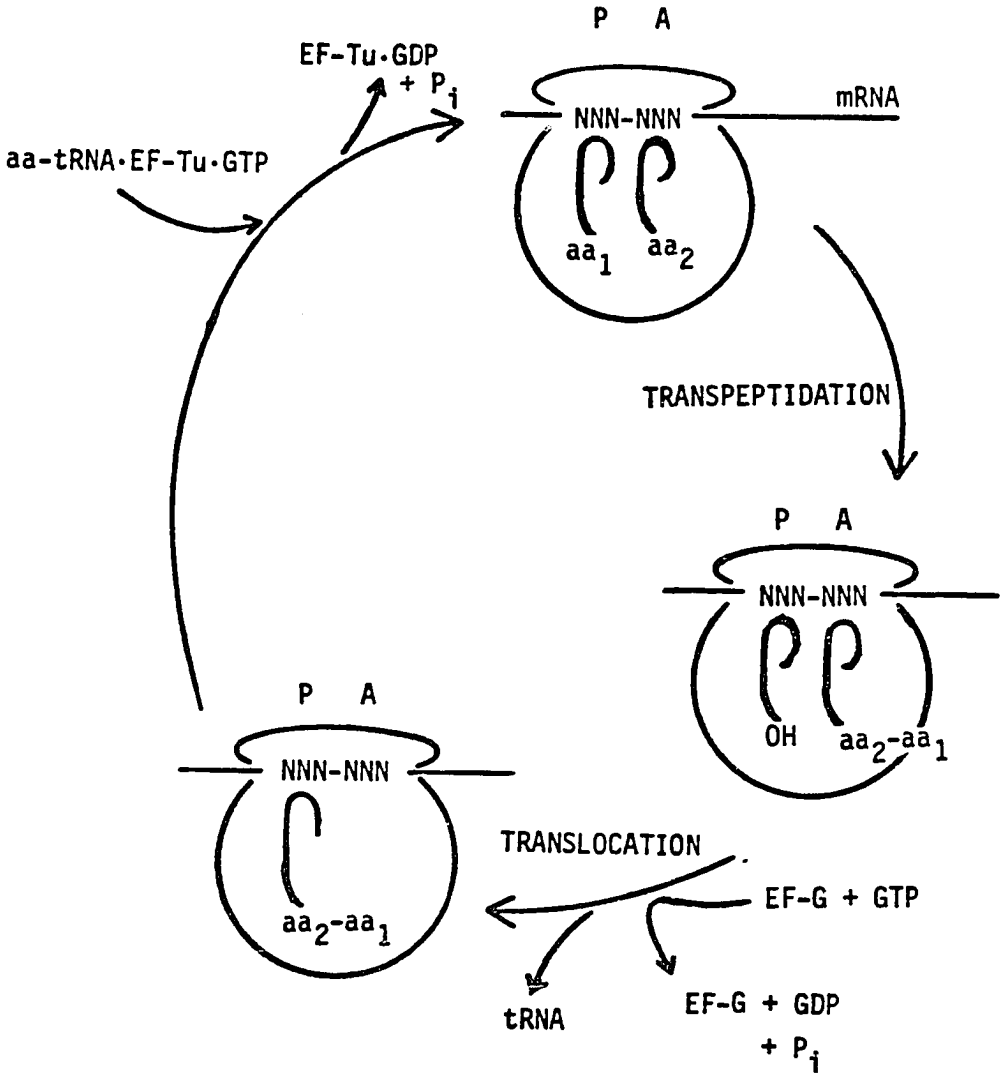

DNA
mRNA
aa–tRNA
Ribosome
Protein

see Kurland, 1977, and Grunberg-Manago et al., 1978.) The initiation process serves to correctly position the mRNA on the ribosome with the nucleotide triplet (codon) for the first amino acid of the peptide base-paired to the initiator aa-tRNA, formyl-Methionine-$tRNA_f^{Met}$ (fMet-$tRNA_f^{Met}$) in bacteria. This aa-tRNA is bound in a functionally-defined site on the ribosome designated the P site.

The elongation process is a cycle, beginning with the positioning of an aa-tRNA in a second functionally-defined binding site on the ribosome, the acceptor or A site (see Figure 2). The aa-tRNA diffuses to the ribosome as part of a ternary complex with guanosine triphosphate (GTP) and a protein, elongation factor Tu (EF-Tu). After the aa-tRNA binds to the mRNA codon on the ribosome, the EF-Tu-bound GTP is hydrolyzed to GDP (guanosine diphosphate), and the EF-Tu*GDP binary complex leaves the ribosome. A peptide bond is spontaneously formed between the amino acid of the aa-tRNA in the A site and the amino acid (or peptide) from the P site-bound fMet- or peptidyl-tRNA; this transfers the nascent protein chain to the tRNA bound in the A site. The now unacylated tRNA in the P site dissociates from the ribosome, and the peptidyl-tRNA in the A site is translocated to the P site by a movement of the mRNA relative to the ribosome. This translocation step is catalyzed by a second non-ribosomal protein, elongation factor G (EF-G), and is accompanied by the hydrolysis of another GTP molecule. The next codon of the mRNA is thus available for another aa-tRNA to bind in the A site to begin the next cycle of elongation.

Termination occurs when one of the three mRNA codons specifying termination is positioned in the A site. During this process, the

Figure 2: Schematic representation of the elongation cycle of protein synthesis.


P A
EF-Tu·GDP
+ P_i
mRNA
NNN-NNN
aa-tRNA·EF-Tu·GTP
aa_1
aa_2
TRANSPEPTIDATION
P A
NNN-NNN
OH
aa_2-aa_1
P A
NNN-NNN
aa_2-aa_1
TRANSLOCATION
EF-G + GTP
tRNA
EF-G + GDP
+ P_i

peptide of the peptidyl-tRNA in the P site reacts with a water molecule rather than another amino acid from an A site bound aa-tRNA. The peptide, now no longer attached to a ribosome-bound tRNA, is therefore released from the ribosome.

Each of the above operations involves specific interactions between proteins and nucleic acids and is catalyzed by non-ribosomal proteins, designated initiation, elongation, and release factors. Although these proteins have been identified, their specific roles in the overall mechanism have yet to be clearly understood.

One of the catalytic non-ribosomal proteins, the elongation factor Tu, is the most abundant protein in Escherichia coli (Furano, 1975; Jacobson and Rosenbusch, 1976; Wittinghofer et al., 1979). The fact that EF-Tu is produced in a large excess over ribosomes and the other elongation factors (Furano, 1975; Skjold, et al., 1973; van der Meide et al., 1983 and references therein) suggests that it may have a role(s) in the cell other than in protein biosynthesis. Some evidence supporting this view has been reported (Travers, 1976; Beck et al., 1978). There are two distinct genes coding for EF-Tu which are under different transcriptional control (Bachman and Low, 1980; van der Meide et al., 1982, 1983). EF-Tu itself has been implicated in the regulation of the expression of these two genes (van der Meide, et al., 1982, 1983). The primary structure of EF-Tu, a single polypeptide chain of 393 amino acids with a molecular weight of 43,200 daltons, has been determined (Jones et al., 1980; Arai et al., 1980). Three laboratories have crystallized EF-Tu (Rubin et al., 1981; Kabsch et al., 1977; Jurnak et al., 1980), but a high resolution x-ray crystal structure has yet to be reported. Low resolution data suggests that the protein has three

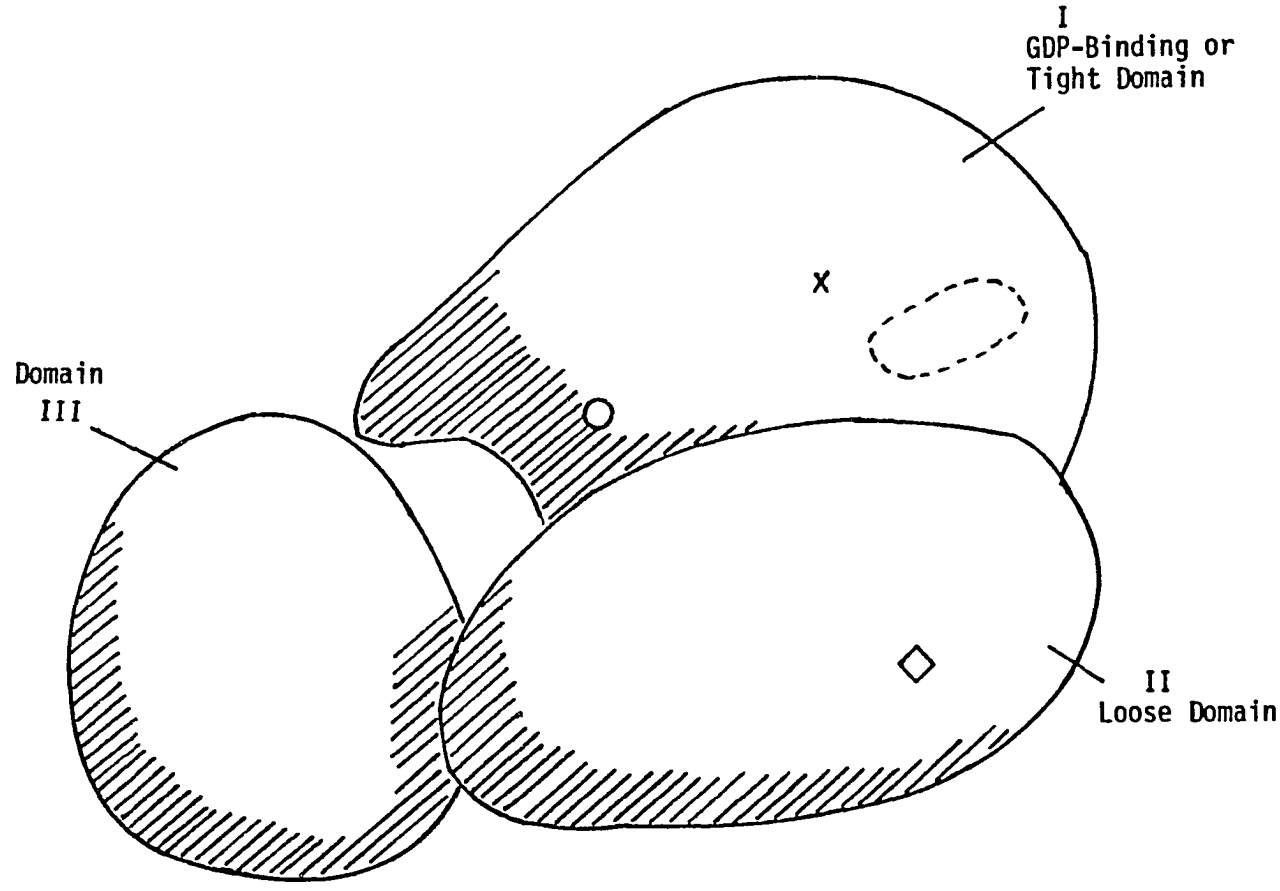
structural domains (see Figure 3), and the approximate location of the GDP binding site has been assigned.

In the presence of GTP, EF-Tu binds very strongly to the various aa-tRNAs which participate in the elongation cycle. However, EF-Tu*GTP binds only weakly to fMet-$tRNA_f^{Met}$, the initiator aa-tRNA in prokaryotes (Tanada et al., 1982). This is consistent with its participation in the elongation cycle for the binding of aa-tRNA to the A site.

How does EF-Tu catalyze the elongation cycle of protein synthesis? After all, aminoacyl-tRNA has been shown to bind to the ribosomal complex in a message-dependent manner without EF-Tu (e.g. Johnson et al., 1976), and in vitro protein synthesis has been demonstrated in the absence of EF-Tu, although at a rate much slower than in vivo (Gavrilova et al., 1976). One possibility is that the EF-Tu-dependent GTP hydrolysis provides the energy necessary to drive the elongation process. Another possibility is that EF-Tu aids in the recognition of the aa-tRNA by the ribosome, perhaps by effecting or facilitating a conformational change in the aa-tRNA which is required for codon-anticodon base-pairing. A third possibility is that catalysis is effected by an interaction of EF-Tu with the ribosome, perhaps by changing the conformation of the ribosomal complex.

The error frequency for protein synthesis predicted on the basis of equilibrium processes involving base-pairing is much greater (100-fold) than has been observed in vivo, where the error rate is about one incorrect amino acid for every 10,000 amino acids incorporated into a protein (Jelenc and Kurland, 1979). It has therefore been suggested that the recognition of ternary complexes by the ribosome is a two-stage process. One specific hypothesis for a two-stage process was proposed

Figure 3: Cartoon representation of the three-dimensional structure of EF-Tu from x-ray crystallographic studies. Dotted line: GDP binding site (on the back side of the domain); X: His-66, the site which is affinity labeled using Nε-bromoacetyl-Lys-tRNA; O: the single tryptophan residue in EF-Tu; ◇: Lys-357, (on back side of the domain) site to which kirromycin cross-links. (Adapted from Duisterwinkel et al., 1984.)

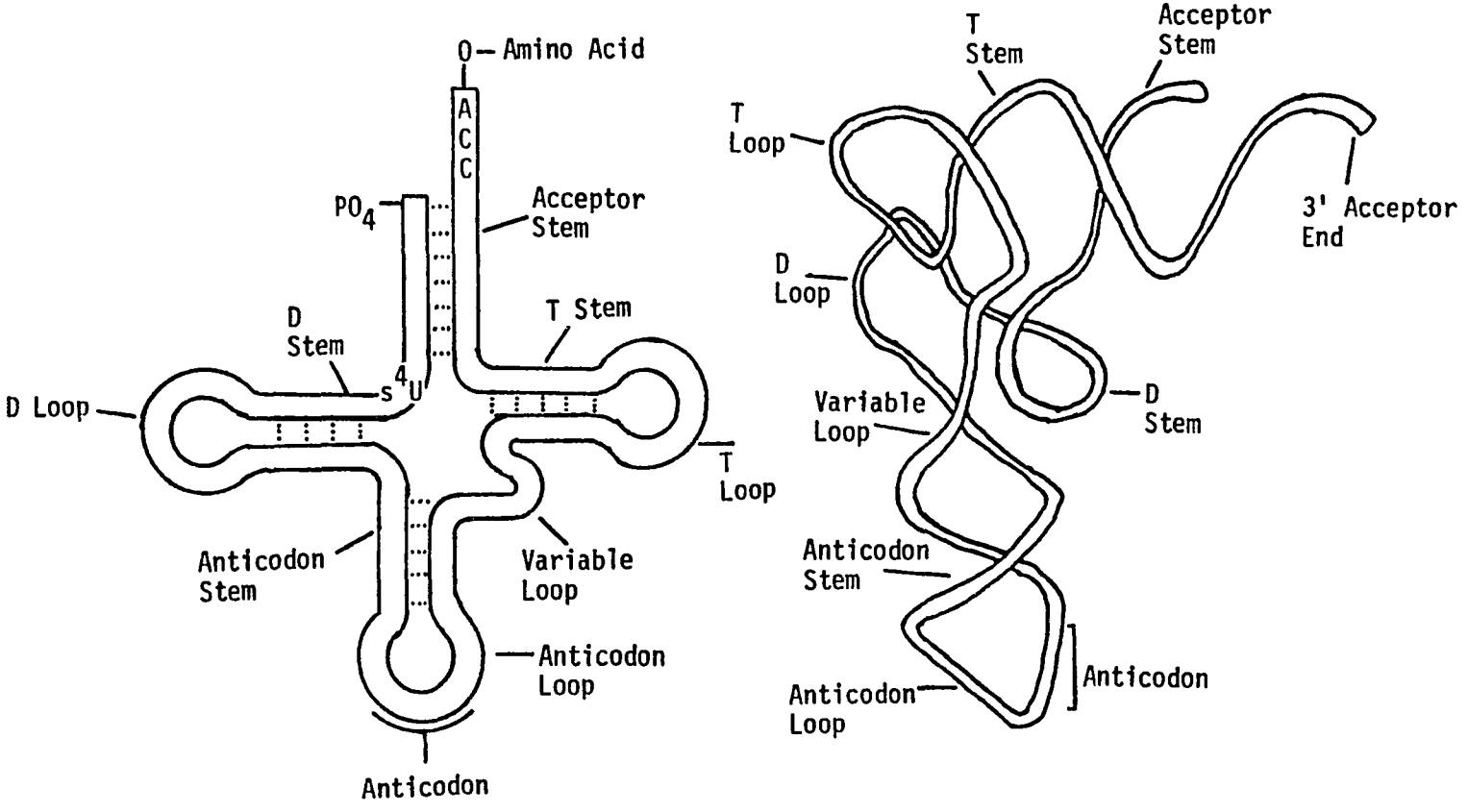

I
GDP-Binding or
Tight Domain
X
Domain
III
II
Loose Domain

independently by Hopfield (1974) and by Ninio (1975). In this scheme, the first stage is an initial discrimination among the various ternary complexes based only on the differences in stability of interactions of cognate and noncognate tRNAs with the codon. The second stage involves the hydrolysis of GTP and the dissociation of EF-Tu*GDP in those ternary complexes which survive the first stage. This proposed second step is referred to as proofreading since it provides an additional opportunity for checking the accuracy of the codon-anticodon base-pairing.

In an attempt to gain a better understanding of this protein-nucleic acid interaction, several investigators have sought to identify the parts of the aa-tRNA which interact directly with EF-Tu. There is strong evidence that EF-Tu interacts with the aminoacyl end of the aa-tRNA (see Figure 4). For example, when EF-Tu forms a ternary complex with aa-tRNA and GTP, the protein both protects the labile aminoacyl bond of the aa-tRNA from spontaneous hydrolysis (Beres and Lucas-Lenard, 1973) and protects the 3' end of the tRNA from digestion by nucleases (see e.g. Jekowsky et al., 1977; Wikman et al., 1982). In contrast, uncharged tRNA and N-α-acetylated aa-tRNAs do not form stable ternary complexes (Ravel et al., 1967). The chemical acylation of the α-amino group of the aa-tRNA is greatly reduced when it is bound to EF-Tu*GTP (Sedlacek et al., 1976). In addition, analogs of the 3'-terminus of the aa-tRNA bind to EF-Tu and block chemical modification of a site of on EF-Tu (Jonák, et al., 1980).

EF-Tu interacts with the aminoacyl group of the aa-tRNA, but will bind aa-tRNAs differing greatly in the aminoacyl moiety. Primary evidence for this property of EF-Tu lies in the fact that EF-Tu can form ternary complexes with all elongator aa-tRNAs. In addition, ternary

Figure 4: The structure of E. coli transfer RNA. Left: two-dimensional representation; right: three-dimensional representation. Dotted lines indicate hydrogen bonding between portions of the RNA present in the helices of the stem regions. The 5' end of the tRNA has a phosphate moiety, and the 3' end is the site for covalent attachment of the amino acid. (Adapted from Rich and Kim, 1978).


O— Amino Acid
A
C
C
PO4
Acceptor Stem
D Stem
T Stem
s4U
D Loop
T Loop
Anticodon Stem
Variable Loop
Anticodon Loop
Anticodon
T Stem
Acceptor Stem
T Loop
3' Acceptor End
D Loop
D Stem
Variable Loop
Anticodon Stem
Anticodon
Anticodon Loop

complex formation has been demonstrated using aa-tRNA lacking its α-amino group (Derwenskus and Sprinzl, 1983). Interestingly, an aa-tRNA analog with a reactive moiety on the side chain of the lysine (Johnson and Cantor, 1980) has been used to affinity label EF-Tu at His-66 (Johnson et al., 1978; Duffy et al., 1981; see Figure 3).

EF-Tu requires certain structural features in the 3' terminus of the aa-tRNA in order to form a ternary complex. EF-Tu is sensitive to the nature of the linkage of the amino acid to the tRNA. When an amide bond replaces the usual ester bond between the amino acid and the tRNA, ternary complex formation is prevented (Sprinzl, et al., 1977). In addition, an intact 2',3'-carbon-carbon bond on the 3'-terminal adenosine of the aa-tRNA is necessary for binding to EF-Tu and GTP (Ofengand and Chen, 1972).

Studies with nuclease-modified tRNAs have been used to obtain information about other portions of the aa-tRNA involved in binding to EF-Tu*GTP. EF-Tu can form a ternary complex with Val-tRNA^{Val} cleaved in its anticodon loop (Krauskopf, et al., 1972), suggesting that the anticodon does not interact directly with EF-Tu. This result is as expected since codon-anticodon binding must occur between the ternary complex and the ribosome-bound mRNA. A weak interaction between EF-Tu and tRNAs lacking all or portions of their C-C-A ends has been reported (Picone and Parmeggiani, 1983). However, 3' half-molecules of Val-tRNA were found by Krauskopf and colleagues (1972) to be completely inactive with respect to interaction with EF-Tu*GTP.

Information about the interactions of EF-Tu with the various regions of the aa-tRNA has also been obtained using various types of protection experiments. Boutorin and coworkers (1981) demonstrated that

the acceptor arm and TψC stem of various aa-tRNAs are protected by EF-Tu from digestion by the double-strand-specific cobra venom ribonuclease. Other nuclease protection experiments using single-strand-specific nucleases have been reported by Jekowsky et al. (1977) and Wikman et al. (1982). Their results indicate accessibility of the dihydrouridine and TψC loops to nuclease attack and protection of the 3' terminus from cleavage. In the presence of EF-Tu*GTP, the D loop and D stem of the aa-tRNA are protected from chemical modification by kethoxal (Bertram and Wagner, 1982). However, these latter data appear to have been interpreted incorrectly. Wintermeyer has shown with fluorescent-labeled tRNA that the D loop does not interact with the protein (personal communication to A. E. Johnson). Instead, the reactivity differences observed by Bertram and Wagner were most likely due to a conformational change in the aa-tRNA which resulted from ternary complex formation (Adkins et al., 1983). Iodide ion quenching experiments using a fluorescent-labeled aa-tRNA (Adkins, et al., 1983) have also shown that EF-Tu does not cover the region of the tRNA around the elbow of the L-shaped tRNA. Taken together, these data are interpreted to mean that EF-Tu binds to the aa-tRNA only along its acceptor and TψC helices.

The aa-tRNA*EF-Tu*GTP ternary complex is one of several multicomponent complexes which participate in the process of discriminating between cognate and noncognate aa-tRNAs at the ribosome. The detailed mechanism for this recognition process is unknown. A characterization of the interactions between the various macromolecules and multicomponent complexes participating in the process is therefore required to understand the mechanism(s) which control recognition. Since the ternary complex is an obligatory intermediate in the

elongation cycle, a thermodynamic characterization of this protein-nucleic acid interaction is essential to clarify its specific role in protein synthesis. Accordingly, it is important to determine accurately the affinity of aa-tRNA for EF-Tu*GTP. In particular, an evaluation of the contributions of different regions of the aa-tRNA to the binding energy of the ternary complex is required to better understand the factors influencing complex formation and complex dissociation at the end of the recognition process.

The equilibrium constant for the dissociation of the aa-tRNA*EF-Tu*GTP ternary complex has been estimated by several groups using three different approaches. One method was based on EF-Tu's protection of the aa-tRNA from nuclease digestion (Knowlton and Yarus, 1980; Tanada et al., 1981, 1982; Derwenskus and Sprinzl, 1983; Louie et al., 1984). A radioactively-labeled aa-tRNA, with the label in the amino acid, was allowed to form a ternary complex with EF-Tu*GTP, and the mixture was then incubated with nuclease. Under these conditions, any aa-tRNA which is not EF-Tu-bound is rapidly degraded, and the radioactive label is no longer attached to the tRNA. Only label which is still intact on the tRNA will be precipitated in cold trichloroacetic acid. Hence, the concentration of the ternary complex-bound aa-tRNA was estimated based on the acid insoluble radioactivity remaining at the time of assay, and was used to calculate a dissociation constant.

Another method for determining the equilibrium constant for the ternary complex relied on EF-Tu's ability to protect the aminoacyl bond of aa-tRNA from spontaneous non-enzymatic hydrolysis (Beres and Lucas-Lenard, 1973; Pingoud et al., 1977b; Pingoud and Urbanke, 1980; Wagner and Sprinzl, 1980). Experimentally, the rates of spontaneous hydrolysis

of the aa-tRNA were compared in the presence and absence of EF-Tu*GTP, using acid insoluble radioactivity to determine the amount of the radioactive label remaining intact on the aa-tRNA. The K_d was calculated by determining the EF-Tu*GTP concentration dependence of the protection of the aminoacyl bond.

A third approach was based on the ability of aa-tRNA to reduce the amount of EF-Tu bound to nitrocellulose filters (Miller et al., 1973; Arai et al., 1974; Ofengand, 1974). In the presence of GDP or GTP, EF-Tu is known to bind to nitrocellulose filters (Miller and Weissbach, 1977). However, in the presence of aa-tRNA and GTP, EF-Tu does not bind the filters. For this type of experiment, a radioactively-labeled GTP was incubated with the EF-Tu in the presence of aa-tRNA. The amount of EF-Tu*GTP bound to filters in the presence and absence of aa-tRNA was measured. The extent of ternary complex formation was deduced by the difference in EF-Tu bound to the filters in the two sets of samples.

The dissociation constants obtained using these methods ranged from less than 10 nM to 1 μM for the various aa-tRNAs tested. For Phe-$tRNA^{Phe}$ the values ranged from 1-10 nM (Miller et al., 1973) to 100 nM (Derwenskus and Sprinzl, 1983). Some of the discrepancies in these equilibrium constants can be attributed to the different experimental protocols (e.g. temperature and ionic strength) which were used. More importantly, each of these investigations had the disadvantage of making measurements under non-equilibrium conditions. In two of the methods, one component of the complex was removed from the equilibrium, by spontaneous hydrolysis or nuclease digestion of the aa-tRNA. In the other situation, the equilibrium was altered by physical separation of one species from the solution, i.e., by binding a component of the

equilibrium to a filter.

Ideally the ternary complex dissociation constant should be evaluated using a technique which permits measurements under equilibrium conditions. This normally requires an optical method, since continuous and non-destructive monitoring of the system is possible. Fluorescence spectroscopy is particularly useful in such studies both because a fluorescent dye is typically very sensitive to changes in its environment and because very low concentrations of a fluorescent probe can be detected. With a probe covalently attached to a single site on a macromolecule, the changes in a single portion of the labeled molecule can be monitored. An advantage of nsing a covalently attached extrinsic fluor is that it can avoid the background fluorescence problems which are frequently encountered with the use of most intrinsic fluors, in part because intensely fluorescent extrinsic dyes can be chosen.

To examine the association of aa-tRNA with EF-Tu*GTP directly and at equilibrium using fluorescence spectroscopy, one needs either the tRNA or the EF-Tu labeled with a fluorescent dye whose environment changes when the two macromolecules associate. EF-Tu labeled with an extrinsic fluor has been prepared (Rychlik et al., 1983), but no report of a change in fluorescence upon binding to aa-tRNA molecules has appeared. Several tRNAs have been prepared with spectral probes, and most show little change in signal in the presence of EF-Tu (Beres and Lucas-Lenard, 1973; Pingoud et al., 1977a; Sprinzl and Faulhammer, 1978). However, an analog of aa-tRNA sensitive to the presence of EF-Tu*GTP has been reported (Johnson et al., 1982; Adkins et al., 1983). This $tRNA^{Phe}$ analog was modified by the covalent attachment of a fluorescein dye on the 4-thiouridine base (s^4U-8) in the corner of the

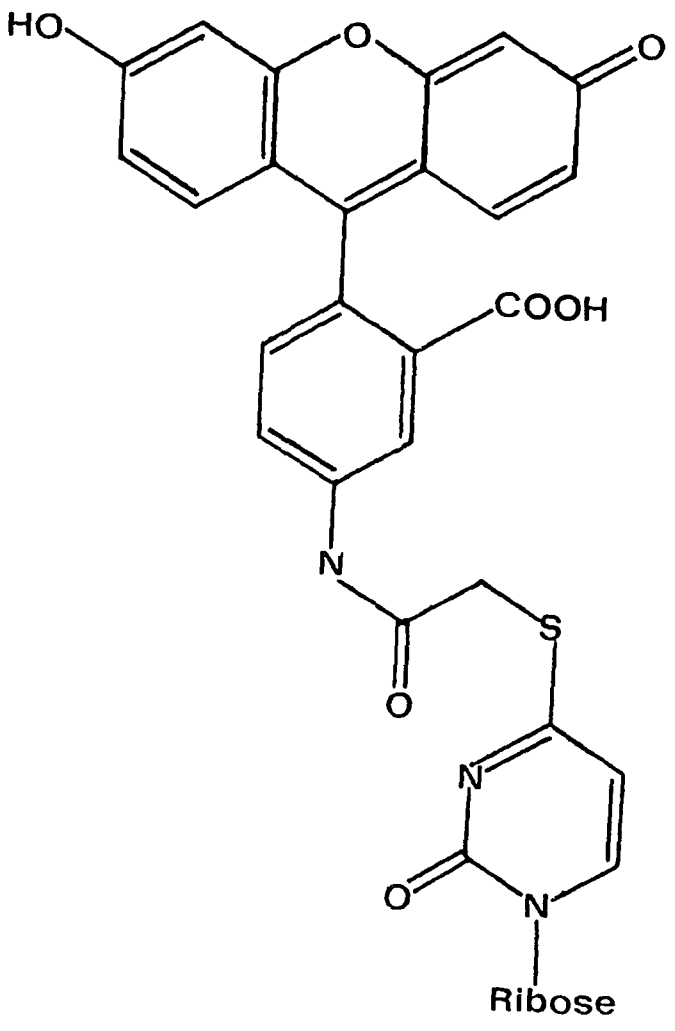
L-shaped molecule, and is designated $tRNA^{Phe}$-F^8 (see Figure 5).

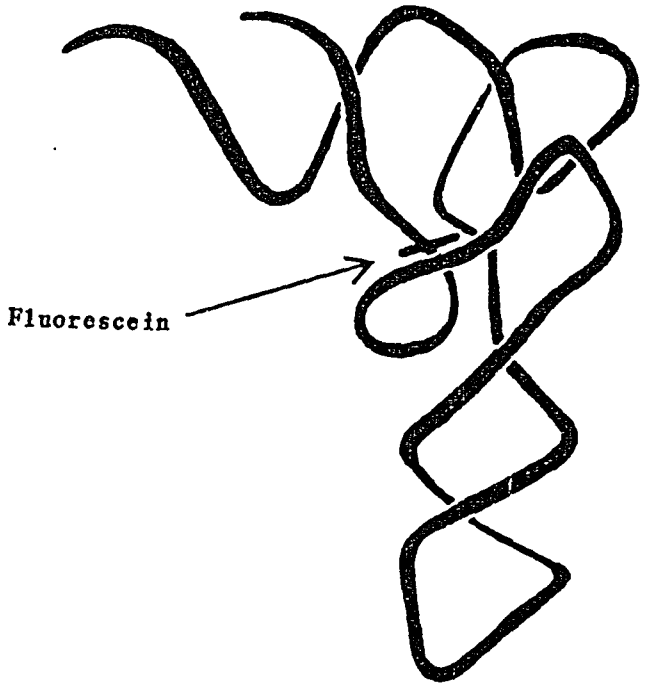
Of course, whenever an investigation utilizes a molecule or macromolecule with a covalent modification, it is essential that the effects of the modification on the molecule's functional activity be examined. Fortunately, $tRNA^{Phe}$-F^8 has proven to be active in its biological functions. $tRNA^{Phe}$-F^8 can be aminoacylated by E. coli aa-tRNA synthetases (Johnson et al., 1982). Phe-$tRNA^{Phe}$-F^8 binds to EF-Tu in the presence of GTP, as demonstrated by the protection of the aminoacyl bond from non-enzymatic hydrolysis (Johnson et al., 1982; Adkins et al., 1983). The EF-Tu-dependent binding to poly(uridylic acid)-programmed ribosomes is the same for Phe-$tRNA^{Phe}$ and for Phe-$tRNA^{Phe}$-F^8 (Johnson et al., 1982). Finally, and most convincingly, Phe-$tRNA^{Phe}$-F^8 has been shown to be as active as Phe-$tRNA^{Phe}$ in polyphenylalanine synthesis (A. E. Johnson, unpublished experiments).

Previous work in Johnson's laboratory characterized some of the spectral properties of this probe. No change in fluorescence emission intensity was observed upon aminoacylation of $tRNA^{Phe}$-F^8 (Adkins et al., 1983). Most interestingly, however, a substantial increase (+28%) in fluorescence emission intensity of Phe-$tRNA^{Phe}$-F^8 accompanied its association with EF-Tu*GTP (Adkins et al., 1983). Since the rate of iodide ion quenching of the Phe-$tRNA^{Phe}$-F^8 fluorescence was not altered by ternary complex formation, it was concluded that the EF-Tu does not directly interact with the fluorescein dye on the tRNA (Adkins et al., 1983). The fluorescence change was therefore interpreted to be due to a conformational change in the aa-tRNA near the s^4U-8.

Thus, $tRNA^{Phe}$-F^8 is a probe which both contains a fluorescent dye sensitive to changes in its environment and is functionally active.

Figure 5: Fluorescein modification of E. coli $tRNA^{Phe}$. Reaction of 5-(iodoacetamido)fluorescein with 4-thiouridine, base 8 in E. coli tRNAs (see Figure 4), results in a thioether-linked adduct (left) between the dye and the tRNA. In the three-dimensional representation of the tRNA (right), the dye is located in the inside of the elbow of the tRNA.


HO
O
O
COOH
N
S
O
N
O
N
Ribose


Fluorescein

Taking advantage of its availability, $tRNA^{Phe}$-F^{8} was therefore used to obtain physiologically meaningful information about the aa-tRNA*EF-Tu*GTP ternary complex, and to better understand the nature of this protein-nucleic acid interaction.

CHAPTER II

MATERIALS AND METHODS

A. Solvent Systems

Titrations were carried out in one of two solvent systems. Buffer A contained 50 mM Hepes[1] (pH 7.6), 10 mM $MgCl_2$, 50 mM NH_4Cl, and 0.1 mM DTT, unless specified otherwise. Buffer B, the polycation-containing solvent (polymix), was prepared using 10X polymix (Jelenc, 1980), and in the final incubations contained 5 mM $MgCl_2$, 0.5 mM $CaCl_2$, 8 mM putrescine-HCl, 1 mM spermidine-HCl, 5 mM NH_4Cl, 95 mM KCl, 0.1 or 1 mM DTT, and 5 mM potassium phosphate (pH 7.0). Because a salt precipitate was observed at pH 7.5 in the Jelenc polymix buffer at 6 °C, the buffer B solutions were titrated to pH 7.0 at 6 °C.

The scintillation cocktail used for counting radioactivity in aqueous samples contained 16.5 g PPO and 0.50 g dimethyl-POPOP per 2 L toluene and 1 L Triton X-100 (Amersham). Four mL of the Triton

---

[1]Abbreviations: Hepes, N-(2-hydroxyethyl)piperazine-N'-2-ethanesulfonic acid; DTT, dithiothreitol; IAAF, 5-(iodoacetamido)fluorescein; PEP, phosphoenolpyruvate; aa-tRNA, aminoacyl-tRNA; EF-Tu, elongation factor Tu; s^4U, 4-thiouridine; PPO, 2,5-diphenyl-1,3-oxazole; POPOP, 1,4-bis-2-(5-phenyloxazolyl)-benzene; dimethyl-POPOP, 1,4-bis-2-(4-methyl-5-phenyloxazolyl)-benzene; poly(rU), poly(uridylic acid); poly(rA), poly(adenylic acid); PEI, polyethyleneimine.

X-100-containing cocktail were used per 400 µL of aqueous radioactive sample. For those radioactive samples which were dried on filters, a second scintillation cocktail was used, and contained 16 g PPO and 0.4 g POPOP per gallon of toluene.

B. Transfer RNA

Escherichia coli $tRNA^{Phe}$ (Plenum Scientific, Hackensack, NJ) and $tRNA_1^{Val}$ (Boehringer, Indianapolis, IN) were reacted with IAAF (Molecular Probes, Junction City, OR) as described previously (Johnson et al., 1982), except that the time of reaction was increased to 17 h. The treatment of the $tRNA_1^{Val}$ reaction product differed from that with $tRNA^{Phe}$ only by the inclusion of 5 mM $MgCl_2$ in the buffers for Sephadex G25 chromatography and for dialysis. The tRNA species with the fluorescein dye covalently attached to s^4U-8, $tRNA^{Phe}$-F^8 and $tRNA_1^{Val}$-F^8, were purified by RPC-5 chromatography (Johnson et al., 1982). The $tRNA_1^{Val}$-F^8 eluted from the RPC-5 column at a position in the NaCl gradient very similar to that observed for $tRNA^{Phe}$-F^8.

After reaction with IAAF, it was necessary to identify the site of the covalent modification of $tRNA_1^{Val}$. A total enzymatic digestion of the modified $tRNA_1^{Val}$ was carried out as described by Johnson et al. (1982). The digestion mixture was dried and anaylzed by thin-layer chromatography on silica gel plates (Analtech) in a benzene/pyridine/acetic acid/ethanol (65:25:4:6, by volume) solvent system using s^4U-fluorescein and pseudouridine-fluorescein dye-nucleoside adducts as markers (Adkins, 1982). Fluorescein-containing material was visually located using an ultraviolet lamp (Mineralight

UVSL-25) to measure R_f values.

Modified and unmodified $tRNA^{Phe}$ and yeast $tRNA^{Phe}$ (Boehringer) were aminoacylated as described earlier (Johnson et al., 1982) using E. coli S-100 enzymes prepared according to Johnson et al. (1976) and radioactive phenylalanine purchased from ICN (Irvine, CA). E. coli MRE 600 $tRNA^{Lys}$ (Boehringer) was aminoacylated using [^{3}H]Lysine (ICN) as described elsewhere (Johnson and Slobin, 1980). The same procedures were used to aminoacylate $tRNA_1^{Val}$-F^8 using [^{14}C]Valine (ICN), except that the dithiothreitol concentration was 1 mM instead of 5 mM. The preparation of f-[^{3}H]Met-$tRNA_f^{Met}$ was similar to that described by Johnson and colleagues (1982) except that the incubation contained 10 mM KCl, 0.1 mM CTP, 1 mM DTT, 9.9 A_{260} units $tRNA_f^{Met}$ (a gift from Dr. P. E. Cole), and 76 μM [^{3}H]Methionine (Amersham). Preparative aminoacylation of unfractionated E. coli tRNA (Boehringer) with a mixture of 20 amino acids was carried out as for $tRNA^{Phe}$, except that the incubation (12.0 mL) contained 40 μM amino acids, 600 A_{260} units tRNA, and 1.2 mg S-100 enzymes.

The advertised specific activities of ICN, New England Nuclear, and Amersham amino acid preparations have occasionally been found to be incorrect, and are frequently incorrect for [^{3}H]Phe. Consequently, the actual specific activity of radioactive amino acid preparations were routinely determined using parallel accepting activity assays (Johnson et al., 1982) that differ only in the ratio of non-radioactive to radioactive amino acid in each incubation.

Transfer RNA concentration was determined using ε_{260}= 6.25×10^5 $M^{-1}cm^{-1}$. The amount of aminoacylated tRNA was determined from the amount of radioactivity precipitated in cold trichloroacetic

acid. Samples were normally precipitated in the presence of 0.3 to 0.4 A_{260} units of added rRNA or tRNA as carrier. However, the efficiency of precipitation for larger aliquots (e.g. 400 μL) was found to be improved by using twice as much carrier RNA. Filters were routinely dried overnight, soaked in 1 mL hyamine hydroxide (Packard) for 1 hr, and counted after the addition of 14 mL of PPO- and POPOP-containing toluene-based scintillation cocktail, on either a Beckman LS-7500 or a LS-100 liquid scintillation counter. The hyamine hydroxide was used to hydrolyze the RNA in the precipitate, maximizing the uniform distribution of radioactivity in the samples relative to the fluor in the scintillation fluid. This procedure also resulted in increased ^3H counting efficiencies over those for the non-hyamine treated filters. The fraction of acid-insoluble radioactivity in a sample of aa-tRNA was found to be the same as the fraction of radioactivity that eluted in the void volume following chromatography on Sephadex G25, at 4 ^oC in 1 mM potassium acetate (pH 5.0), 5 mM $MgCl_2$.

C. EF-Tu

Crystalline EF-Tu*GTP was purified from *E. coli* B cells as described elsewhere (Miller and Weissbach, 1974). EF-Tu*GDP concentrations were determined using ε_{280}= 41,600 $M^{-1}cm^{-1}$. (A 1.0 mg/mL solution of EF-Tu*GDP had an absorbance at 280 nm of 0.96; Dr. D. L. Miller, personal communication.) GDP-binding assays showed that the EF-Tu was completely active in binding nucleotide.

The nucleotide binding activity of the EF-Tu was routinely measured using [^3H]GDP in a nitrocellulose filter binding assay similar to that

described by Miller and Weissbach (1974), except that no EF-Ts was present. For this assay, duplicate aliquots of a solution containing 20 μM [^{3}H]-GDP (167-236 dpm/pmol) and 1.1 mg/mL bovine serum albumin in the same buffer as the EF-Tu stock solution (see Section E below) (but without the pyruvate kinase, PEP, and GTP) were placed in polystyrene assay tubes on ice. To each tube an equal volume aliquot of the EF-Tu*GTP solution was added, typically containing 130 to 300 pmol EF-Tu. Duplicate aliquots of each of two different sizes were usually assayed. The samples were incubated on ice for 8 to 10 min and diluted with 2 mL ice cold wash buffer (10 mM Tris-Cl, pH 7.4, 10 mM $MgCl_2$, 10 mM NH_4Cl) before pouring over prewetted nitrocellulose filters (0.45 μm pore size; Gelman GN-6, or Millipore HAWP) Each tube was rinsed three times with 3 mL ice cold wash buffer. Filters were dried overnight before counting in a PPO- and POPOP-containing toluene-based scintillator. Polystyrene tubes and BSA were found to be useful in minimizing variations in filter binding results, presumed to be due to adsorption of the EF-Tu*GTP to the sides of the assay tubes. The 8 to 10 min incubation period was found adequate to permit the exchange of GTP bound to EF-Tu for the tighter binding GDP.

The GDP-binding activity of an EF-Tu sample was also estimated using gel filtration following an 8 min, 0 ^oC incubation in the presence of 10 μM [^{3}H]GDP (167-236 dpm/pmol) and 0.55 mg/mL bovine serum albumin. In this case, the minimum amount of active EF-Tu was calculated from the total radioactivity eluted in the void volume from the Sephadex G-25 column (0.6 cm ID x 19 cm) at 4 ^oC.

The specific activity of the [^{3}H]GDP was periodically redetermined using two different methods. First, the mole fraction of GDP was

determined by chromatography on thin layer plates (PEI Cellulose F; Merck) as described by Jelenc and Kurland (1979). Small aliquots of [^{3}H]GDP, [^{1}H]GDP and [^{1}H]GTP were spotted 5 mm from the lower edge of 11-12 cm long plates in separate lanes. After developing in a 0.75 M potassium phosphate (pH 3.5) buffer, the plates were dried, and the [^{1}H]-GTP and -GDP markers were located by absorption using short wavelength ultraviolet light to measure their respective R_f values. Strips about 4 mm wide were cut from the lanes containing the [^{3}H]GDP, placed in scintillation vials with 0.4 mL 2 N HCl, incubated 10 min, and counted in a Triton-X100-containing scintillation cocktail. The positions and amplitudes of the radioactive peaks were compared to those of the markers to quantitate the [^{3}H]GDP relative to the presumed hydrolysis product, [^{3}H]GMP.

Secondly, an evaporation test was used to determine the amount of ^{3}H exchange into H_2O. An aliquot of [^{3}H]GDP was diluted with cold H_2O and split into 10-12 equal samples in scintillation vials. Half the samples were immediately diluted with cold H_2O, mixed with a Triton-containing scintillation cocktail, and counted. The remaining samples were allowed to evaporate to dryness under a fume hood before dilution and counting. The ratio of the average radioactive counts in the dried to the undried samples yielded the fraction of the ^{3}H remaining on the nucleotide.

D. Protection and Deacylation Assays

Samples (160 µL) were prepared in 1.5-ml capped polypropylene tubes and contained 10 µM GTP, 8 µg pyruvate kinase, 1 mM PEP, 0.1 mM

dithiothreitol, and 1.77 μg EF-Tu*GDP, in buffer B, buffer A, buffer A at pH 7.0, or in buffer A with 50, 300, or 1000 mM KCl instead of 50 mM NH_4Cl. Deacylation assays differed from the protection assays only in that EF-Tu was omitted from the samples. Following an initial 20-min incubation at 37 °C to convert all GDP to GTP, 9.6 to 11.7 pmol aa-tRNA (0.18 to 0.27 A_{260} units for unfractionated tRNAs, or 0.013 to 0.015 A_{260} units for purified tRNAs) was added to each sample. Immediately after mixing, aliquots were removed and assayed for cold acid insoluble radioactivity as described by Johnson and Adkins (1984). The sample tubes were then capped and placed at the desired incubation temperature (6, 15, or 25 °C). Duplicate aliquots were removed and assayed two more times between 2 and 8 hours after the beginning of the incubation. Since it was expected that the deacylation rates would be greater at higher temperatures, lower at pH 7.0, and lower for Val-$tRNA_1^{Val}$-F^8, the times for assay were chosen to yield significant levels of deacylation without the loss of all precipitable radioactivity. Accordingly, the final assays for samples incubated at 25 °C were taken after 4 hr, and for Val-$tRNA_1^{Val}$-F^8 and pH 7.0 samples after 8 hr. The deacylation ranged from 58% at 25 °C for Phe-tRNA, to 12% at 6 °C for Val-$tRNA_1^{Val}$-F^8 incubations.

E. Fluorescence Measurements

All fluorescence measurements were made using a Spex Fluorolog spectrofluorimeter interfaced either to a Tektronix 31 programmable calculator (Adkins et al., 1983), or to an Apple II Plus microcomputer. The band-pass was usually 10 nm on both excitation and emission. Slits

were kept closed except during scans to avoid photodegradation of the sample. Temperature control was maintained with a Lauda K2R circulating bath attached to the four-position cell holder. Temperatures in the sample cells, determined using a temperature probe (Fisher Scientific) in a cell containing only solvent, were between 5 and 7 ^{o}C during all experiments, unless specified otherwise. The cell holder compartment was flushed throughout each experiment with a steady stream of N_2 in order to prevent condensation on the faces of the cuvettes.

All samples were excited at 480 nm. The absorbance of the samples at 480 nm was less than 0.001, so no corrections in the fluorescence emission intensities for inner filter effects were necessary. Spectra were obtained by measuring 1 nm increments, typically at an integration time of 2 seconds. Emission intensity was quantified by integration of the uncorrected fluorescence signal from 500-600 nm. A minimum of two emission scans were done at each titration point, and fewer than 5% of the duplicate emission intensities differed from their average by more than 0.5%. In all experiments, the background signal due to solvent was subtracted, and all data were corrected for dilution due to the addition of titrant.

In order to monitor the stability of the instrument, the emission intensity of a 8 nM solution of disodium fluorescein in 0.1 N KOH was measured prior to each set of sample scans during a titration. In 52 separate experiments of 3-9 h duration, individual measurements did not differ more than 1.2% from the mean for that experiment, and most were within 0.6% of the mean value. Hence, the lamp intensity was essentially constant during each experiment.

F. Titration Procedures

All titrations used the following procedures unless specified otherwise. Prior to a titration, EF-Tu was incubated with pyruvate kinase and PEP in buffer A or B at 37 °C for 20 min to convert all of the GDP to GTP and thereby ensure that all of the EF-Tu was bound to GTP. This EF-Tu*GTP stock solution was then kept on ice, or at the temperature of the sample cells, during the course of the titration.

Samples were prepared without EF-Tu directly in 1x1 cm quartz fluorescence cuvettes. All samples (3.0 mL) contained 10 μM GTP, 135-168 μg pyruvate kinase (Sigma), 1 mM PEP and usually 0.01 A_{260} units of [^{14}C]Phe-tRNA^{Phe}-F^{8} (900-1080 pmol Phe/A_{260} unit tRNA; 405-450 Ci/mol Phe) in buffer A or B.[2] Thus the concentration of Phe-tRNA^{Phe}-F^{8} in the samples typically ranged from 2.2 to 4.6 nM. A teflon-coated magnetic stirrer was added to each cuvette to permit mixing without removal of the cuvette from the cell holder; this prevented any spectral fluctuations due to temperature changes in the sample. The initial fluorescence emission intensity of each sample, F_o, was determined by averaging a minimum of four separate scans. The initial scans sometimes showed a monotonic increase in emission intensity. In those cases, scans were repeated until a constant emission was observed over six scans. Typically, a stable F_o was established within two hours. However, in a few cases, as much as 3.3 hours were required to obtain a

---

[2]The buffer B used in the experiments described in this dissertation differs from the polymix used by Jelenc and Kurland (1979) for the optimal translation assay system in pH, in the GTP and PEP concentrations (0.5 mM vs. 10 μM, and 6 mM vs. 1 mM respectively for Jelenc and Kurland's and my experiments), and in lacking ATP.

stable fluorescence signal. Robertson and Wintermeyer (1981) also observed that a pre-incubation of fluorescent tRNA samples was necessary in their experiments.

Following the determination of F_o, two 250 or 300 µL aliquots from each sample were assayed for acid-insoluble radioactivity to establish the initial concentration of aa-tRNA. GDP-binding to the EF-Tu in the stock solution was also measured at this time using filter assays.

Titrations were performed by one of two methods. In the first method, aa-tRNA was titrated with an EF-Tu stock solution containing PEP and pyruvate kinase (see above). In order to span a wider range of EF-Tu*GTP concentrations in a titration, this method was varied for some experiments. A portion of the EF-Tu stock solution was diluted 16-fold in the buffer for that experiment (including the GTP, PEP, and pyruvate kinase) after the 37 ^{o}C incubation. This diluted stock solution was only used for the initial titration points.

The second method was used when the Phe-$tRNA^{Phe}$-F^{8}*EF-Tu*GTP ternary complex was titrated with a competing tRNA species. In these experiments, the samples initially contained 3.2 to 3.6 nM[^{14}C] Phe-$tRNA^{Phe}$-F^{8} in buffer B. After obtaining an F_o and removing aliquots to assay for acid-insoluble radioactivity, a small aliquot of EF-Tu*GTP in buffer B was added to the cuvette, to give a final concentration of 6.9 nM. Three or four sets of duplicate scans were taken as above to ensure attainment of equilibrium. The samples in the cuvettes were then titrated with the competing tRNA.

Titrations were accomplished by the sequential addition of the titrant solution (in volumes ranging from 1 to 250 µL) to the samples in the cuvettes. After each addition, the solution was gently stirred for

1 min. Emission scans were not initiated until seven minutes later in order to ensure complete equilibration and to permit the evaporation of any condensation on the cuvettes. This procedure usually resulted in an interval of 16 to 18 min between successive pairs of scans. After the final addition of EF-Tu*GTP, 3 to 5 sets of duplicate scans were taken at 8 minute intervals in order to ensure attainment of equilibrium.

At the end of each experiment, three or four 400 μL aliquots of each sample were assayed for cold acid-insoluble radioactivity. In addition, three 400 μL aliquots of each sample were usually assayed for total radioactivity in the Triton X-100-containing scintillation cocktail. The Triton assays served to verify the amount of the aa-tRNA initially added to the solution. The GDP-binding activity of the EF-Tu in the stock solution was also measured by filter binding assay. The total volume of titrant added to a sample during a titration did not exceed 12% of the original sample volume (2.4 or 2.5 mL), except in the experiments at higher temperatures or high ionic strength, where a greater [EF-Tu] was required for saturation of binding.

Titrations of Val-$tRNA_1^{Val}$-F^8 were carried out as above, except that they initially contained from 6.1 to 7.4 nM [^{14}C]Val-$tRNA_1^{Val}$-F^8 (790 pmol Val/A_{260} unit tRNA; 240 Ci/mol Val).

G. Ionic Strength Dependence of K_d

The dependence of K_d on the ionic strength was determined in titrations as described above using [^{14}C]Phe-$tRNA^{Phe}$-F^8 in buffer A containing 50, 120, 300, 550, or 1000 mM KCl instead of 50 mM NH_4Cl. In each case, fewer titration points were used in order to minimize the

duration of the experiment and thus the deacylation of the Phe-tRNA^{Phe}-F^{8}.

H. Determination of K_d Values for Fluorescent aa-tRNAs

In any sample, the total observed fluorescence emission intensity (F) is given by

$$F = R_u E_u + R_f E_f + R_b E_b \quad , \qquad (1)$$

where R is the concentration, and E is the fluorescence intensity per molecule, of unacylated tRNA^{Phe}-F^{8} (u), free Phe-tRNA^{Phe}-F^{8} (f), and Phe-tRNA^{Phe}-F^{8} bound to EF-Tu*GTP (b). Since the aminoacylation of tRNA^{Phe}-F^{8} does not change its emission intensity (Adkins et al, 1983), $E_u = E_f$. In the absence of EF-Tu*GTP, the fluorescence intensity, F_o, equals $R_t E_f$, where R_t is the total concentration of tRNA^{Phe}-F^{8} ($R_u + R_f + R_b$). When EF-Tu*GTP is in excess, so that all Phe-tRNA^{Phe}-F^{8} is in a ternary complex, the observed emission intensity is at a maximum and the relative fluorescence emission intensity (F/F_o) is given by

$$(F/F_o)_{max} = \frac{(R_b E_b + R_u E_f)}{R_t E_f} \quad . \qquad (2)$$

Rearrangement of equation 2 yields

$$\frac{E_b}{E_f} = \frac{(F/F_o)_{max} + y - 1}{y} \quad , \qquad (3)$$

where $y = R_a/R_t$ and $R_a = R_f + R_b$. E_b/E_f was determined for each experiment using equation 3. The same equations were used to analyze the

Val-$tRNA_1^{Val}$-F^8 titrations.

The K_a for the association of EF-Tu with GTP is 2.5×10^6 M^{-1} (Arai et al., 1974). Since incubations always included 10 μM GTP, essentially all of the EF-Tu present was associated with GTP. Hence, the dissociation of the ternary complex is given by

$$\text{aa-tRNA*EF-Tu*GTP} \rightleftharpoons \text{aa-tRNA} + \text{EF-Tu*GTP}, \qquad (4)$$

and this equilibrium is described by the following equation:

$$K_d = \frac{[\text{aa-tRNA}][\text{EF-Tu*GTP}]}{[\text{aa-tRNA*EF-Tu*GTP}]} = \frac{R_f(T_t - R_b)}{R_b}, \qquad (5)$$

where the concentration of the free EF-Tu*GTP (T_f) is given by the difference between the total EF-Tu*GTP concentration (T_t) and the concentration of EF-Tu*GTP bound in the ternary complex ($T_b = R_b$). Combining equations 1 and 5 yields an expression for the relative fluorescence intensity in terms of the experimentally-determined parameters (R_t, R_a, T_t, E_b/E_f) and the unknown, K_d:

$$F/F_o = 1 + \frac{[(E_b/E_f)-1]}{2R_t}\{(R_a+T_t+K_d)-[(R_a+T_t+K_d)^2-4R_aT_t]^{1/2}\}. \qquad (6)$$

Values of K_d were obtained by performing a nonlinear least squares fit of the data from individual fluorescence experiments to equation 6 using the NLIN procedure of SAS (Statistical Analysis System, SAS Institute, Inc., Cary, NC). A sample of the actual programs written for use with NLIN on an IBM 3081 is found in Appendix A. For this analysis, the intercept of one (equation 6) was considered a variable since the initial fluorescence measurement does have uncertainty associated with

it (see Chapter III, Section M). The intercept was initially set to 1. The best-fit value of this initial fluorescence measurement ranged from 0.993 to 1.002 for the four sets of data in Table II. Initial estimates for K_d were calculated from the individual data points for each experiment using a BASIC program written for an Apple II Plus microcomputer (see Appendix B). This program calculates a K_d for each point in the titration from the fluorescence change and an approximation of the value of E_b/E_f for that particular experiment. This procedure neglected the deacylation of the aa-tRNA, since it was only used to obtain K_d estimates (see discussion of deacylation of aa-tRNA below). Each K_d value reported in Tables II and III was obtained from a nonlinear least squares analysis of a data set that included all of the data points collected in titrations of a particular type.

The best-fit K_d values returned by NLIN were reported with symmetric, asymptotic 95% confidence intervals. As pointed out by Johnson and Frasier (1984), such confidence limits can be seriously misleading. Therefore, the 67% confidence intervals were obtained by searching the parameter space for the variance ratios predicted by the F-statistic (Johnson et al., 1981; Johnson, 1983; Johnson and Frasier, 1984). The programs used in determining the 67% confidence intervals are listed and described in Appendix C. These 67% confidence intervals were frequently asymmetric and larger than the 95% confidence intervals returned by NLIN. Tests for goodness-of-fit were done as described by Johnson et al. (1981). The residuals of the nonlinear fit, examined both as a function of F/F_o and as a function of T_t, were scrutinized for systematic deviations graphically and by fitting to polynomials to the third degree.

Neglecting the deacylation of the aa-tRNA during the experiment was found to result both in significant systematic deviations in the residuals of the fit and in broader confidence intervals for K_d. Hence, the effect of deacylation on the total concentration of aa-tRNA (R_a) was taken into account at each titration point (i) using

$$R_{ai} = R_{bi-1} + [R_{ai-1} - R_{bi-1}]e^{-k\Delta t}, \qquad (7)$$

where Δt is the time between titration points i-1 and i. In this model, only the free aa-tRNA deacylates. R_b was calculated using the best estimate of K_d from previous iterations with NLIN, and the rate constant k was determined from deacylation assays (see Section D above). All K_d values at 6 ^{o}C reported here were obtained using the deacylation rates listed in Table I. The expression in equation 7 was found to yield values for R_{ai} which were consistent with aa-tRNA concentrations calculated from the acid insoluble radioactivity determined at the ends of experiments.

I. Competition Experiments

Experiments to determine the affinity of a second tRNA species for EF-Tu were based on its ability to compete with Phe-$tRNA^{Phe}$-F^8 for binding to EF-Tu, and two different methods were used. In the first method, samples initially contained 2.8-4.0 nM [^{14}C]Phe-$tRNA^{Phe}$-F^8 in buffer A or B and either [^{3}H]Phe-$tRNA^{Phe}$, [^{3}H]Lys-$tRNA^{Lys}$, or yeast [^{3}H]Phe-$tRNA^{Phe}$ at concentrations between 3.9 and 14.8 nM. Those experiments using Val-$tRNA_1^{Val}$-F^8 initially contained 5.5-5.6 nM [^{14}C]Val-$tRNA_1^{Val}$-F^8 and 4.4-4.8 nM [^{3}H]Phe-$tRNA^{Phe}$ in buffer A.

Table I

DEACYLATION RATE CONSTANTS FOR AMINOACYL-tRNAS[a]

aa-tRNA	Buffer	Temperature	k (min^{-1})[b]
Phe-tRNA[c]	A	6 °C	1.1×10^{-3}
Phe-tRNA	A, pH 7.0	6 °C	3.0×10^{-4}
Phe-tRNA	B	6 °C	3.0×10^{-4}
Lys-tRNA[d]	B	6 °C	3.0×10^{-4}
Val-$tRNA_1^{Val}$-F[8]	A	6 °C	2.2×10^{-4}
Phe-tRNA	A	15 °C	2.5×10^{-3}
Phe-tRNA	A	25 °C	7.2×10^{-3}

[a] Experimental details are described in Chapter II, Section D.

[b] The rate constants were calculated assuming a first-order decay process, using the relationship:

$$k = \frac{-\ln(c/c_o)}{t}$$

where c_o and c represent the amounts of acid insoluble radioactivity at two assay times (c is from the later assay), and t is the time (min) between these assays.

[c] Unfractionated tRNA aminoacylated using only phenylalanine.

[d] Unfractionated tRNA aminoacylated using only lysine.

Titrations with EF-Tu*GTP were carried out as described above. In general, fewer titration points were used in the competition experiments than in the experiments using only one tRNA species, to avoid the greater amounts of deacylation anticipated when two aa-tRNA species were competing for binding to the EF-Tu. The data from this type of competition experiment was used for determining dissociation constants using the nonlinear least squares analysis (see Section J below).

Other competition experiments were carried out by forming a ternary complex with Phe-$tRNA^{Phe}$-F^8 and EF-Tu*GTP first, and then titrating with a second tRNA competitor species. Samples were prepared containing 3.2 to 3.6 nM [^{14}C]Phe-$tRNA^{Phe}$-F^8 in buffer B. For the titrant, f-[^{3}H]Met-$tRNA_f^{Met}$ or unfractionated tRNA, either unacylated or aminoacylated with a mixture of all 20 amino acids (totally aminoacylated tRNA), was used. When very concentrated tRNA solutions were required to reach high concentrations at the end of a titration, rather than diluting the tRNA in buffer B, undiluted tRNA stock solutions were used. Therefore, as a control, in each case a second identically prepared cuvette was titrated with only the buffer in which the titrant tRNA was stored, either H_2O or 5 mM $MgCl_2$.

J. Determination of K_d Values for Unmodified Non-Fluorescent tRNAs

Since fluorescence changes are associated only with Phe-$tRNA^{Phe}$-F^8 binding to EF-Tu*GTP, the expression relating the relative emission intensity to the concentration of Phe-$tRNA^{Phe}$-F^8 in the ternary complex is the same whether or not non-fluorescent aa-tRNA is also present in the sample. From equations 1, 2, and 3, this expression is:

$$F/F_o = 1 + [(E_b/E_f)-1](R_b/R_t). \quad (8)$$

When a sample contains two different aa-tRNA species, R_b at a particular T_t value will depend upon the concentration of the competing aa-tRNA and its affinity for EF-Tu*GTP, since the following two equilibria must hold simultaneously:

$$K_{dR} = \frac{R_f T_f}{R_b}, \quad (9a)$$

and

$$K_{dS} = \frac{S_f T_f}{S_b}, \quad (9b)$$

where R refers to the fluorescent aa-tRNA and S to the non-fluorescent aa-tRNA. Since K_{dR} is determined in the single component titration experiments, and since:

$$T_f = T_t - S_b - R_b, \quad (10)$$

one can derive an equation that relates the amount of bound fluorescent aa-tRNA (R_b) to the experimentally determined quantities (T_t, R_t, R_a, S_t, S_a, and K_{dR}) and the single unknown, K_{dS}:

$$(K_{dR}-K_{dS})R_b^3 + (T_tK_{dS}+2R_aK_{dS}+K_{dR}K_{dS}-R_aK_{dR}+S_aK_{dR}-T_tK_{dR}-K_{dR2})R_b^2 +$$

$$(R_aT_tK_{dR}-R_aS_aK_{dR}-2R_aT_tK_{dS}-R_a^2K_{dS}-R_aK_{dR}K_{dS})R_b + K_{dS}R_a^2T_t = 0 \quad (11)$$

The solutions to this equation are three real, unequal roots, and an algorithm was used to select the correct non-negative root which was within the range of the possible concentrations for R_b. Nonlinear least

squares analyses were then performed to fit equation 8 with convergence on the values of K_{dS} and the intercept as described above. A listing of a representative program which was used for this analysis is given in Appendix D. In these experiments, the best-fit intercepts ranged from 1.02 to 1.07. The deacylation of each aa-tRNA was included in the analysis, as detailed earlier. The confidence intervals and the goodness-of-fit were also determined as above (see Section H).

In the experiments where Phe-$tRNA^{Phe}$-F^8*EF-Tu*GTP was titrated with tRNA, the same expression relating the relative emission intensity to the concentration of Phe-$tRNA^{Phe}$-F^8 in a ternary complex is still valid (equation 8). For these titrations, the concentration of ternary-complex bound Phe-$tRNA^{Phe}$-F^8 (R_b=T_b) at each titration point was calculated from equation 8 using experimentally determined values for F/F_o and R_t, and the average E_b/E_f value for buffer B, 1.55 (see Table II). T_f can be obtained from equation 9a, since R_f is given by R_a-R_b, and K_{dR} was experimentally determined from single component titrations. S_f is calculated from S_b (= T_t-R_b-T_f; see equation 10) and S_a, since S_f=S_a-S_b. Thus, K_{dS}, the K_d for the second tRNA species, is calculated from equation 9b. K_d values were calculated at each point using a BASIC program written for an Apple II Plus microcomputer (see Appendix E for program listing). Since there was an excess of tRNAs over EF-Tu in these experiments, the concentration of Phe-$tRNA^{Phe}$-F^8 was corrected for deacylation using the expression in equation 7. The results of these experiments were not analyzed by nonlinear least squares, because there were not sufficient data to perform a statistically significant analysis.

K. Titration of $tRNA^{Phe}$-F^8 with EF-Tu*GTP

$tRNA^{Phe}$-F^8 was titrated with EF-Tu*GTP to determine the affinity of EF-Tu*GTP for this modified tRNA relative to its aminoacyl form, Phe-$tRNA^{Phe}$-F^8. A sample initially contained 9.86×10^{-7} M $tRNA^{Phe}$-F^8 in buffer B. The absorbance of the sample at 480 nm was about 0.05, high enough to exhibit a small inner filter effect (5%). However, the absorbance of the sample was approximately constant throughout the experiment, so the inner filter effects were constant and could be neglected. The EF-Tu*GTP stock solution was prepared as described above, except that the GTP concentration was increased to 1 mM. Titrations were carried out as described in Section F, using a 5 nm bandpass on both excitation and emission, except that no assays for cold acid insoluble radioactivity were required. For each titration point, two pairs of emission scans were done, with stirring of the sample and an additional delay (as though for an addition) between the pairs of scans.

The dissociation constant for the complex of $tRNA^{Phe}$-F^8 with EF-Tu*GTP was calculated for each point in a titration using the BASIC program listed in Appendix B.

CHAPTER III

RESULTS

A. Fluorescence-detected Ternary Complex Formation

The addition of EF-Tu*GTP to a solution of Phe-tRNA^{Phe}-F^{8} caused a substantial increase in its fluorescence emission intensity (Figure 6). This enhancement resulted from the association of EF-Tu*GTP with Phe-tRNA^{Phe}-F^{8} and a subsequent EF-Tu*GTP-induced conformational change in the aa-tRNA near the s^{4}U-8 base (Adkins, et al., 1983).

The extent of this emission intensity increase was solvent dependent. The largest fluorescence change was observed in buffer B, where it averaged 55%. The fluorescence change was 36% in buffer A, and 28% in the Hepes-containing buffer (pH 8.0) reported by Adkins, et al. (1983). To identify the source of these differences, the EF-Tu*GTP-dependent fluorescence change of Phe-tRNA^{Phe}-F^{8} was examined in a buffer A solution which had been adjusted to pH 7.0. The size of this fluorescence increase was found to be the same as in buffer B (see Table II). These results suggest that the magnitude of the observed fluorescence change is primarily pH-, rather than buffer-, dependent, and decreases with increasing pH.

The EF-Tu*GTP-induced increase in fluorescence emission intensity

Figure 6: Fluorescence change upon ternary complex formation. Uncorrected emission spectra for Phe-$tRNA^{Phe}$-F^8 in buffer B (polymix) before (——) and after (- - -) the addition of excess EF-Tu*GTP. The emission intensity of the Phe-$tRNA^{Phe}$-F^8 in the sample prior to EF-Tu addition was arbitrarily defined to be 1.0. Since the addition of EF-Tu*GTP does not alter the emission of $tRNA^{Phe}$-F^8 (see Figure 8), its contribution to the fluorescence signal has been subtracted.

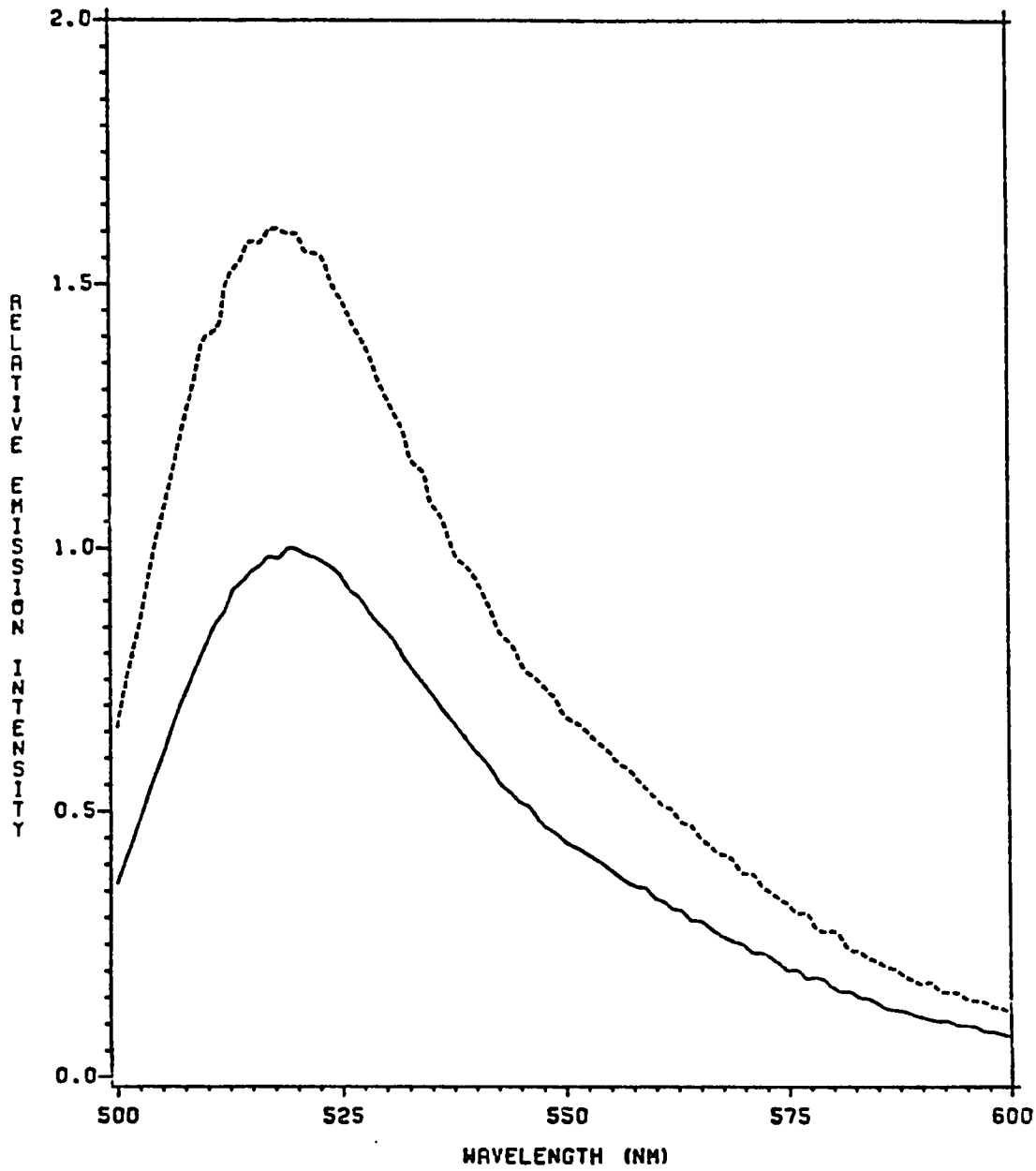

2.0
1.5
1.0
0.5
0.0
RELATIVE EMISSION INTENSITY
500
525
550
575
600
WAVELENGTH (NM)

Table II

ASSOCIATION OF FLUORESCENT-LABELED AA-tRNA WITH EF-Tu*GTP[a]

aa-tRNA	Buffer	Expts	$\frac{E_b}{E_f}$[b]	K_d, nM[c]
Phe-tRNA^{Phe}-F^8	A	4	1.36 (1.29-1.42)	0.85 (0.31-0.97) [0.49-1.21]
Phe-tRNA^{Phe}-F^8	A (pH 7.0)	2	1.55	1.2 (0.77-1.8) [0.89-1.5]
Phe-tRNA^{Phe}-F^8	B	13	1.55 (1.47-1.62)	4.7 (3.6-6.2) [4.2-5.2]
Val-tRNA$_1^{Val}$-F^8	A	4	1.69 (1.63-1.79)	4.3 (2.8-6.5) [3.4-5.2]

(a) Experimental details are given in Chapter II, Section F.

(b) Average value of E_b/E_f; range of values obtained is shown in parentheses.

(c) Best-fit K_d returned by the nonlinear least squares analysis of all of the titration data. The values in parentheses indicate the 67% confidence interval. The values in brackets indicate the 95% confidence interval returned by NLIN (see Chapter II, Section H).

for Val-tRNA$_1^{Val}$-F^8 was larger than that observed for Phe-tRNA^{Phe}-F^8 in the same buffer (A). This suggests that the conformation of the Val-tRNA$_1^{Val}$-F^8 differs from that of the Phe-tRNA^{Phe}-F^8. Also, it is interesting to note that the fluorescence emission intensity per mole of free Val-tRNA$_1^{Val}$-F^8 was less than that for free Phe-tRNA^{Phe}-F^8, both in the presence and the absence of EF-Tu*GTP.

No changes in spectral shape upon ternary complex formation were observed in either buffer A or buffer B.

B. Titration of Fluorescent-labeled aa-tRNA with EF-Tu*GTP

In order to determine the affinity of EF-Tu*GTP for Phe-tRNA^{Phe}-F^8, the concentration dependence of the association of EF-Tu*GTP with Phe-tRNA^{Phe}-F^8 was determined. The formation of the ternary complex was monitored by the change in fluorescence, and, as expected, the emission intensity reached a maximum when sufficient EF-Tu*GTP had been added (Figure 7). The fluorescence change occurred over a two-log change in EF-Tu*GTP concentration (Figure 8), which indicates that the fluorescence change monitors a single binding event (Klotz, 1982). This conclusion was further supported by the fact that the data were fit successfully to a model that includes only a single binding event. The fluorescence change was reversible upon the addition of an excess of aminoacyl-tRNA (see Section I below).

The formation of EF-Tu*GTP was ensured by including pyruvate kinase, PEP, and 10^{-5}M GTP in both the aa-tRNA- and the EF-Tu-containing solutions. Experiments were done at 6 ^{o}C to reduce the rate of

Figure 7: EF-Tu*GTP dependence of Phe-tRNA^{Phe}-F^{8} fluorescence intensity. The titration initially contained 3.2 nM Phe-tRNA^{Phe}-F^{8} (●) in buffer B at 6 ^{o}C as described in Chapter II, Section F. No fluorescence change was observed when 5.4 nM tRNA^{Phe}-F^{8} was titrated with EF-Tu*GTP (▲). The data in the inset are from the same experiments, but are plotted on a reduced scale in order to demonstrate the saturation of the fluorescence change.

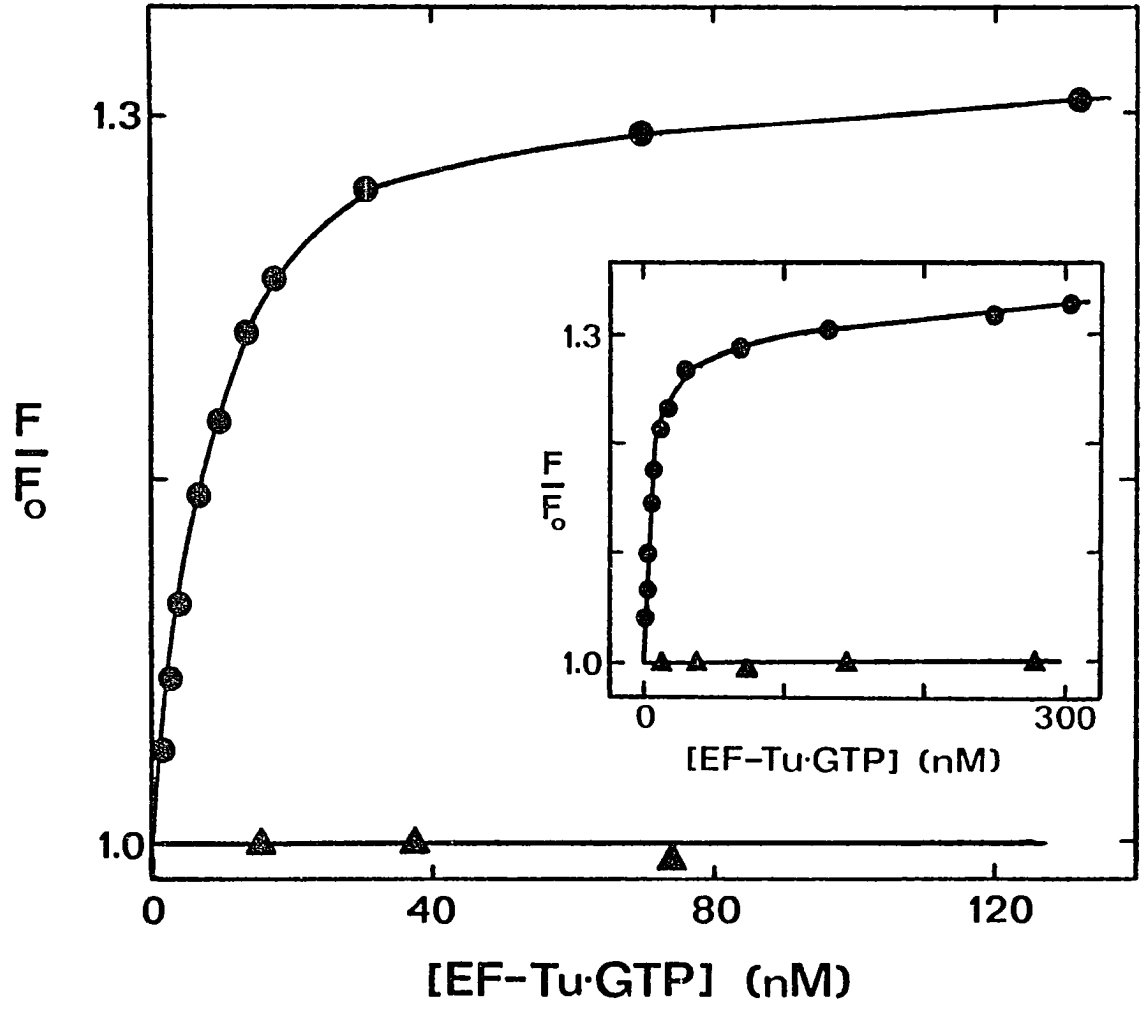
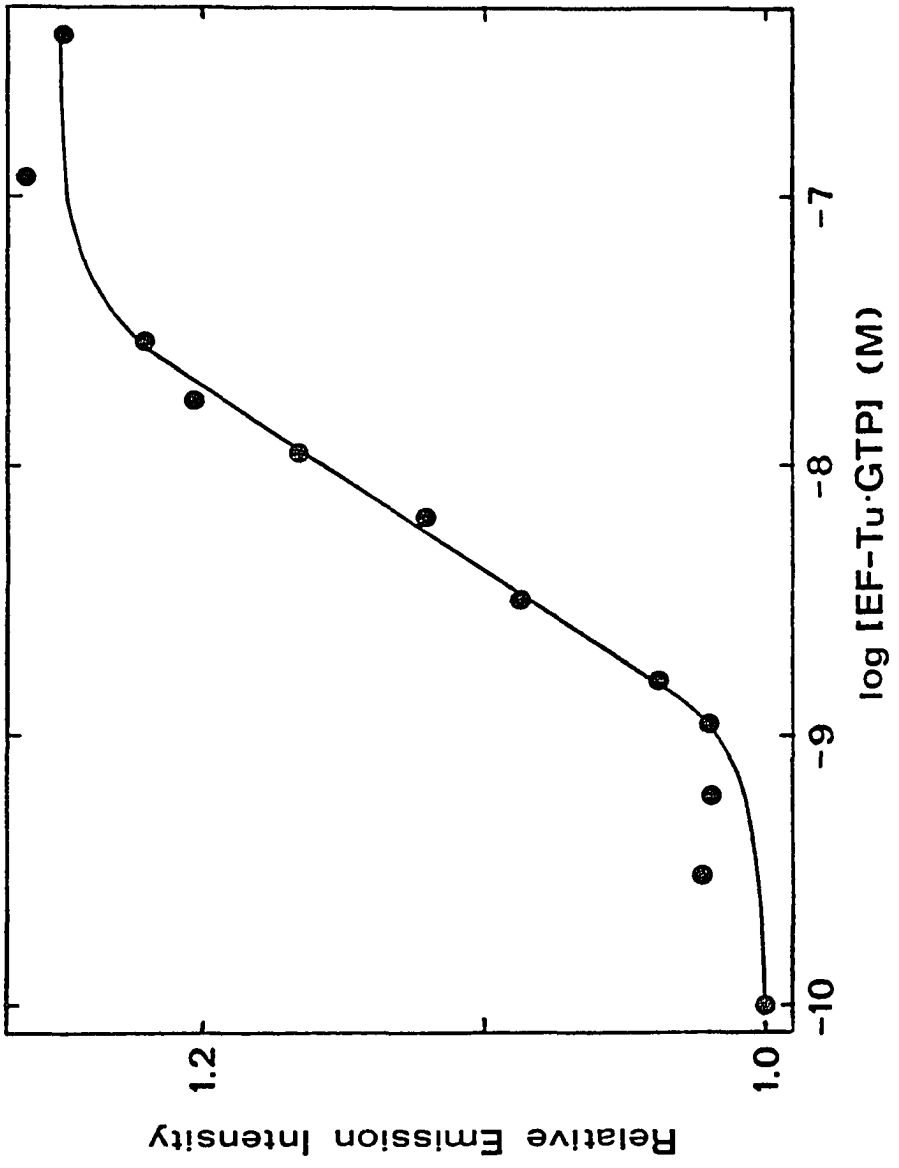

1.3
1.0
F/F0
0
40
80
120
[EF-Tu·GTP] (nM)
1.3
1.0
F/F0
0
300
[EF-Tu·GTP] (nM)

Figure 8: The change in fluorescence for Phe-tRNA^{Phe}-F^{8} occurs within a 2-log change in EF-Tu*GTP concentration. The sample initially contained 2.40 nM Phe-tRNA^{Phe}-F^{8} in buffer B and was titrated as described in Chapter II, Section F. For this experiment, a portion of the EF-Tu*GTP stock solution was diluted 16-fold in buffer B after the 37 ^{o}C incubation, and was used for the initial titration points.


Relative Emission Intensity
1.0
1.2
-10
-9
-8
-7
log [EF-Tu·GTP] (M)

hydrolysis of the aa-tRNA. Although experiments lasted as long as 9 hr, the total deacylation never exceeded 13% at 6 °C, and in nearly all cases was less than 10%. In the experiments at 15 and 25 °C, as well as in the titrations at high ionic strength, the total deacylation was greater. However, the data analysis procedures included corrections for the deacylation in all cases.

Within the concentration ranges used in the ternary complex titrations, no fluorescence change was observed when Phe-$tRNA^{Phe}$-F^8 was titrated with EF-Tu*GDP, or when either $tRNA^{Phe}$-F^8 or $tRNA_1^{Val}$-F^8 was titrated with EF-Tu*GTP (see Figure 7).[3] These results are consistent with those reported by Adkins et al. (1983), and support the conclusion that the change in fluorescence emission intensity is due to the binding of Phe-$tRNA^{Phe}$-F^8 to EF-Tu*GTP in a ternary complex.

The titrations of Val-$tRNA_1^{Val}$-F^8 in buffer A proceeded like those with Phe-$tRNA^{Phe}$-F^8 with respect to the EF-Tu*GTP dependence and the saturability of the fluorescence change. In buffer B, I was unable to obtain a stable initial fluorescence intensity. The fluorescence increase observed was perhaps due to a slow equilibration for the Val-$tRNA_1^{Val}$-F^8 with the polycations in buffer B.

C. Calculation of K_d for Fluorescent-labeled Aminoacyl-tRNAs

The K_d values reported in Table II were obtained by nonlinear least squares analysis of the combined data from all of the titrations of a

---

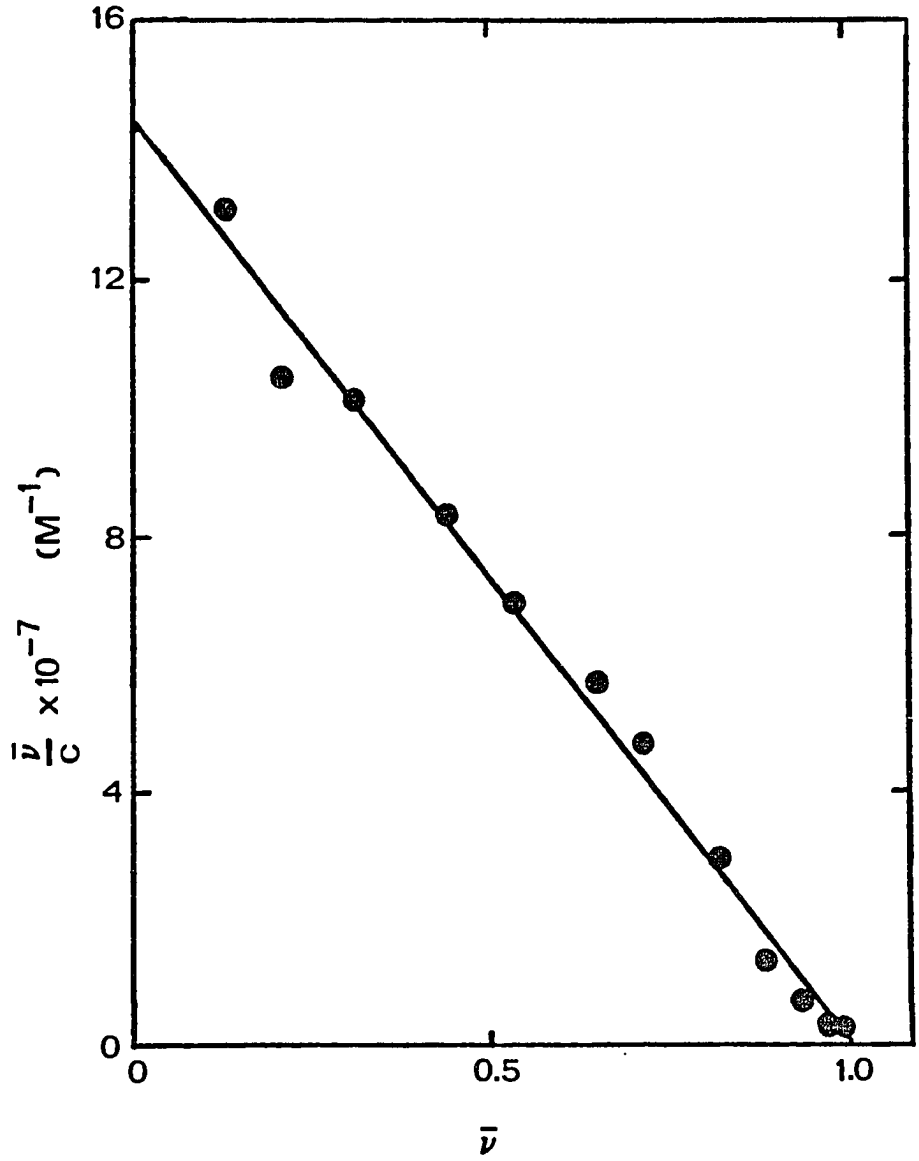
[3]However, a fluorescence change was observed at higher concentrations of $tRNA^{Phe}$-F^8 and EF-Tu*GTP (see Section H below).

particular type, as detailed in Chapter II, Section H. The 67% confidence intervals for these best-fit K_d values determined as described in Chapter II (Section H) and the symmetric, asymptotic 95% confidence intervals from NLIN are also shown in Table II. The lower limits of the 95% confidence intervals from NLIN were sometimes less than zero, especially when individual rather than combined data sets were analyzed. Such unrealistic limits were obtained because the titration data were asymmetrically distributed about the K_d values, with only very little data at concentrations lower than the K_d values.

The values in Table II were obtained using two different preparations of Phe-tRNA^{Phe}-F^8. Dissociation constants calculated from experiments using a higher concentration of Phe-tRNA^{Phe}-F^8 (10.6-13.4 nM) were not significantly different from those using lower concentrations of Phe-tRNA^{Phe}-F^8 (2.2-4.6 nM), and are also included in the average K_d (for buffer B) listed in Table II. These data indicate that the calculated K_d was independent of both the concentration and preparation of the Phe-tRNA^{Phe}-F^8. Similarly, the same K_d was obtained using two different preparations of EF-Tu.

A Scatchard plot of the binding data of Figure 7 is shown in Figure 9. Linear least squares regression analysis of the data from this particular experiment gave n = 1.0 and $K_d = 7.0 \times 10^{-9}$M.

These results demonstrate that EF-Tu*GTP has a very high affinity for aa-tRNA. Whether the K_d values were obtained using NLIN, a BASIC program (Appendix B), or Scatchard analysis, the values were all in reasonable agreement with each other. As noted in Chapter II, Section C, the EF-Tu concentration in these experiments was determined by absorbance. Hence, the K_d values reported here actually constitute the


16
12
8
4
0
0
0.5
1.0
$\frac{\bar{\nu}}{C} \times 10^{-7}$ (M^{-1})
$\bar{\nu}$

maximum values for K_d, since the possibility that a fraction of the EF-Tu was unable to participate in ternary complex formation cannot be ruled out.

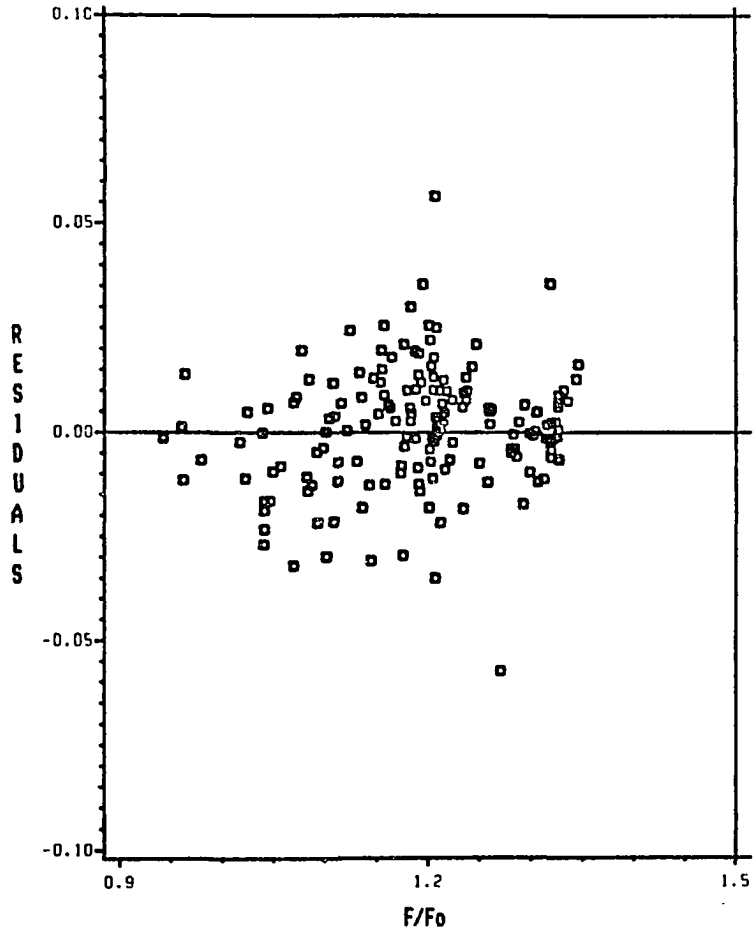
D. Nonlinear Least Squares Analysis of Titration Data

To find the best way to fit titration data using a nonlinear least squares analysis, variations of the model represented in equation 6 (or equation 11 for competition experiments) were tried. Each was assessed in terms of their effects on the best-fit value for K_d and the goodness-of-fit. For example, attempts to converge simultaneously on both K_d and $(F/F_o)_{max}$ or K_d, $(F/F_o)_{max}$, and F_i were unsuccessful due to the very high correlation coefficient for K_d and $(F/F_o)_{max}$.

As noted in Chapter II, Section H, the residuals of the nonlinear fits were examined both as a function of F/F_o and T_t. The graphically analyzed residuals of the fit were found useful in assessing the goodness-of-fit. For example, the residuals obtained from fits of the data both accounting for and neglecting the deacylation of the aa-tRNA (Figures 10 and 11, respectively) were compared. Significant systematic deviations in the residuals of the fit, such as those apparent in Figure 11, were found to result when deacylation was neglected. Thus, the relation given in equation 7 was used for all data analyzed using nonlinear least squares to minimize the systematic deviations in the residuals of the fits.

The sensitivity of the K_d obtained to the value used for the molar absorptivity for the tRNA was examined. The value of $\varepsilon_{260}=6.25 \times 10^5 M^{-1}cm^{-1}$ is equivalent to 1600 pmol tRNA per A_{260}

Figure 10: Residuals of the nonlinear least squares fit of the combined data for titrations of Phe-tRNA^{Phe}-F^{8} with EF-Tu*GTP in buffer B, plotted as a function of F/F_o (left) and T_t (right). As for all data fitted using NLIN, the effects fo deacylation on the concentration of the aa-tRNA was taken into account. Note the lack of systematic deviations in the residuals and the symmetrical distribution of points above and below zero.


0.10
0.05
0.00
-0.05
-0.10
RESIDUALS
0.9
1.2
1.5
F/Fo

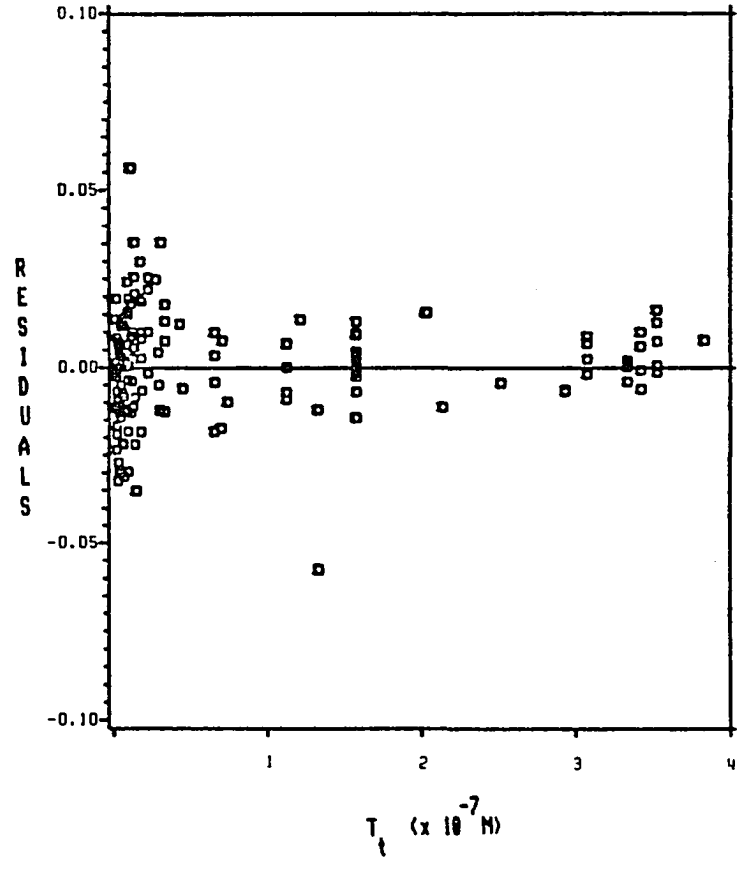
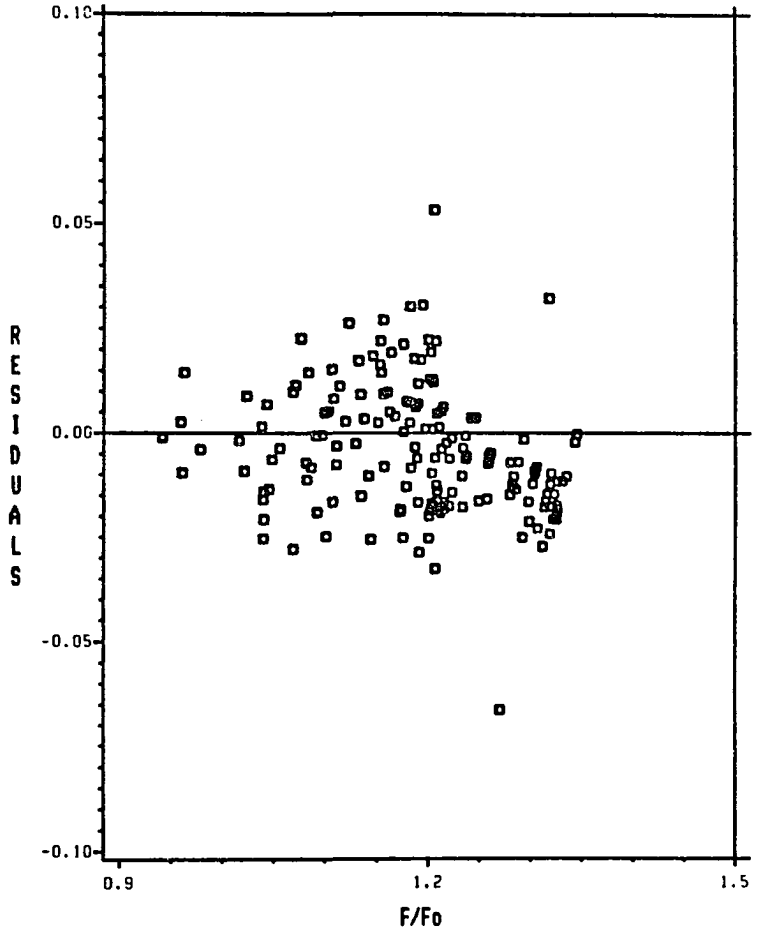
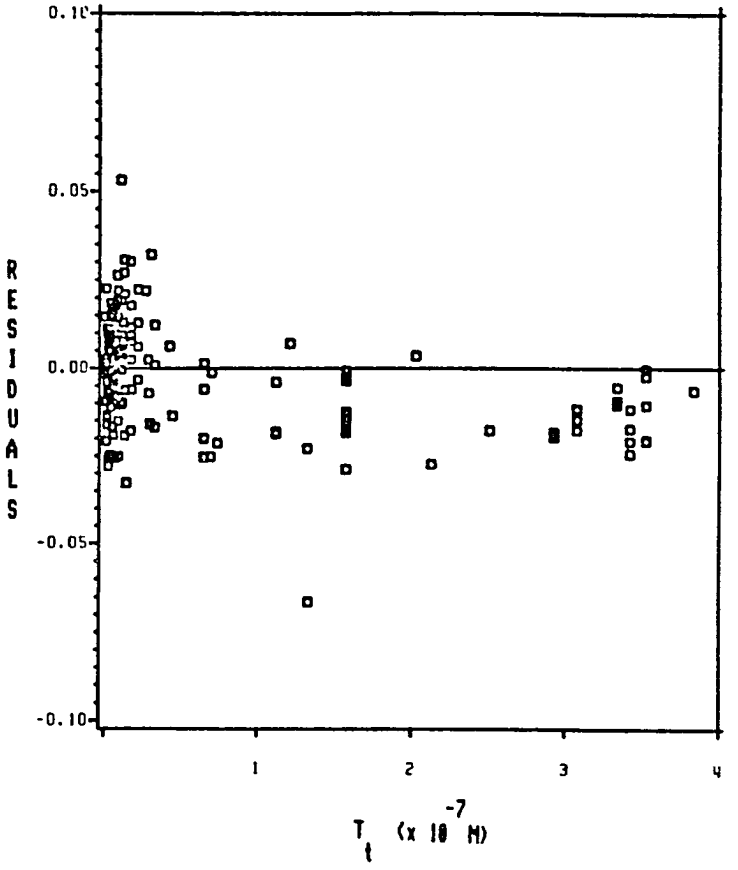

0.10
0.05
0.00
-0.05
-0.10
RESIDUALS
1
2
3
4
T (x 10^-7 M)
t

Figure 11: Residuals of the nonlinear least squares fit of the combined data for titrations of Phe-tRNA^{Phe}-F^{8} with EF-Tu*GTP in buffer B, not corrected for deacylation of the aa-tRNA. Note the pronounced systematic deviations in the residuals plotted as a function of F/F_o (left) and of T_t (right).


0.10
0.05
0.00
-0.05
-0.10
RESIDUALS
0.9
1.2
1.5
F/Fo


0.10
0.05
0.00
-0.05
-0.10
RESIDUALS
1
2
3
4
T (x 10^-7 M)
t

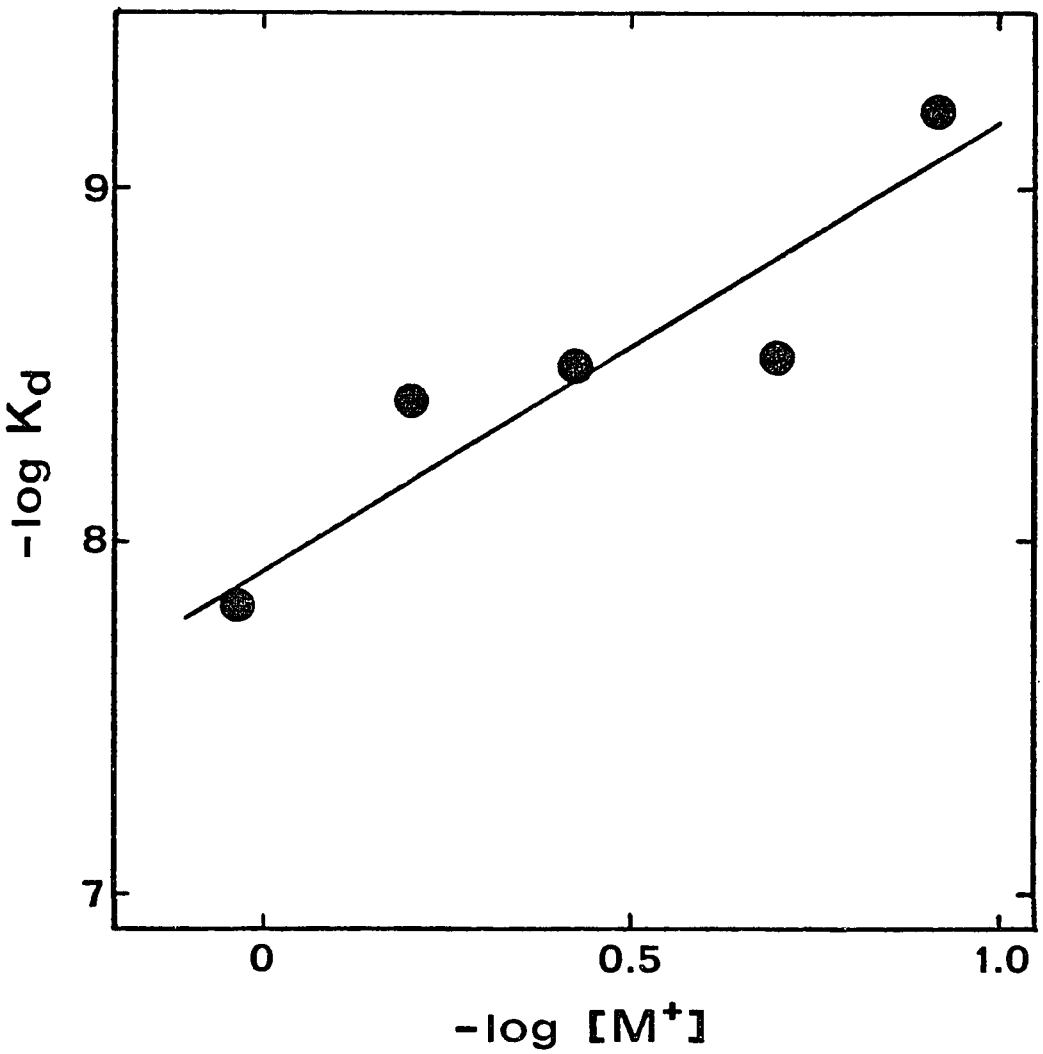
unit. However, purified tRNA preparations aminoacylate to various levels, with the differences presumably being due to impurities of other tRNA species or functionally less-active tRNAs, to differences in molar absorptivity values, to incorrect radioisotope specific activity values (see Section B above), to varying losses during sample preparation, and to synthetase preparations with varying activities. No significant difference in the fitted K_d values was observed with ε_{260} values ranging from 5.86 to 6.64 x $10^5 M^{-1} cm^{-1}$ (corresponding to 1500 to 1700 pmol/A_{260}). Thus, even if the true molar absorptivities for the tRNAs used in any experiment were not in accord with that which was used, no significant affect on the fitted K_d would be anticipated.

E. Ionic Strength Effects

The electrostatic contribution to the interaction between a particular protein and nucleic acid can be evaluated by examining the ionic strength dependence of the K_d (Record et al., 1976, 1978; Lohman et al., 1980). The ionic strength dependence of the ternary complex K_d is shown in Figure 12. The increase in K_d with increasing ionic strength demonstrates that the affinity of EF-Tu*GTP for aa-tRNA does involve ionic interactions. It is also clear that there is a major non-electrostatic component to the binding, since the K_d is quite low even in 1 M KCl (see Record et al., 1976).

Under some circumstances, the number of ion pairs involved in a protein-nucleic acid interaction can be determined using the analysis procedures detailed by Record et al. (1976) and Lohman et al. (1980). If it is assumed that no anions are displaced during the EF-Tu*GTP

Figure 12: Ionic strength dependence of the ternary complex dissociation constant. Titrations were carried out in the presence of 50 to 1000 mM K^+ as described in Chapter II, Section G. $[M^+]$ represents the total concentration of monovalent cations in the samples. Each of the K_d values was obtained from the nonlinear least squares best-fit of the combined data from two or three separate experiments. The straight line was generated by a linear least squares regression analysis of the data.

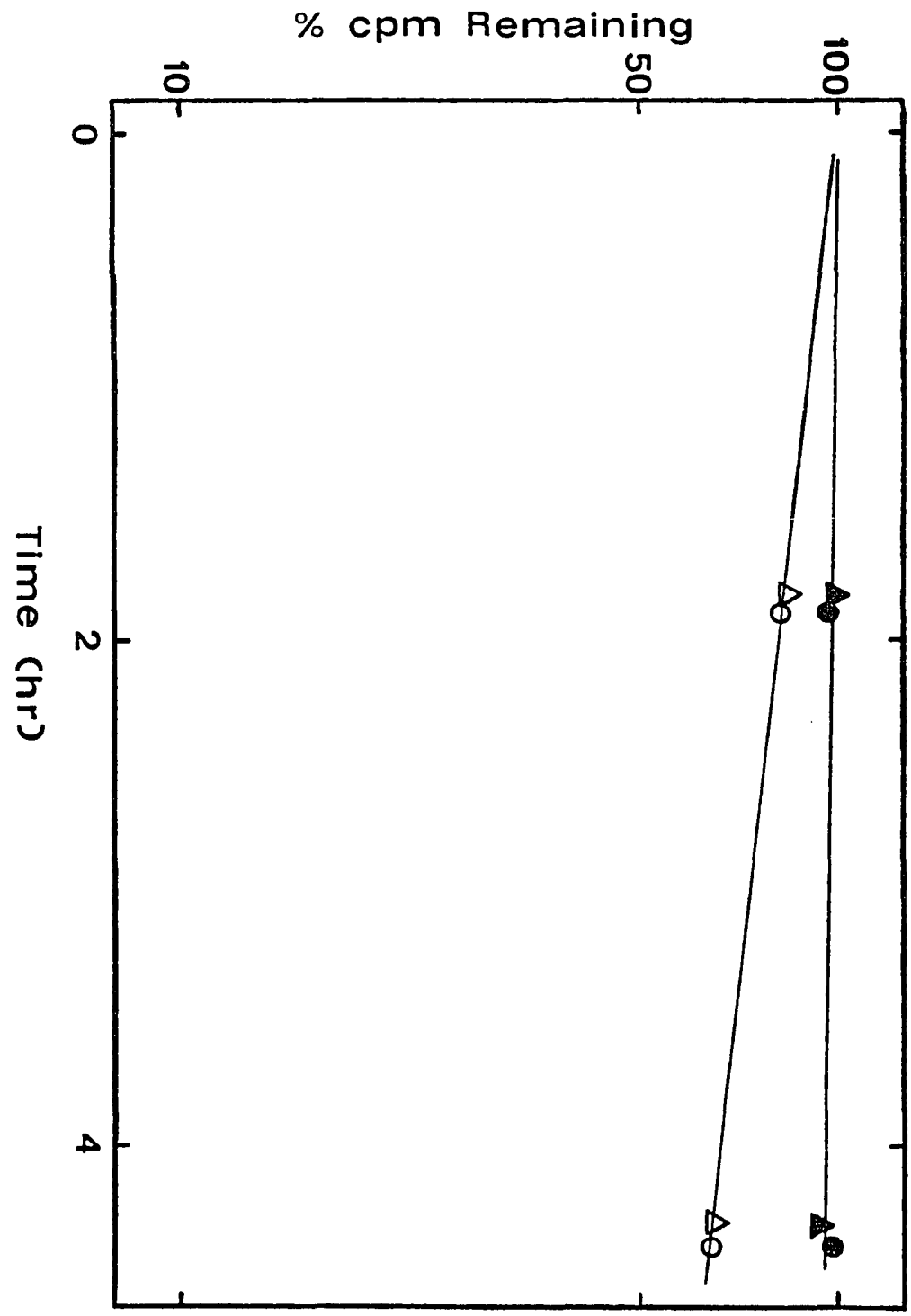

9
8
7
-log K_d
0
0.5
1.0
-log [M^+]

association with aa-tRNA, and that Mg^{2+} effects are limited to electrostatic competition with K^+ and EF-Tu, then, using the results of Lohman et al. (1980), calculations using the data in Figure 12 indicate that there are between 1.4 and 1.9 ion pairs involved in ternary complex formation. The 1.4 value is obtained if one assumes that the protein binds only to double-stranded RNA and that the Ψ value of 0.89 found for poly(rA)*poly(rU) (Record et al., 1976) is appropriate. The 1.9 value is obtained using the Ψ value of 0.68 for single-stranded poly(rU). Unfortunately, it is not known to what extent EF-Tu binds single-stranded and double-stranded regions of the aa-tRNA (see Chapter IV).

The data in Figure 12 indicate the extent of K^+ ion release during ternary complex formation under these conditions (i.e., in the presence of Mg^{2+}). Hence, the number of ion pairs calculated above represents the minimum number of ion pairs involved in ternary complex formation. EF-Tu does not bind GTP in the absence of Mg^{2+} (Ravel and Shorey, 1969; Leupold et al., 1983), thereby precluding a determination of the ionic strength dependence of ternary complex formation in the absence of divalent cations. In addition, numerous studies have shown that the conformation of tRNA is sensitive to $[Mg^{2+}]$ (e.g., Crothers and Cole, 1978), and, consistent with such observations, the fluorescence of $tRNA^{Phe}$-F^8 is dependent upon the Mg^{2+} concentration (see section M below). Thus, the above assumption that the only role of Mg^{2+} is to compete with K^+ and EF-Tu for binding to the tRNA phosphates is probably not justified, and hence the total number of salt bridges between EF-Tu and aa-tRNA cannot be calculated.

The formation of the ternary complex at high ionic strength was confirmed by protection assays which showed an EF-Tu-dependent reduction

Figure 13: Protection of the aminoacyl bond of Phe-tRNA by EF-Tu*GTP from spontaneous hydrolysis in the presence of 1 M KCl. Samples (160 μL) were prepared as described in Chapter II, Section D, with 11.1 pmol [^{14}C]-Phe-tRNA (0.27 A_{260} units), and were incubated at 6 ^{o}C following the addition of 40.9 pmol EF-Tu. Incubations containing EF-Tu (●,▲) showed complete protection of the aminoacyl bond from hydrolysis, while parallel samples lacking EF-Tu (○,△) demonstrated spontaneous hydrolysis. KCl was added to a final concentration of 1 M either before (circles) or after (triangles) the 37 ^{o}C incubation of EF-Tu. Acid-insoluble radioactivity at t = 0 totalled approximately 1450 cpm.


% cpm Remaining
10
50
100
0
2
4
Time (hr)

of aminoacyl ester bond hydrolysis even at 1 M KCl (see Figure 13). It was also important to demonstrate that the presence of 1 M KCl in the samples did not hinder EF-Tu*GTP formation and thereby prevent ternary complex formation. Protection assays were performed in which the KCl was added both before and after the incubation of EF-Tu with pyruvate kinase and PEP at 37 °C, prior to the addition of aa-tRNA and incubation at 6 °C. No difference in protection of the aminoacyl bond was observed in the two samples (see Figure 13).

F. Temperature Dependence of K_d

The ternary complex dissociation constants for Phe-$tRNA^{Phe}$-F^8 in buffer A were determined to be 1.4 nM at 15 °C and 5.4 nM at 25 °C, using the same procedures as described in Chapter II, Section F, except that the time of individual scans was reduced in order to minimize deacylation during the experiment. The best-fit K_d values were obtained as described (Chapter II, Section H) using deacylation rate constants (k) listed in Table I, determined as described in Chapter II, Section D. A van't Hoff plot (ln K_a versus 1/T) of the K_d values at 6, 15, and 25 °C indicates that the ΔH^o of this interaction is -16 kcal/mol of complex.

G. Determination of K_d Values for Unmodified Non-fluorescent Aminoacyl-tRNAs

The affinities of non-fluorescent unmodified aa-tRNAs for EF-Tu*GTP can be determined by their ability to compete with the fluorescent-

labeled aa-tRNAs for binding to the protein. Thus, a mixture of unmodified non-fluorescent aa-tRNA and fluorescent-labeled aa-tRNA was titrated with EF-Tu*GTP. As expected, at the end of the titration, when EF-Tu*GTP was in excess, the total fluorescence change was the same in a sample containing only Phe-tRNA^{Phe}-F^{8} at 3.2 nM as in a sample containing Phe-tRNA^{Phe}-F^{8} at 3.2 nM and Phe-tRNA^{Phe} at 14.8 nM (Figure 14). (The small difference in the total fluorescence change observed in these two samples is due to increased deacylation of Phe-tRNA^{Phe}-F^{8} in the sample containing Phe-tRNA^{Phe}.) However, in the early stages of the titration when EF-Tu*GTP was limiting, a smaller rate of increase in emission intensity was observed in the latter sample due to competition between Phe-tRNA^{Phe}-F^{8} and Phe-tRNA^{Phe} for the available EF-Tu*GTP.

The ternary complex dissociation constants for three unmodified aa-tRNAs under different conditions are listed in Table III, along with the 67% and 95% confidence intervals. These K_d values were obtained by nonlinear least squares analysis of the combined data from all of the titrations with a particular pair of aa-tRNAs, as described in Chapter II, Section J. For all nonlinear least squares analyses, the effects of deacylation on the total concentrations of both aa-tRNAs was taken into account at each point in a titration using the relationship given in equation 7. The same K_d values were obtained when competition experiments used a range of concentrations of the unmodified aa-tRNA (see Chapter II, Section I). The confidence intervals for the titrations in Table III are larger than for the titrations in Table II because fewer data points were used in the analysis of the competition experiments. The larger confidence intervals also reflect the fact that errors in K_{dR} strongly influence the value obtained for K_{dS}. In

Figure 14: Titration of Phe-tRNA^{Phe}-F^{8} with EF-Tu*GTP in the presence or absence of competing Phe-tRNA^{Phe}. One sample (●) initially contained Phe-tRNA^{Phe}-F^{8} (3.2 nM), while the second sample (■) contained both Phe-tRNA^{Phe}-F^{8} (3.2 nM) and Phe-tRNA^{Phe} (14.8 nM). Titrations were performed as described in Chapter II, Section I.

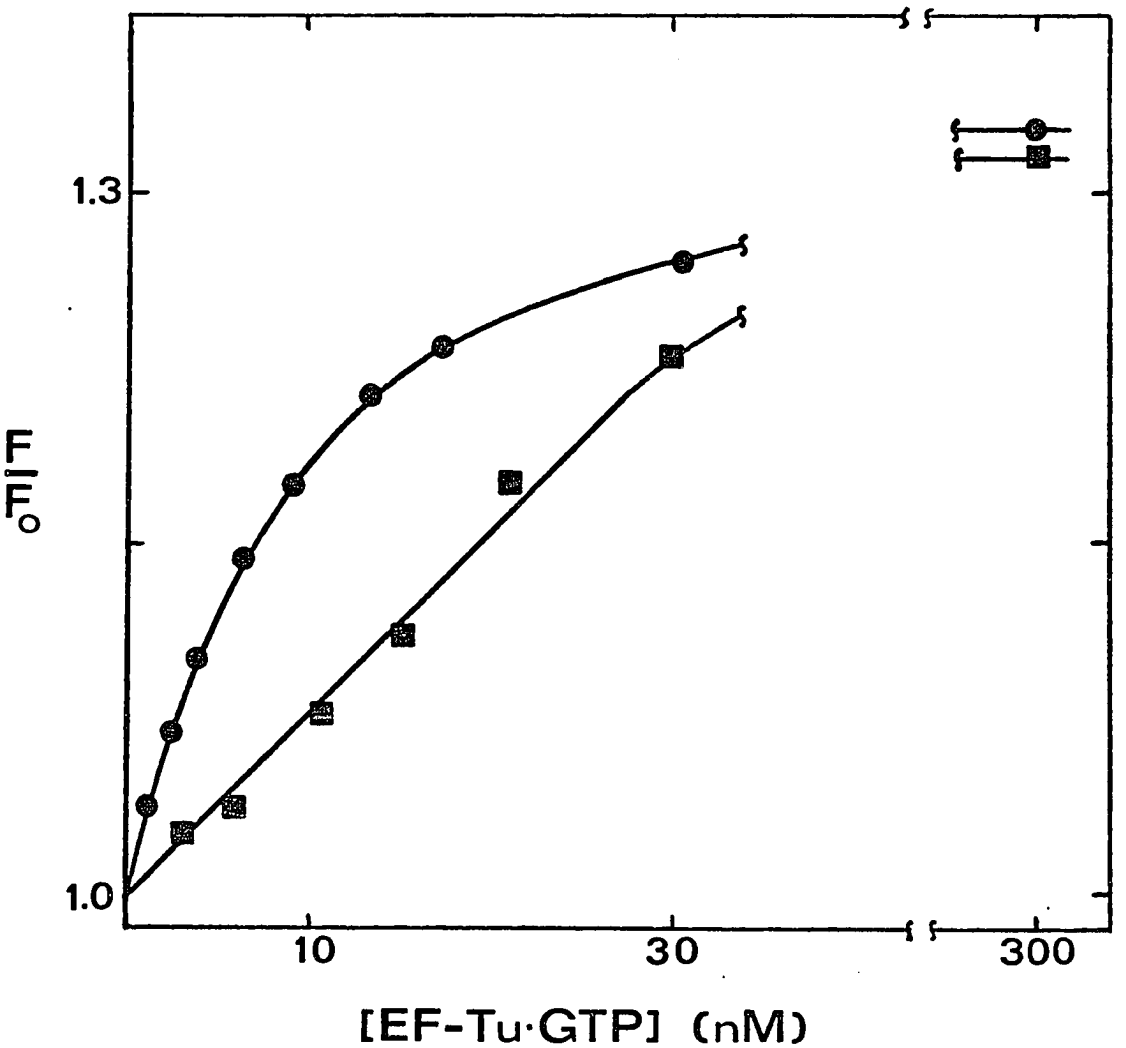

1.3
1.0
F/F0
10
30
300
[EF-Tu·GTP] (nM)

Table III

ASSOCIATION OF UNMODIFIED aa-tRNA WITH EF-Tu•GTP[a]

Unmodified aa-tRNA	aa-tRNA-F	Buffer	Expts	K_{dS}, nM[b]
E. coli Phe-tRNA^{Phe}	Phe-tRNA^{Phe}-F^{8}	B	5	1.16 (0.55-2.3) [0.72-1.6]
Yeast Phe-tRNA^{Phe}	Phe-tRNA^{Phe}-F^{8}	B	3	0.72 (0.27-1.9) [0.29-1.2]
E. coli Lys-tRNA^{Lys}	Phe-tRNA^{Phe}-F^{8}	B	7	7.7 (3.6-14.4) [4.6-10.8]
E. coli Phe-tRNA^{Phe}	Phe-tRNA^{Phe}-F^{8}	A	4	0.10 (0.02-0.26) [0.03-0.16]
E. coli Phe-tRNA^{Phe}	Val-tRNA$_1^{Val}$-F^{8}	A	5	0.28 (0.03-2.75) [-0.95-0.66]

[a] Experimental details are described in Chapter II, Section I.

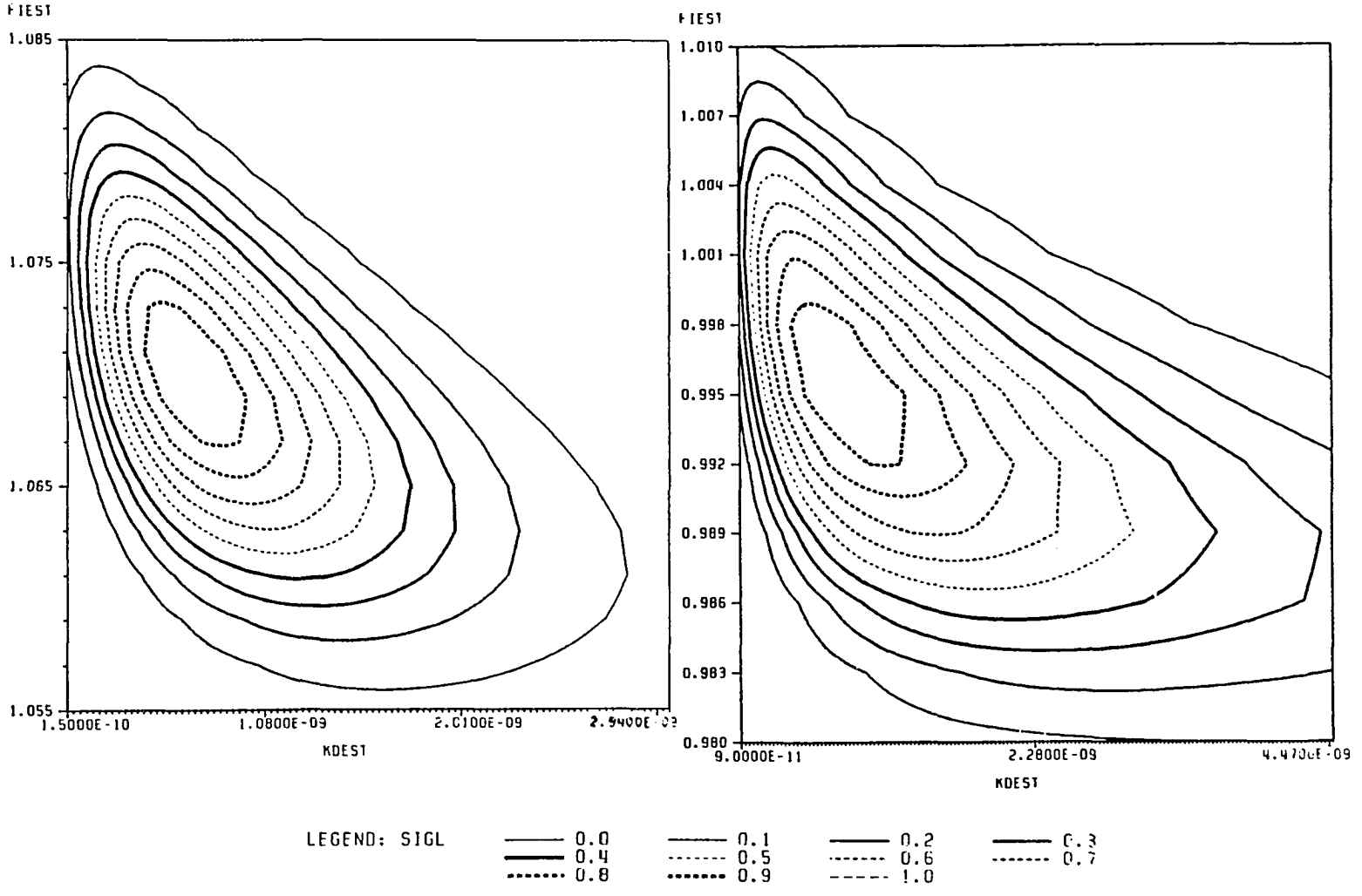
[b] The best fit K_d values for the unmodified aa-tRNAs ($=K_{dS}$) were determined as detailed in Chapter II, Section J, using the K_d values for the fluorescent-labeled aa-tRNAs given in Table II. The values in parentheses indicate the 67% confidence interval. The values in brackets indicate the 95% confidence interval returned by NLIN (see Chapter II, Section H).

addition, because the K_d values were lower than anticipated, the data points were asymmetrically disposed about the K_d; the consequences of such asymmetry are discussed by Johnson and Frasier (1984). As pointed out in Chapter II, Section H, the confidence intervals were frequently asymmetric. The two plots in Figure 15 clearly show the asymmetry of the confidence intervals from two different sets of combined data.

In principle, the K_d value found for a particular unmodified non-fluorescent aa-tRNA should be independent of the nature of the fluorescent-labeled aa-tRNA used in the competition experiments. Since Phe-$tRNA^{Phe}$-F^8 and Val-$tRNA_1^{Val}$-F^8 differ in their affinity for EF-Tu*GTP (Table II), we investigated whether or not competition experiments using these two fluorescent probes would yield the same K_d value for Phe-$tRNA^{Phe}$. As can be seen from the data in Table III, the K_d values obtained for Phe-$tRNA^{Phe}$ using two different spectral probes were very similar. This similarity is particularly noteworthy becuase the value obtained for the K_d of an unmodified aa-tRNA ternary complex is very sensitive to the value used in the calculations for the K_d of the fluorescent aa-tRNA ternary complex. Thus, the K_d values determined using this approach appear to be independent of the spectral probe used in the titration.

Based on the data shown in Tables II and III, Phe-$tRNA^{Phe}$-F^8 has a lower affinity for EF-Tu*GTP than does Phe-$tRNA^{Phe}$. This suggests that the fluorescein dye somehow interferes with the protein-nucleic acid interaction. Such an effect by the dye would have to be allosteric, since EF-Tu does not cover this region of the aa-tRNA when in the ternary complex (Adkins et al., 1983). Conceivably, $tRNA^{Phe}$ which is modified with fluorescein may have a slightly altered conformation

Figure 15: Asymmetry of the confidence intervals for K_d for two sets of combined data. The contour lines represent points of equal significance level (SIGL), as calculated using the program in Appendix C and plotted as a function of both F_i (FIEST) and K_{dS} (KDEST). The range of the 67% confidence interval was obtained from the maximum and minimum values for each variable (KDEST and FIEST) for a significance level of 0.33. Left: confidence intervals obtained for the combined data for EF-Tu*GTP titrations of Phe-tRNA^{Phe}-F^8 and yeast Phe-tRNA^{Phe} in buffer B, using K_{dR} = 4.7 nM and $K_{dS(est)}$ = 0.72 nM. Right: confidence intervals obtained for the combined for EF-Tu*GTP titrations of Val-tRNA$_1^{Val}$-F^8 and *E. coli* Phe-tRNA^{Phe} in buffer A, using K_{dR} = 4.3 nM and $K_{dS(est)}$ = 0.84 nM.

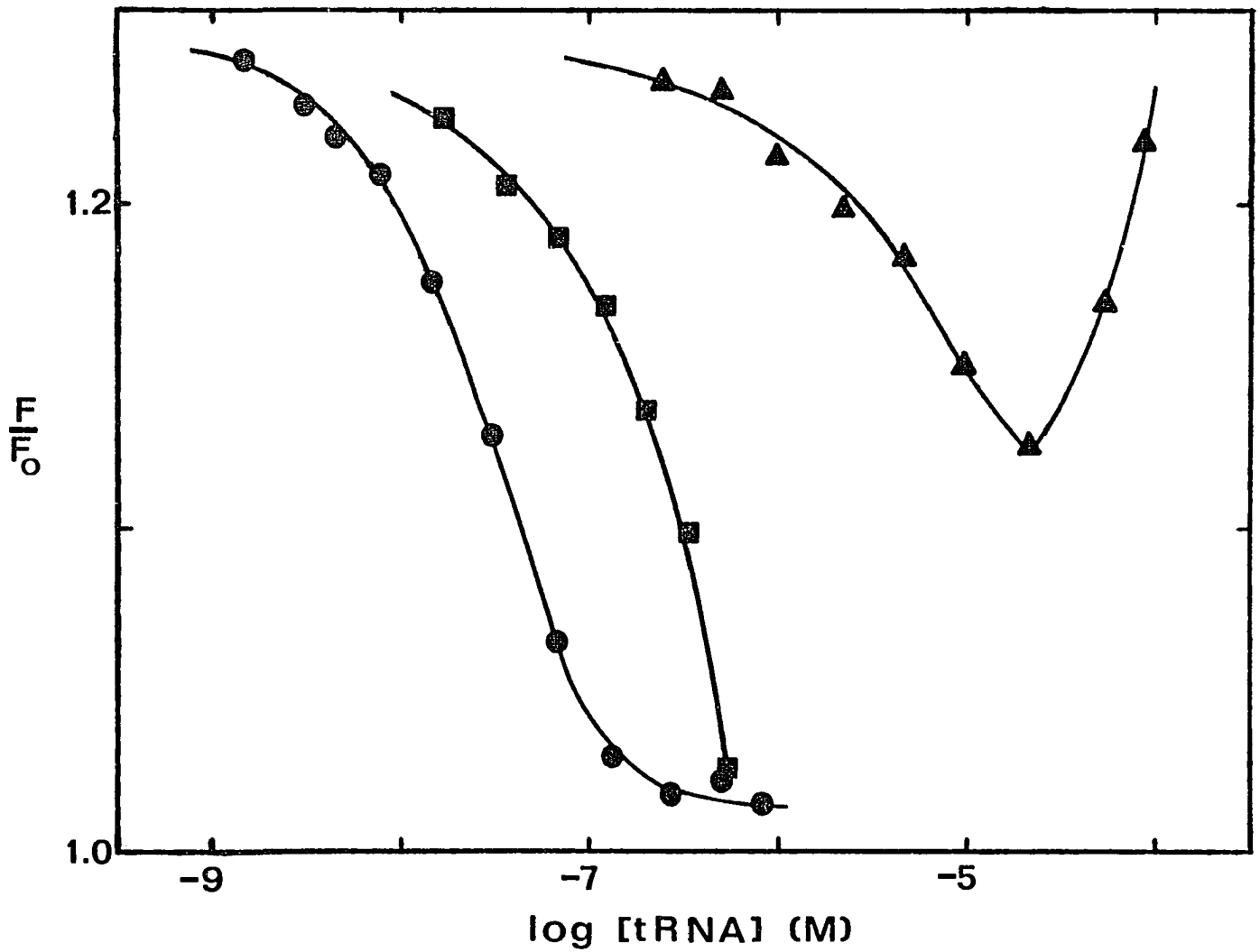

FIEST
1.085
1.075
1.065
1.055
1.5000E-10
1.0800E-09
2.0100E-09
KDEST
FIEST
1.010
1.007
1.004
1.001
0.998
0.995
0.992
0.989
0.986
0.983
0.980
9.0000E-11
2.2800E-09
KDEST
LEGEND: SIGL
0.0
0.1
0.2
0.3
0.4
0.5
0.6
0.7
0.8
0.9
1.0

relative to the unmodified $tRNA^{Phe}$. However, Adkins et al. (1983) observed some heterogeneity in Phe-$tRNA^{Phe}$-F^8 preparations, with respect to the EF-Tu-dependent protection of the aminoacyl bond from hydrolysis. It is possible that the fluorescent-labeled aa-tRNA solutions contain molecules with a reduced capacity to bind or interact with EF-Tu*GTP.

The affinities of fMet-$tRNA_f^{Met}$ and totally aminoacylated unfractionated tRNA for EF-Tu were determined by their abilities to compete with ternary complex-bound Phe-$tRNA^{Phe}$-F^8 for binding to EF-Tu*GTP. Thus, when a sample containing Phe-$tRNA^{Phe}$-F^8*EF-Tu*GTP was titrated with either fMet-$tRNA_f^{Met}$ or totally aminoacylated unfractionated tRNA, the fluorescence of the sample decreased (see Figure 16). As expected, the rate of the decrease in emission intensity was slower for the titration with fMet-$tRNA_f^{Met}$, since this aa-tRNA species is known to have a lower affinity for EF-Tu*GTP than elongator aa-tRNAs.

The dissociation constant for the complex of the competing aa-tRNA with EF-Tu*GTP was determined for each point in the titration (see Figure 16) using a BASIC program which uses the fluorescence to calculate the concentration of the ternary complex-bound Phe-$tRNA^{Phe}$-F^8, and from this the other concentrations needed to calculate a K_d (see Appendix E). Using this method, for those points where the fluorescence decrease was small, and consequently more sensitive to errors in the fluorescence measurement, the calculated K_d values were highly inconsistent and therefore disregarded. Only the points past the beginning of a titration were used in calculating an average K_d. For a titration with fMet-$tRNA_f^{Met}$, the average K_d was 3×10^{-7}M. The average K_d calculated from a titration with totally aminoacylated tRNA was

Figure 16: Titration of the Phe-tRNA^{Phe}-F^{8}*EF-Tu*GTP ternary complex with aminoacylated or unacylated tRNA in buffer B. Ternary complexes were formed by the addition of EF-Tu*GTP (final concentration = 6.9 nM) to samples initially containing Phe-tRNA^{Phe}-F^{8} (●: 3.6 nM; ■ : 3.3 nM;▲: 3.5 nM), prepared as described in Chapter II, Section F. The samples were titrated with totally aminoacylated unfractionated tRNA (in buffer B; ●), f-[^{3}H]Met-tRNA$_{f}^{Met}$ (in 1 mM K-acetate, pH 5, 5 mM $MgCl_2$; ■), or unacylated, unfractionated tRNA (in 5 mM $MgCl_2$;▲).


1.2
1.0
$\frac{F}{F_o}$
-9
-7
-5
log [tRNA] (M)

8×10^{-9}M.

H. Titration of Ternary Complex with Unacylated tRNA

As noted above, the affinities of non-fluorescent unmodified aa-tRNAs for EF-Tu*GTP can be determined by their ability to compete with the fluorescent-labeled aa-tRNAs for binding to the protein. Similarly, the affinity of unacylated tRNA for the aa-tRNA binding site on EF-Tu can be evaluated by its ability to compete with Phe-tRNA^{Phe}-F^{8} for binding to EF-Tu. When a sample containing Phe-tRNA^{Phe}-F^{8}*EF-Tu*GTP was titrated with either unfractionated aa-tRNA or unfractionated tRNA, the fluorescence emission intensity increase resulting from the binding to EF-Tu*GTP was reversed (see Figure 16). The concentration of tRNA required to cause a 50% decrease in the fluorescence emission intensity was three orders of magnitude larger for unacylated tRNA than for aa-tRNA. Titration of a similarly prepared ternary complex with the 5 mM $MgCl_2$ solution in which the unacylated tRNA had been dissolved resulted in no significant decrease in fluorescence.

At the end of a titration with aa-tRNA, the fluorescence decreased to a level near F_o, i.e. that of the Phe-tRNA^{Phe}-F^{8} before addition of EF-Tu*GTP. Surprisingly, however, in the titration with unacylated tRNA, the fluorescence of the sample began to increase as the tRNA concentration increased. To investigate this unexpected fluorescence increase further, a Phe-tRNA^{Phe}-F^{8} sample lacking EF-Tu*GTP was titrated with unacylated tRNA. In this case, the fluorescence emission intensity was constant until it the tRNA concentration reached 20 μM, the level at which the fluorescence was found to increase in the presence of EF-Tu.

The magnitude of the fluorescence at tRNA concentrations above 200 μM was the same both in the presence and absence of EF-Tu (Figure 17). Hence, this increase in fluorescence is not caused by an interaction of the fluorescent tRNA with EF-Tu. No cloudiness was observed in any of the samples, suggesting that light-scattering effects did not contribute to the fluorescence changes.

The exact nature of the effect responsible for the fluorescence increase in the presence of high concentrations of unacylated tRNA is not known. The possible causes of the fluorescence increase include tRNA-tRNA interactions, for example in codon-anticodon or loop-loop base-pairing.

To test the possibility that base-pairing interactions could cause the observed fluorescence increase, EF-Tu*GTP-bound Phe-$tRNA^{Phe}$-F^8 was titrated with synthetic polyribonucleotides. When the ternary complex was titrated with poly(rU) (Sigma), a polynucleotide complementary to the $tRNA^{Phe}$ anticodon, at concentrations in excess of 50 A_{260} mL^{-1} the fluorescence of the sample increased to about 21% beyond the EF-Tu-dependent increase (Figure 18). This result suggests that the fluorescence increase observed in the presence of either poly(rU) or tRNA was due to base pairing with the anticodon of Phe-$tRNA^{Phe}$-F^8. In contrast, titration to similar concentrations with poly(rA) (Boehringer) resulted in a reversal of the Tu-induced fluorescence increase (Figure 18). Although the data are not conclusive, this decrease may have been caused by competition between the poly(rA) and Phe-$tRNA^{Phe}$-F^8 for binding to EF-Tu.

In any case, this secondary effect did not occur until tRNA concentrations were high enough to demonstrate a substantial competition

Figure 17: Titration of Phe-tRNA^{Phe}-F^{8} with unacylated unfractionated tRNA in the presence and absence of EF-Tu*GTP. Samples were prepared as described in Chapter II, Section F, and initally contained 3.5 (●) or 3.4 (▲) nM Phe-tRNA^{Phe}-F^{8} in buffer B. EF-Tu*GTP was added to one sample (⊖) to a concentration of 6.9 nM to form the ternary complex. Both samples were titrated with unfractionated unacylated tRNA in 5 mM $MgCl_2$. In each case, parallel samples were titrated with only 5 mM $MgCl_2$ as a control (data not shown), demonstrating that dilution did not affect the observed fluorescence, either in the presence or absence of EF-Tu*GTP.

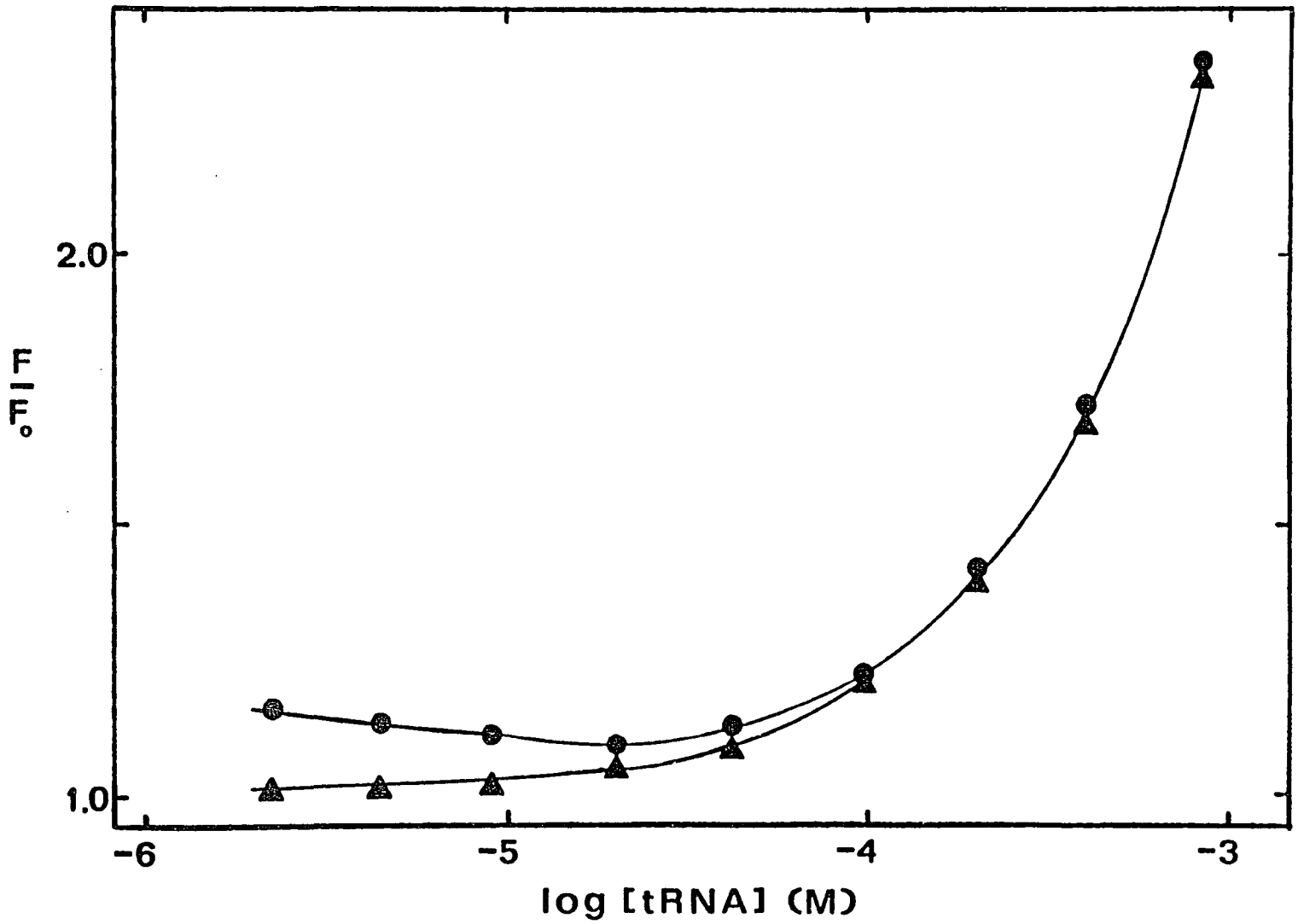
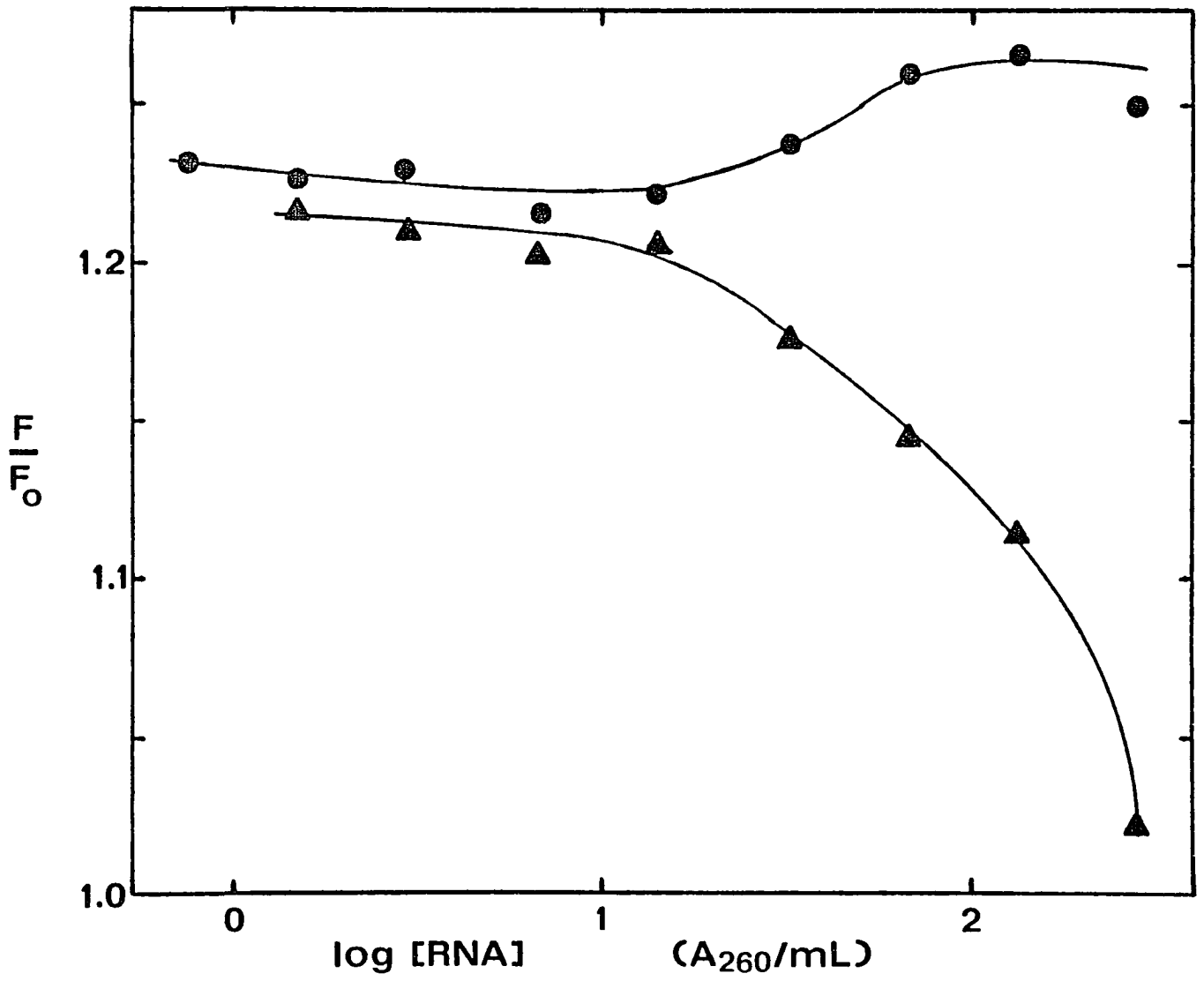

2.0
1.0
F/F₀
-6
-5
-4
-3
log [tRNA] (M)

Figure 18: Titration of Phe-tRNA^{Phe}-F^{8}•EF-Tu•GTP with poly(rU) or poly(rA). EF-Tu•GTP was added (final concentration = 6.9 nM) to samples which initially contained 3.3 nM Phe-tRNA^{Phe}-F^{8} in buffer B, prepared as described in Chapter II, Section F. One sample was titrated with poly(rU) (●), while the a second sample was titrated with poly (rA) (▲). Both polynucleotides were dissolved in 5 mM $MgCl_2$ The fluorescence (F/F_o) of both samples was 1.22 prior to the titrations. As in the experiments in Figure 17, control titrations with 5 mM $MgCl_2$ showed no change in fluorescence.


1.2
1.1
1.0
F/F0
0
1
2
log [RNA] (A260/mL)

with Phe-tRNA^{Phe}-F^{8} for binding to EF-Tu*GTP. In spite of the secondary fluorescence change, the data suggest that the affinity of unacylated tRNA for the protein is about three orders of magnitude weaker than that of aa-tRNA.

I. Determination of K_d for Unacylated tRNA

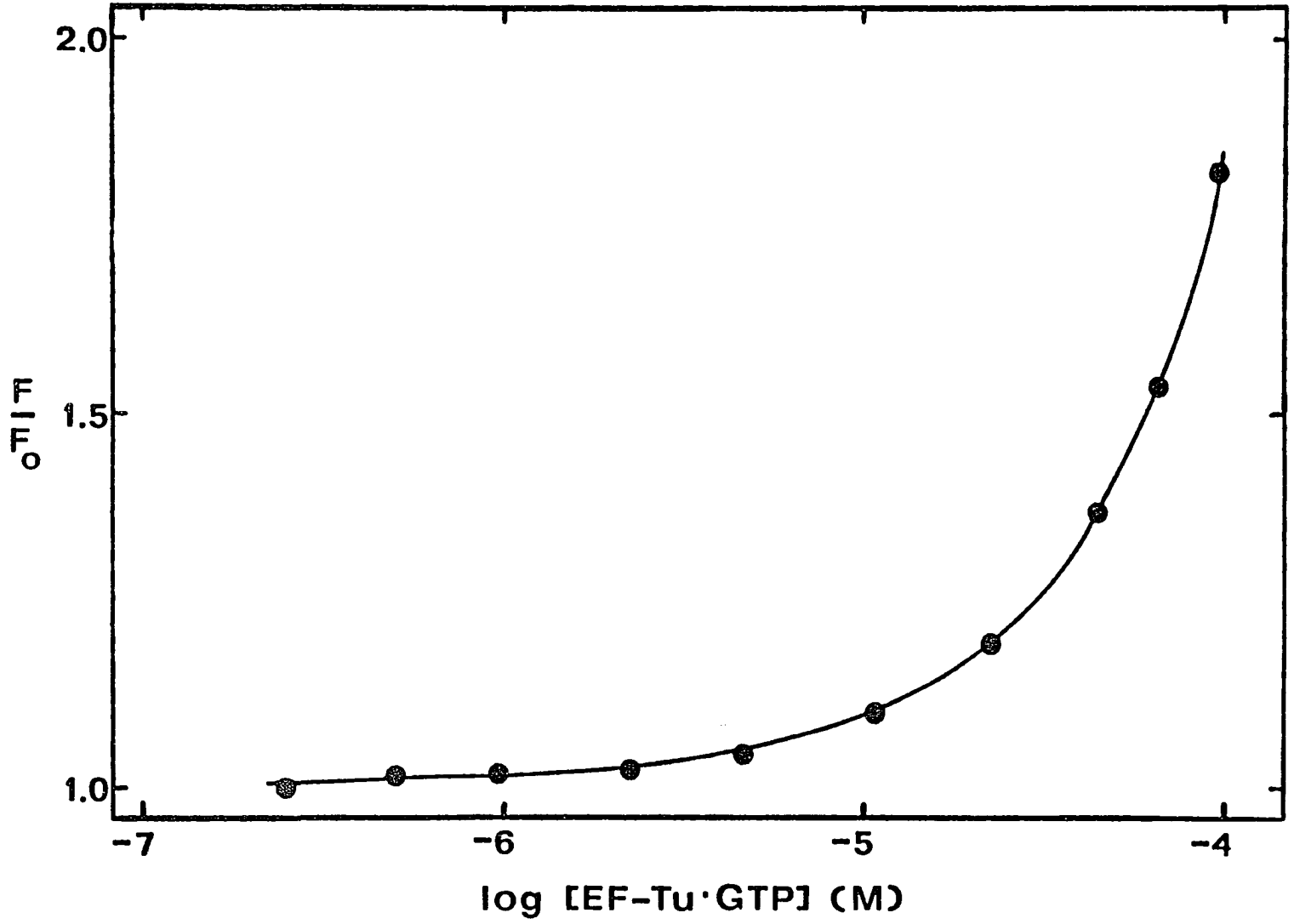
The dissociation constant for the complex of unacylated tRNA with EF-Tu*GTP was determined for each point in a titration (cf. Figure 16) using a BASIC program which uses the fluorescence to calculate the concentration of the ternary complex-bound Phe-tRNA^{Phe}-F^{8}, and from this, the other concentrations needed to calculate a K_d (see Appendix E). However for those points where the fluorescence decrease was small, and consequently more sensitive to errors in the measurement, the calculated K_d's were highly inconsistent and therefore disregarded. Those points later in the titration where the fluorescence began to show increases (cf. Figure 16) were also unreliable for obtaining a K_d, since the fluorescence intensities were influenced by effects other than the competition between Phe-tRNA^{Phe}-F^{8} and tRNA for binding to EF-Tu*GTP. Thus, an average K_d for a particular experiment was calculated from the intermediate points in a titration which resulted in larger fluorescence decreases, but before the fluorescence began to increase again. The K_d for the dissociation of the complex of tRNA with EF-Tu*GTP was found to be about 1×10^{-5} M.

J. Determination of K_d for $tRNA^{Phe}$-F^8

Since an affinity of unacylated tRNA for EF-Tu*GTP was demonstrated, two questions were raised. First, can $tRNA^{Phe}$-F^8 also bind to EF-Tu*GTP? Secondly, if $tRNA^{Phe}$-F^8 does bind to the protein, can a change in fluorescence be induced? As stated earlier, within the range of EF-Tu*GTP concentrations used in titrations to determine the ternary complex dissociation constant for Phe-$tRNA^{Phe}$-F^8, no fluorescence change was observed when the unacylated $tRNA^{Phe}$-F^8 was titrated with EF-Tu*GTP. In addition, when a sample containing a much higher concentration of $tRNA^{Phe}$-F^8 (9.86×10^{-7} M) was titrated with EF-Tu*GTP to 2.2×10^{-6}M, no change in fluorescence emission intensity resulted. Thus, although titrations of Phe-$tRNA^{Phe}$-F^8 with EF-Tu*GTP also contained $tRNA^{Phe}$-F^8 because of deacylation, no interaction between $tRNA^{Phe}$-F^8 and EF-Tu contributed to the observed changes in fluorescence.

However, further titration of $tRNA^{Phe}$-F^8 with EF-Tu*GTP to 97 μM results in a fluorescence increase of 85% (see Figure 19). Although saturation of the fluorescence change was not demonstrated, a minimum K_d can be calculated if the fluorescence level at the end of the titration is taken to be the maximum. Assuming that the increase was indeed a result of the formation of a ternary complex between EF-Tu*GTP and $tRNA^{Phe}$-F^8, a <u>minimum</u> K_d of 3×10^{-5} M for this interaction was calculated, using the BASIC program in Appendix B.

Figure 19: Titration of $tRNA^{Phe}$-F^8 with EF-Tu*GTP. The sample initially contained 9.9×10^{-7}M $tRNA^{Phe}$-F^8 in buffer B, and was titrated with EF-Tu*GTP in the presence of 1 mM GTP. Each point represents the average fluorescence from four scansμ in each case the range of the fluorescence emission intensities was within the size of the point.


2.0
1.5
1.0
F/F0
-7
-6
-5
-4
log [EF-Tu·GTP] (M)

K. Characterization of the Fluorescein-modified $tRNA_1^{Val}$

Thin-layer chromatographic analysis of the product of the covalent reaction of IAAF with $tRNA_1^{Val}$ was used to identify the site of modification on the $tRNA_1^{Val}$. Visual inspection of the plate with an ultraviolet lamp revealed one fluorescent spot displaced from the origin with an R_f corresponding to that of the s^4U-F dye-nucleoside adduct marker (see Adkins, 1982). No other fluorescent spots were observed from the modified $tRNA_1^{Val}$ digestion mixture. It was therefore concluded that the $tRNA_1^{Val}$ was singly and covalently labeled with fluorescein at s^4U-8. The similarity of the chromatographic behavior on the RPC-5 column of the modified $tRNA_1^{Val}$ to that of the modified $tRNA^{Phe}$ supported this conclusion.

L. Activity of EF-Tu

Considerable variability was observed in the results from the EF-Tu nitrocellulose filter binding assays. It was found that decomposition of the [^{3}H]GDP was a major contributor to this variability. In spite of storage of the [^{3}H]GDP solution at -20 ^{o}C, as much as 5% of the ^{3}H exchanged into H_2O per month. Thin layer chromatographic analysis indicated hydrolysis of 12% of the [^{3}H]GDP to [^{3}H]GMP after 15 months, and 29% hydrolysis after 22 months. It was therefore necessary to redetermine the specific activity of the [^{3}H]GDP periodically to obtain meaningful filter binding results.

The ability of EF-Tu to bind GDP was confirmed using gel filtration on a Sephadex G-25 column. In more than one experiment, the GDP binding

activity of an EF-Tu solution was unusually low (e.g. 30%) when assayed using the nitrocellulose filters. However, when aliquots of the same EF-Tu solution were tested for GDP binding using gel filtration, the protein was determined to be nearly completely active. These results suggest that problems other than those related to the specific activity of the [^{3}H]GDP contributed to the variability in the filter assays. This notion is supported by the fact that the wetting ability of filters was occasionally very poor, although all the filters used from one company were from the same lot. Variations in results obtained using filter assays have been noted previously (Dr. D. L. Miller, personal communication), and were the cause of difficulties in using this assay to estimate the K_d for the ternary complex. Differences in the material used to make the nitrocellulose filters appeared to be the source of the problems with these assays.

The molar absorptivity used in determining concentrations of EF-Tu differed from one reported in the literature. Block and Pingoud (1981) determined the ε_{280} to be 32,900 $M^{-1}cm^{-1}$, for EF-Tu, apparently in the absence of any bound nucleotide. All EF-Tu solutions used in this dissertation were measured in the presence of bound GDP, so the ε_{280} value of 41,600 $M^{-1}cm^{-1}$, derived from the absorbance of a 1.0 mg(dry weight)/mL solution, (see Chapter II, Section C) was deemed more appropriate. This ε_{280} value is consistent with that reported by Block and Pingoud if the ε_{280} contribution for GDP is included.

M. Factors Influencing the Fluorescence of the Probe

The possible effects of Mg^{2+} on $tRNA^{Phe}$-F^8 conformation and

fluorescence were investigated, since the $tRNA^{Phe}-F^8$ was stored in buffers lacking Mg^{2+}. Thus, $Phe-tRNA^{Phe}-F^8$ and $tRNA^{Phe}-F^8$ samples were prepared in buffer A lacking Mg^{2+} and DTT, and the fluorescence emission intensities at the emission maximum (519 nm) were followed at 6 °C. After the addition of enough $MgCl_2$ to equal that for buffer A, more than a three-fold increase in fluorescence was observed. A stable fluorescence signal was obtained within 8 minutes, the length of the usual interval allowed for equilibration between groups of scans. It was therefore concluded that any Mg^{2+} equilibration in the fluorescence experiments occured relatively rapidly, and that other factors were responsible for instabilities in the initial fluorescence scans.

In order to avoid potential fluorescence reproducibility problems caused by reorienting the cuvette after removing it for mixing, a teflon-coated magnetic stirrer was added to each cuvette to permit mixing before and during titrations without removal of the cuvettes from the cell holder. The use of a stirrer also prevented any spectral fluctuations due to temperature changes in the sample, caused by removing the cuvette from the cell holder to achieve mixing of the solution. Such temperature-associated problems could be especially dramatic in experiments performed at 6 °C.

Since other investigators have reported the loss of fluorescent or radioactive labels attached via thioethers (Eshaghpour et al., 1979; Kruse et al., 1980), similar losses could be another possible source of unstable fluorescence emission intensities. It was suspected that reducing agents could cause the fluorescein dye to be displaced from the tRNA, because the dye is attached to the s^4U-8 base via a thioether bond (see Figure 5). To test this possibility, samples of $tRNA^{Phe}-F^8$ and

$tRNA_1^{Val}$-F^8 were incubated in buffer B in the presence of 0.1, 1.0, and 10 mM DTT at 37 °C for 12 to 14 hr under an N_2 atmosphere. Each mixture was dried and analyzed by thin-layer chromatography on silica gel plates (Analtech) using a benzene/pyridine/acetic acid/ethanol (65:25:4:6, by volume) solvent system (Adkins, 1982). Fluorescent spots which were not at the origin were observed only in the lanes for samples incubated with 1.0 or 10 mM DTT. Each of these spots had an R_f greater than that of the s^4U-fluorescein adduct marker. This result suggested that the dye was no longer covalently attached to the tRNA, but instead a free fluorescein dye. Based on this apparent displacement of the fluorescein dye from the tRNA at high levels of DTT, 0.1 mM DTT was used in all subsequent experiments, although early experiments in polymix had been carried out using 1 mM DTT as described by Jelenc (1980)[4]. The sensitivity of $tRNA^{Phe}$-F^8 to reducing agents was also demonstrated with 2-mercaptoethanol. The fluorescence emission intensity of Phe-$tRNA^{Phe}$-F^8 increased by at least 25% when incubated at 5 °C for 210 min in buffer A solutions containing 5 or 100 mM 2-mercaptoethanol in place of DTT.

The sensitivity of the fluorescence emission intensity of the $tRNA^{Phe}$-F^8 probe to nucleases was also examined. The fluorescence of a sample containing 5.9 nM $tRNA^{Phe}$-F^8 in 50 mM Hepes (pH 7.6) and 10 mM $MgCl_2$ in a volume of 2.5 mL was prepared in a 1x1 cm polystyrene fluorescence cuvette and placed in the cell holder at 37 °C. The

---

[4]Titrations using 1 mM DTT in buffer B did not yield K_d values significantly different from those using 0.1 mM DTT and were therefore included in the analyses of the combined data for experiments of a particular type.

fluorescence emission intensity of the sample was monitored before and after the addition of 0.3 units alkaline phosphatase (Sigma), 40 μg ribonuclease A (Grand Island Biological), 4 μg snake venom phosphodiesterase (Worthington), and 1 μg ribonuclease T1 (Sigma), all in a volume of 11 μL. The amounts of the digestive enzymes used are the same as are typically used in this laboratory to characterize the fluorescent modification of a tRNA, by total digestion of the tRNA in a 20 μL incubation at 37 °C for 18 hr (Johnson et al., 1982). An increase of 220% was observed within 30 min after the addition of the nucleases and mixing of the sample. Thus, it is clear that the fluorescence changes associated with digestion of the tRNA by nucleases are substantially larger than those resulting from the formation of the Phe-$tRNA^{Phe}$-F^{8}*EF-Tu*GTP ternary complex.

N. Experimental Considerations

All buffer B solutions, containing the polymix solvent, were titrated to pH 7.0 to avoid precipitates observed at the higher pH (7.5) which was specified by Jelenc (1980). Under certain conditions (e.g. high salt or with significant amounts of alcohol in the solution), Jelenc encountered precipitation also, indicating a high tendency of the polymix buffers toward precipitation. The assays in which Jelenc used the polymix buffers were all at 37 °C, so it is likely that the precipitation observed in the present study was due to the lower temperatures at which the experiments were performed.

The presence of pyruvate kinase in titrated samples was found to be useful in minimizing problems due to apparent adsorption to the teflon

stirrer. Such adsorption was only deduced when titration of Phe-$tRNA^{Phe}$-F^8 with EF-Tu*GDP was attempted in the absence of pyruvate kinase and PEP. In these experiments, the initial fluorescence intensities decreased at least 10% and as much as 25% in 90 min. However, the fluorescence increased to approximately that of the initial scans upon addition of the usual amount of pyruvate kinase. Additionally, the amounts of cold acid-insoluble radioactivity were lower at the beginning than at the end of a titration in the absence of pyruvate kinase. This suggests that a fraction of the tRNA was initially removed from the solution by adsorption, and returned to the solution only after sufficient EF-Tu was added to form ternary complexes or to compete for adsorption sites.

Solvent pH has a major influence on the intensity of fluorescent emission (cf. Table II). This was also evident when a sample containing Phe-$tRNA^{Phe}$-F^8 was prepared in a quartz cuvette lacking both a stirrer and pyruvate kinase. Initially, no decrease in fluorescence was observed. Subsequent addition of an aliquot of pyruvate kinase to the cuvette caused a drop in fluorescence. A control sample showed a similar decrease when an equivalent aliquot containing only the 2.2 M $(NH_4)_2SO_4$, (pH 6.0) buffer in which the pyruvate kinase was suspended was added to the cuvette. The fluorescence emission intensity decrease was presumably due to the lower pH of the buffer for the enzyme. Pyruvate kinase was therefore included in titrations with EF-Tu*GDP, where GDP necessarily replaced GTP, and PEP was omitted.

Due to the possible inaccuracies in the calculated concentrations of aa-tRNA caused by adsorption to the teflon stirrer, titrations of Phe-$tRNA^{Phe}$-F^8 with EF-Tu*GTP in buffer B were carried out in the

absence of stirrers. The titrations proceeded in a manner similar to those with stirrers, except that some mixing problems seemed to be present, as evidenced by greater variability in the titration curves. The K_d values from these stirrer-less experiments did not differ significantly from those in which stirrers were used. These titrations were therefore included in the combined data sets used in determining a K_d for buffer B.

CHAPTER IV

DISCUSSION

The mechanism by which the ribosomal complex enhances the discrimination between aa-tRNAs that are correctly and incorrectly base-paired to the mRNA codon is unknown. An essential prerequisite to elucidating that mechanism is the characterization, both thermodynamic and kinetic, of the interactions between the various macromolecules and multicomponent complexes which participate in the recognition process. I have investigated the formation of the aa-tRNA*EF-Tu*GTP ternary complex by monitoring a fluorescence change which accompanies the association of Phe-$tRNA^{Phe}$-F^{8} with EF-Tu*GTP (Adkins et al., 1983; Figure 6). This approach facilitated the examination of the protein-nucleic acid interaction directly and at equilibrium.

The importance of examining this interaction under equilibrium conditions is demonstrated by comparing the K_d values obtained spectroscopically and those obtained by other techniques (see Table IV). The ternary complex dissociation constant measured at low temperature using non-equilibrium techniques ranged from 1-10 nM to 100 nM for *E. coli* Phe-$tRNA^{Phe}$. Although variations in the ionic strengths and temperatures of the incubations make direct comparisons impossible, it is apparent that, in general, the higher K_d values obtained by these

Table IV

COMPARISON OF REPORTED K_d VALUES FOR AMINOACYL-tRNAs[a]

Method	aa-tRNA	Temperature	K_d (nM)	Ref.
Fluorescence	*E. coli* Phe-tRNA^{Phe}	6 °C	0.13	Table III
Spectroscopy	*E. coli* Phe-tRNA^{Phe}-F^8	6 °C	0.85	Table II
	E. coli Phe-tRNA^{Phe}-F^8	25 °C	5.4	Chapter III
	Yeast Phe-tRNA^{Phe}	6 °C	0.72	Table II
	E. coli Lys-tRNA^{Lys}	6 °C	7.7	Table III
Filter	*E. coli* Phe-tRNA^{Phe}	0 °C	1-10	(b)
Assay	*E. coli* Phe-tRNA^{Phe}	0 °C	72	(c)
Nuclease	*E. coli* Phe-tRNA^{Phe}	0 °C	79	(d)
Protection	*E. coli* Phe-tRNA^{Phe}	0 °C	100	(e)
Assay	Yeast Phe-tRNA^{Phe}	0 °C	54	(f)
Hydrolysis	*E. coli* Phe-tRNA^{Phe}	25 °C	20	(g)
Protection	Yeast Phe-tRNA^{Phe}	25 °C	20	(h)
Assay	*E. coli* Lys-tRNA^{Lys}	25 °C	250	(g)

[a] All measurements were made in buffers of similar pH and ionic strength.

[b] Miller et al., 1973

[c] Arai et al., 1974

[d] Tanada et al., 1981

[e] Derwenskus and Sprinzl, 1983

[f] Tanada et al., 1982

[g] Pingoud and Urbanke, 1980

[h] Pingoud et al., 1977

methods reflect an underestimation of the strength of the ternary complex with Phe-tRNA^{Phe}, shown by my results to have a K_d of 0.13 nM at 6 ^{o}C in a buffer similar to those used in the other studies. At 25 ^{o}C, the value for the Phe-tRNA^{Phe} ternary complex K_d determined by protection assay was 20 nM (Pingoud and Urbanke, 1980), while the K_d for Phe-tRNA^{Phe}-F^{8} at 25 ^{o}C was found to be 5.4 nM (see Chapter III, Section F). Because the K_d of Phe-tRNA^{Phe} is less than that of Phe-tRNA^{Phe}-F^{8} (Tables II and III), the 20 nM figure considerably underestimates the affinity of Phe-tRNA^{Phe} for EF-Tu*GTP. This underestimation is to be expected, because only the spectroscopic measurements were obtained under equilibrium conditions. On the other hand, the non-equilibrium methods do provide an indication of the relative affinities of various aa-tRNAs for EF-Tu*GTP: the K_d for Lys-tRNA^{Lys} is 6.6-fold higher than the K_d for Phe-tRNA^{Phe} by spectroscopy (Table III), it is 3.2- to 4.3-fold higher by nuclease protection experiments (Louie et al., 1984), and 12.5-fold higher by aminoacyl bond protection experiments (Pingoud and Urbanke, 1980). These differences in the relative affinities may result from the differences in the experimental conditions.

It is also important to emphasize that the spectroscopic method described in this dissertation does not require the modification of an aa-tRNA to determine the K_d of its ternary complex. Instead, the affinity of an unmodified aa-tRNA for EF-Tu*GTP is determined by its ability to compete with a fluorescent-labeled aa-tRNA for binding to the protein. The identity of the fluorescent aa-tRNA is irrelevant: the fluorescent aa-tRNA only provides a mechanism for monitoring the extent of association of the unmodified aa-tRNA with the protein. The approach

utilized in this dissertation is therefore a general approach for the determination of the binding affinity of a nucleic acid for EF-Tu*GTP. Additionally, this approach can be used to study various mutant EF-Tu molecules, various undermodified tRNAs, fragments of tRNAs, and various nucleotides for their influences on ternary complex formation.

It is worthwhile to note that although modification of $tRNA^{Phe}$ with a fluorescein dye weakens the interaction of its aminoacylated form with EF-Tu, the K_d is still within the range of values for other unmodified aa-tRNAs (see Tables II and III). Consistent with the relative affinities of Phe-$tRNA^{Phe}$-F^8 and Phe-$tRNA^{Phe}$ for the protein, the affinity of $tRNA^{Phe}$-F^8 for EF-Tu*GTP also appears to be weaker than that of tRNA (Chapter III, Section H; see discussion below). The apparently weakened binding of the fluorescent tRNA to the protein could be due to heterogeneity in $tRNA^{Phe}$-F^8 preparations (see Chapter III, Section G) and/or to a structural alteration in the tRNA caused by the dye.

The K_d values reported in this dissertation were obtained using a nonlinear least squares analyisis of the data, fitting to a model with only a single binding event: the association of aa-tRNA with EF-Tu*GTP. The validity of this model is supported by titrations which demonstrated the absence of interactions between $tRNA^{Phe}$-F^8, $tRNA_1^{Val}$-F^8, or unacylated tRNA with EF-Tu in the range of concentrations employed to study aa-tRNA*EF-Tu*GTP ternary complex equilibria. The lack of any fluorescence change in titrations of Phe-$tRNA^{Phe}$-F^8 with EF-Tu*GDP is in agreement with the EF-Tu*GTP-dependence of the interaction and of the concomittant fluorescence increase. More importantly, even if there were any EF-Tu*GDP in the titrant solutions, in spite of the GTP-regenerating pyruvate kinase and PEP, no effect on the observed

fluorescence would result. The fluorescence changes associated with ternary complex formation are also substantially smaller than those resulting from nuclease digestion of the tRNA. Clearly, the fluorescence changes observed in titrations of Phe-tRNA^{Phe}-F^{8} with EF-Tu*GTP resulted only from ternary complex formation.

My experiments demonstrate that EF-Tu*GTP has a high affinity for aa-tRNA, and it is appropriate to consider why the binding between aa-tRNA and EF-Tu*GTP is so tight. Since the intracellular concentrations of EF-Tu and aa-tRNA are in excess of 100 μM (Ingraham et al., 1983), K_d values on the order of 1 μM would be sufficient to ensure ternary complex formation. However, the actual K_d values are approximately 100-fold lower. This suggests that the strong affinity of EF-Tu*GTP for aa-tRNA is required for something besides ternary complex formation. A reasonable hypothesis is that the tight association between the protein and the aa-tRNA is necessary to take full advantage of the discriminatory mechanisms of the ribosomal complex. Stated most simply, because of the high affinity of EF-Tu*GTP for the aa-tRNA, the aa-tRNA will be released from the protein and free to bind to the ribosome only after the correct codon-anticodon interaction triggers a mechanism to disrupt the ternary complex. This mechanism would presumably involve the hydrolysis of the GTP to GDP and the formation of the EF-Tu*GDP complex, which has a low affinity for aa-tRNA.

Hopfield (1974) and Ninio (1975) have independently proposed that the recognition process is a two-stage mechanism involving proofreading. In their schemes, an initial codon-anticodon-mediated discrimination of various ternary complexes is followed by a second discriminatory stage (= proofreading) that is initiated by the hydrolysis of GTP and the

dissociation of EF-Tu*GDP in those ternary complexes which successfully complete the first stage. There is some experimental evidence which supports this hypothesis. Thompson and coworkers demonstrated that while some non-cognate ternary complexes bound without any GTP hydrolysis, near-cognate ternary complexes exhibited an abortive binding reaction with ribosomes that involved GTP hydrolysis and the dissociation of the aa-tRNA before it stably binds in the A site (Thompson and Stone, 1977; Thompson et al., 1981). These data are interpreted as demonstrating a GTP-dependent proofreading step in aa-tRNA recognition on the ribosome. Experiments reported by other laboratories are consistent with Thompson's findings (Yamane et al., 1981; Ruusala et al., 1982; Andersson and Kurland, 1983). If this is indeed the mechanism, then the tight binding between EF-Tu*GTP and aa-tRNA may be required to ensure that the ternary complex remains intact during the first stage of the recognition process. This would minimize the chances of premature release of the factor from the aa-tRNA and the possible passage of aa-tRNA into the proofreading stage prior to completion of the first stage. In effect, the high affinity of EF-Tu*GTP for aa-tRNA would reduce translational errors by ensuring that maximum discrimination was achieved during the first stage of the recognition process.

The importance of the solvent milieu on the ternary complex K_d is clearly shown by my results (Tables II and III; Figure 12). It is particularly noteworthy that the protein-nucleic acid binding is much tighter in a commonly-used Hepes-based <u>in vitro</u> milieu than in the more physiological polymix milieu. This difference does not result from a difference in solvent pH (Table II), but rather from the difference in

solvent ionic strength: the K_d in polymix is approximately the K_d expected in a Hepes-buffered solution of the same ionic strength (Figure 12). In any event, the differences in K_d obtained in polymix compared with that obtained in other solvent systems will have to be considered when comparing data from the different solvent systems.

The pH of the solvent influences the magnitude of the fluorescence change observed upon ternary complex formation. Larger fluorescence changes were observed in solvents at pH 7.0 than at pH 7.6. Also, the fluorescence emission intensity of Phe-tRNA^{Phe}-F^8 is lower in buffer A at pH 7.0 than in buffer A at pH 7.6, both in the presence and absence of EF-Tu*GTP. These differences in fluorescence emission intensities are probably attributable to the the molar absorptivity of fluorescein, which is known to be highly pH-sensitive, decreasing with decreasing pH (Mercola et al., 1972). The similarity of the conformational states of the Phe-tRNA^{Phe}-F^8 which is EF-Tu-bound in the buffers differing only in pH therefore cannot be assessed.

The various studies whose aims were to identify the portion of the aa-tRNA which interacts directly with EF-Tu have been interpreted to mean that the EF-Tu binds to the aa-tRNA along its acceptor arm (see Chapter I). Since EF-Tu must bind to all elongator aa-tRNAs, no matter what the base sequence, one might expect that the putative binding along the acceptor arm would involve salt bridges between the protein and the phosphates on the aa-tRNAs. This view would appear to be supported by the fact that the ternary complex K_d values are nearly the same for yeast and E. coli Phe-tRNA^{Phe} (Table III; Pingoud and Urbanke, 1980; Tanada et al., 1982), despite the considerable difference in their acceptor arm sequences (Sprinzl et al., 1978).

My data indicate that there are a minimum of 2 salt bridges involved in ternary complex formation. However, as detailed in Chapter III, Section E, the actual number of ionic interactions cannot be determined. In the case of another protein-nucleic acid interaction, that of phage R17 coat protein with its RNA binding site, an upper limit of five ionic contacts between the protein and RNA was obtained using assumptions similar to those made in the present study (Carey and Uhlenbeck, 1983b). These investigators interpreted the ionic contacts as contributing to the observed high specificity of the binding. Although studies with several DNA binding proteins have led to the idea that ionic contacts are characteristic of nonspecific protein-DNA interactions, ionic contacts may be a characteristic of specific RNA-protein interactions. The secondary and tertiary structure of RNA create protein binding sites which have unique three dimensional arrays of nucleotide phosphates and hence enhance the specificity of interactions (see Carey and Uhlenbeck, 1983b).

However, it is important to note that there is a substantial non-electrostatic component of the binding between EF-Tu and aa-tRNA. Using protection assays, Pingoud et al. (1977b) observed an ionic strength dependence of the Tyr-tRNA^{Tyr} ternary complex K_d which was very similar to that of Figure 12. In agreement with my results, they also concluded that there was a considerable non-electrostatic contribution to the binding energy. Because of the polyanionic nature of tRNA, an electrostatic component to tRNA-protein interactions would not be surprising. Also, as noted above, the ability of EF-Tu to bind to all elongator aa-tRNAs points to an electrostatic contribution to this protein-nucleic acid interaction. However, the large contribution of

non-electrostatic interactions to the binding energy of the ternary complex can be viewed as consistent with the relative weakness of the interaction of EF-Tu*GTP with unacylated tRNA (see Chapter III, Section J). It is conceivable that non-electrostatic interactions of EF-Tu with the aminoacyl group of the aa-tRNA are responsible for the much of the specificity and the strength of the association with EF-Tu. This view is also supported by the relatively weak affinity of fMet-$tRNA_f^{Met}$ for EF-Tu*GTP (Chapter III, Section G), and by the reported differences affinities for EF-Tu*GTP of aa-tRNAs which differ only in their aminoacyl groups (Pingoud and Urbanke, 1980; Wagner and Sprinzl, 1980; Tanada, et al. 1982).

The affinity of unacylated tRNA for EF-Tu is about 1000-fold weaker than that for aa-tRNA (Figure 16). The affinity of $tRNA^{Phe}$-F^8 is also much weaker than Phe-$tRNA^{Phe}$-F^8 for EF-Tu*GTP (see Chapter III, Section J). If the K_d at 6 ^oC in buffer B is not less than 3×10^{-5}M (Chapter III, Section H), the ΔG^o for the $tRNA^{Phe}$-F^8 ternary complex is therefore at most -5.8 kcal/mol[5]. In contrast, the ΔG^o for the Phe-$tRNA^{Phe}$-F^8 ternary complex at 6 ^oC in buffer B is -10.6 kcal/mol. Thus the interaction of $tRNA^{Phe}$ with EF-Tu has at best one-half the binding energy of the Phe-$tRNA^{Phe}$-F^8*EF-Tu*GTP ternary complex. In other words, the aminoacyl moiety contributes a substantial fraction of the energy for ternary complex formation.

---

[5]Note however that there are other possible explanations for the large increase in fluorescence observed in titration of $tRNA^{Phe}$-F^8 with EF-Tu*GTP. For example, the fluorescence could have been influenced by depletion of Mg^{2+} in the buffer due to the high concentration of GTP, or by other unrecognized effects caused by the unusually high concentrations of the $tRNA^{Phe}$-F^8 and EF-Tu*GTP.

The interaction between EF-Tu*GTP and aa-tRNA can be further characterized in terms of enthalpy and entropy changes. At 6 ^{o}C in buffer A, the ΔG^{o} for the Phe-tRNA^{Phe}-F^{8} ternary complex is -11.6 kcal/mol, as calculated directly from K_a. From the temperature dependence of the ternary complex dissociation, a ΔH^{o} of -16 kcal/mol and a ΔS^{o} of -16 cal mol^{-1}deg^{-1} are calculated.

Comparison of the thermodynamic parameters describing the interaction of Phe-tRNA^{Phe}-F^{8} with EF-Tu*GTP to those for other RNA-protein interactions aids in evaluating the significance of these measured values. The value for ΔG^{o} is very similar to that reported for the sequence-specific binding of phage R17 coat protein to its RNA binding site (see Table V). The enthalpy change for the Phe-tRNA^{Phe}-F^{8}-EF-Tu*GTP interaction is less than the large favorable ΔH^{o} for the R17 coat protein-RNA interaction, but the latter is offset somewhat by the entropic contributions to ΔG^{o}.

A highly specific RNA-protein interaction which has been the subject of much investigation is that between tRNA and aminoacyl-tRNA synthetases. Krauss and coworkers (1976) measured thermodynamic parameters for both specific (cognate, homologous) and nonspecific (noncognate, heterologous) tRNA-synthetase interactions. Both the specific and the nonspecific interactions were characterized by a large favorable gain in entropy resulting from the release of bound H_2O molecules upon association of the two macromolecules. The specific interaction has a small negative ΔH^{o} and a positive ΔS^{o}, but the nonspecific interaction has a positive ΔH^{o} which is counteracted by a large positive ΔS^{o} (see Table V). The authors concluded that the nonspecific binding is stabilized by electrostatic interactions (e.g.

Table V

THERMODYNAMIC PARAMETERS DESCRIBING RNA-PROTEIN INTERACTIONS

RNA Protein	K_d (nM)	ΔG^o (kcal/mol)	ΔH^o (kcal/mol)	ΔS^o (cal mol deg)	Ref.
Phe-$tRNA^{Phe}$-F^8	0.85	-11.6[a]	-16	-16	b
EF-Tu*GTP	5.4	-11.3[c]	-16	-16	d
tRNA					
Synthetase					
Specific	100	-9.4[e]	-3.5	+20	f
Nonspecific	2000	-7.8[e]	+15	+75	f
21-Nucleotide					
RNA Binding Site[g]	1[g]	-11[h]	-19	-30	i
R17 Coat Protein					

[a]Buffer A (50 mM Hepes pH 7.6, 10 mM $MgCl_2$, 50 mM NH_4Cl), 6 °C

[b]Table II; Chapter III.

[c]Buffer A, 25 °C.

[d]Chapter III, Section F.

[e]0.03 M Potassium phosphate pH 7.2, 0.05 M KCl, 10 mM $MgCl_2$, 24 °C.

[f]Krauss et al., 1976.

[g]see Carey and Uhlenbeck, 1983a.

[h]0.1 M Tris-HCl pH 8.5, 10 mM magnesium acetate, 80 mM KCl, 2 °C.

[i]Carey and Uhlenbeck, 1983b.

ion pairs) which result in a positive ΔH.

As noted by Carey and Uhlenbeck (1983b), in general, favorable contributors to ΔH are relatively weak contacts of the van der Waals' and hydrogen-bond types which result when there is a good steric fit between the associating macromolecules, and favorable contributors to ΔS include ionic contacts and hydrophobic forces, because both permit greater disorder of the solvent molecules (e.g. H_2O) when no longer constrained in a highly ordered state around the charged or hydrophobic surfaces of the macromolecule. Thus, similar to the assessment of the R17 coat protein system, the favorable ΔH value for aa-tRNA association with EF-Tu*GTP appears to reflect a relatively large number of hydrogen-bonding and van der Waals' interactions between protein and RNA, although perhaps fewer in number than for the R17 coat protein-RNA association. In both cases, a close steric fit between the RNA and the protein is indicated, consistent with the need for specificity in each interaction. Some unfavorable hydrophobic interactions or configurational constraints may contribute to the unfavorable change in entropy in these association processes. Since only few ion contacts were indicated for the complexes of these polyanionic RNA molecules with their respective proteins, it is not too surprising that there is not a favorable entropic contribution to the binding energy.

In contrast, the interaction of aa-tRNA with EF-Tu*GTP is quite different from that of tRNA with synthetase enzymes, since the latter is not stabilized by a large number of hydrogen-bonding and van der Waals' interactions. Instead, the tRNA-synthetase association presumably uses ionic contacts made available by the release of bound H_2O molecules to

provide stability, compensating for a lack of weak contacts to favor the association of the macromolecules.

The weak affinity of unacylated tRNA for EF-Tu*GTP reported here is consistent with the data from other studies indicating the formation of a tRNA*EF-Tu*GTP complex. While at lower concentrations of tRNA and EF-Tu*GTP, no interaction between the protein and RNA is demonstrable (Chapter III, Section B; Adkins, 1982), at 8 x 10^{-4}M concentrations of both $tRNA^{Glu}$ and EF-Tu*GTP, Shulman and coworkers (1974) deduced complex formation using high-resolution n.m.r. spectroscopy. In another study, the protection from covalent labeling with N-tosyl-L-phenylalanylchloromethane provided for EF-Tu*GTP by aa-tRNA was observed in the presence of about 10^{-4}M $tRNA^{Glu}$ (Jonák et al., 1980). Picone and Parmeggiani (1983) have reported an interaction between unacylated tRNA and EF-Tu based on an assay for the GTPase activity of EF-Tu. Based on my results, the relatively high concentrations of tRNA and protein used in each of these investigations are in accord with what one would expect to be necessary to observe tRNA-EF-Tu*GTP interactions.

Although the exact nature of the aa-tRNA structural changes which cause the changes in fluorescence emission have not been identified, I have now shown that two different fluorescent-modified aa-tRNAs behave similarly when confronted with EF-Tu*GTP. My data indicate that it is also possible for EF-Tu*GTP to alter the fluorescence emission intensity in $tRNA^{Phe}$-F^{8}. Curiously, this evidence also implies that the binding of the aminoacyl group by EF-Tu*GTP is not essential to effect a conformational change in aa-tRNA, although other experiments presented here suggest that the aminoacyl group is a major contributor to the binding energy of the ternary complex. Further investigations will be

required to clarify the possibility that the EF-Tu-induced fluorescence changes in Phe-tRNA^{Phe}-F^8 and tRNA^{Phe}-F^8 are caused by similar structural changes, but limitations of the system will hinder such a study using fluorescence.[6]

The conformational or environmental changes in Phe-tRNA^{Phe}-F^8 associated with the additional fluorescence increase observed in the presence of high concentrations of tRNA or poly(rU) are also unknown. Other preliminary data demonstrate that the binding of Phe-tRNA^{Phe}-F^8 to ribosomes elicits an additional change in fluorescence emission (A.E. Johnson, unpublished data). If in fact the fluorescence increase is due to base pairing at the anticodon, a conformational change in aa-tRNA upon binding to mRNA would be implied.

The emission intensities of both Phe-tRNA^{Phe}-F^8 and Val-tRNA$_1^{Val}$-F^8 increase when they associate with EF-Tu*GTP. The sensitivity of the s^{4}U-conjugated dye to the binding of EF-Tu*GTP (allosterically; Adkins et al., 1983) suggests that the region of the aa-tRNA near the s^{4}U is particularly susceptible to conformational changes, since aa-tRNAs with fluorescent moieties elsewhere have not exhibited spectral changes upon association with EF-Tu*GTP (Beres and Lucas-Lenard, 1973; Pingoud et

---

[6]In short, to attempt to saturate the fluorescence change observed when tRNA^{Phe}-F^8 was titrated with EF-Tu*GTP, higher concentrations of either the tRNA of the protein (or both) will be necessary. Increasing the concentration of the tRNA^{Phe}-F^8 will require the use of smaller fluorescence cuvettes to minimize inner filter effects. Reproducible fluorescence measurements have been found very difficult to obtain with such cuvettes, because (a) mixing requires the use of either a micropipet or a polystyrene stirring rod, and (b) measurements are highly dependent upon the exact repositioning of the cuvette every time the cell holder is rotated. In addition, such high concentrations of EF-Tu would be rather costly to use, especially considering the unreliability of measurements made in the smaller fluorescence cuvettes.

al., 1977a; Sprinzl and Faulhammer, 1978). This region has also been shown to be sensitive to the presence or absence of Mg^{2+} (see Chapter III, Section M; Heerschap et al., 1983). Since the binding of Phe-$tRNA^{Phe}$-F^8 to ribosomes elicits an additional change in fluorescence emission (A.E. Johnson, unpublished data), it is possible that the aa-tRNA undergoes an additional conformational change upon binding to the ribosomal complex. Whatever the case, the additional spectral change will permit the evaluation of the thermodynamics and kinetics of the aa-tRNA interaction with the ribosomal complex and its dependence upon EF-Tu.

LITERATURE CITED

Adkins, H. J., Ph.D. dissertation, University of Oklahoma (1982).

Adkins, H. J., Miller, D. L., and Johnson, A. E. (1983) Biochemistry 22, 1208-1217.

Andersson, D. I., and Kurland, C. G. (1983) Mol. Gen. Genet. 191, 378-381.

Arai, K., Kawakita, M., and Kaziro, Y. (1974) J. Biochem. (Tokyo) 76, 293-306.

Arai, K., Clark, B. F. C., Duffy, L., Jones, M. D., Kaziro, Y., Laursen, R. A., L'Italien, J., Miller, D. L., Nagarkatti, S., Nakamura, S., Nielsen, K. M., Petersen, T. E., Takahashi, K., and Wade, M. (1980) Proc. Natl. Acad. Sci. U.S.A. 77, 1326-1330.

Bachman, B. J., and Low, K. B. (1980) Microbiol. Rev. 44, 1-56.

Beck, B. D., Arscott, P. G., and Jacobson, A. (1978) Proc. Natl. Acad. Sci. U.S.A. 75, 1250-1254.

Beres, L., and Lucas-Lenard, J. (1973) Biochemistry 12, 3998-4002.

Bertram, S., and Wagner, R. (1982) Biochemistry Int. 4, 117-126.

Block, W., and Pingoud, A. (1981) Anal. Biochem. 114, 112-117.

Boutorin, A. S., Clark, B. F. C., Ebel, J. P., Kruse, T. A., Petersen, H. U., Remy, P., and Vassilenko, S. (1981) J. Mol. Biol. 152, 593-608.

Carey, J., and Uhlenbeck, O. C. (1983a) Biochemistry 22, 2601-2610.

Carey, J., and Uhlenbeck, O. C. (1983b) Biochemistry 22, 2610-2615.

Crothers, D. M., and Cole, P. E. (1978) in Transfer RNA (Altman, S., Ed.) pp 196-247, MIT Press, Cambridge, MA.

Derwenskus, K.-H. and Sprinzl, M. (1983) FEBS Lett. 151, 143-147.

Duffy, L. K., Gerber, L., Johnson, A. E., and Miller, D. L. (1981)

Biochemistry 20, 4663-4666.

Duisterwinkel, F. J., Kraal, B., De Graaf, J. M., Talens, A., Bosch, L., Swart, G. W. M., Parmeggiani, A., La Cour, T. F. M., Nyborg, J., and Clark, B. F. C. (1984) EMBO Journal 3, 113-120.

Eshaghpour, H., Soll, D., and Crothers, D. M. (1979) Nucleic Acids Res. 7, 1485-1495.

Furano, A. V. (1975) Proc. Natl. Acad. Sci. U.S.A. 72, 4780-4784.

Gavrilova, L. P., Kostiashkina, O. E., Koteliansky, V. E., Rutkevitch, N. M., and Spirin, A. S. (1976) J. Mol. Biol. 101, 537-552.

Grunberg-Manago, M., Buckingham, R. H., Cooperman, B. S, and Hershey, J. W. B. (1978) Symp. Soc. Gen. Microbiol. 28, 27-110.

Heerschap, A., Haasnoot, C. A. G., and Hilbers, C. W., (1983) Nucleic Acids Res. 11, 4501-4520.

Hopfield, J. J. (1974) Proc. Natl. Acad. Sci. U.S.A. 71, 4135-4139.

Ingraham, J. L., Maaløe, O., and Neidhardt, F. C. (1983) Growth of the Bacterial Cell, p. 3, Sinauer Associates, Sunderland, MA.

Jacobson, G. R., and Rosenbusch, J. P. (1976) Nature 261, 23-26.

Jekowsky, E., Schimmel, P., and Miller, D. L. (1977) J. Mol. Biol. 114, 451-458.

Jelenc, P. C. (1980) Anal. Biochem. 105, 369-374.

Jelenc, P. C., and Kurland C. G. (1979) Proc. Natl. Acad. Sci. U.S.A. 76, 3174-3178.

Johnson, A. E., and Adkins, H. J. (1984) Anal. Biochem. 137, 351-359.

Johnson, A. E., and Cantor, C. R. (1980) J. Mol. Biol. 138, 273-297.

Johnson, A. E., and Slobin, L. I. (1980) Nucleic Acids Res. 8, 4185-4200.

Johnson, A. E., Miller, D. L., and Cantor, C. R. (1978) Proc. Natl. Acad. Sci. U.S.A. 75, 3075-3079.

Johnson, A. E., Adkins, H. J., Matthews, E. A., and Cantor, C. R. (1982) J. Mol. Biol. 156, 113-140.

Johnson, A. E., Woodward, W. R., Herbert, E., and Menninger, J. R. (1976) Biochemistry 15, 569-575.

Johnson, M. L. (1983) Biophys. J. 44, 101-106.

Johnson, M. L., and Frasier, S. G. (1984) Methods Enzymol., in press.

Johnson, M. L., Correia, J. J., Halvorson, H. R., and Yphantis, D. A. (1981) Biophys. J. 36, 575-588.

Jonák, J., Smrt, J., Holý, A., and Rychlík, I. (1980) Eur. J. Biochem. 105, 315-320.

Jones, M. D., Petersen, T. E., Nielsen, K. M., Magnusson, S., Sottrup-Jensen, L., Gausing, K., and Clark, B. F. C. (1980). Eur. J. Biochem. 108, 507-526.

Jurnak, F., McPherson, A., Wang, A. H. J., and Rich, A. (1980) J. Biol. Chem. 255, 6751-6757.

Kabsch, W., Gast, W. N., Schulz, G. E., and Leberman, R. (1977) J. Mol. Biol. 117, 999-1012.

Knowlton, R. G., and Yarus, M. (1980) J. Mol. Biol. 139, 721-732.

Klotz, I. M. (1982) Science 217, 1247-1249.

Krauskopf, M., Chen, C.-M., and Ofengand, J. (1972) J. Biol. Chem. 247, 842-850.

Krauss, G., Riesner, D., and Maass, G. (1976) Eur. J. Biochem. 68, 81-93.

Kruse, T. A., Clark, B. F. C., and Sprinzl, M. (1978) Nucleic Acids Res. 5, 879-892.

Kruse, T. A., Siboska, G. E., Sprinzl, M., Clark, B. F. C. (1980) Eur. J. Biochem. 107, 1-6.

Kurland, C. G. (1977) Annu. Rev. Biochem. 46, 173-200.

Leupold, C. M., Goody, R. S., and Wittinghofer, A. (1983) Eur. J. Biochem. 135, 237-241.

Lohman, T. M., deHaseth, P. L., and Record M. T., Jr. (1980) Biochemistry 19, 3522-3530.

Louie, A., Ribiero, N. S., Reid, B. R., and Jurnak, F. (1984) J. Biol. Chem. 259, 5010-5016.

Mercola, D. A., Morris, J. W. S, and Arquilla, E. R. (1972) Biochemistry 11, 3860-3874.

Miller, D. L., and Weissbach, H. (1974) Methods Enzymol. 30, 219-232.

Miller, D. L., and Weissbach, H. (1977) in Nucleic Acid-Protein Recognition (Vogel, H. J., Ed.) pp 409-440, Academic Press, New York.

Miller, D. L., Cashel, M., and Weissbach, H. (1973) Arch. Biochem. Biophys. 154, 675-682.

Ninio, S. (1975) Biochimie 57, 587-595.

Ofengand, J. (1974) Methods Enzymol. 29, 661-667.

Ofengand, J., and Chen, C.-M. (1972) J. Biol. Chem. 247, 2049-2058.

Picone, D., and Parmeggiani, A. (1983) Biochemistry 22, 4400-4405.

Pingoud, A, and Urbanke, C. (1980) Biochemistry 19, 2108-2112.

Pingoud, A., Kownatzki, R., and Maass, G. (1977a) Nucleic Acids Res. 4, 327-338.

Pingoud, A., Urbanke, C., Krauss, G., Peters, F., and Maass, G. (1977b) Eur. J. Biochem. 78, 403-409.

Ravel, J. M. and Shorey, R. L. (1969) J. Cell. Physiol. 74: Sup. 1, 103-116.

Ravel, J. M., Shorey, R. L., and Shive, V. (1967) Biochem. Biophys. Res. Commun. 29, 68-73.

Record, M. T., Jr., Anderson, C. F., and Lohman, T. M. (1978) Q. Rev. Biophys. 11, 103-178.

Record, M. T., Jr., Lohman, T. M., and deHaseth, P. (1976) J. Mol. Biol. 107, 145-158.

Rich, A., and Kim, S. H. (1978) Sci. Am. 238, 52-62.

Robertson, J. M., and Wintermeyer, W. (1981) J. Mol. Biol. 151, 57-79.

Rubin, J. R., Morikawa, K., Nyborg, J., La Cour, T. F. M., Clark, B. F. C., and Miller, D. L. (1981) FEBS Lett. 129, 177-179.

Ruusala, T., Ehrenberg, M., and Kurland, C. G. (1982) EMBO Journal 1, 741-745.

Scatchard, G. (1949) Ann. N.Y. Acad. Sci. 51, 660-672.

Sedlacek, J., Jonák, J., and Rychlík, I. (1976) FEBS Lett. 68, 208-210.

Shulman, R. G., Hilbers, C. W., and Miller, D. L. (1974) J. Mol. Biol. 90, 601-607.

Skjold, A. C., Juarez, H., and Hedgcoth, C. (1973) J. Bacteriol. 115, 177-187.

Sprinzl, M., and Faulhammer, H. (1978) Nucleic Acids Res. 5, 4837-4853.

Sprinzl, M., Gruter, F., and Gauss, D. H. (1978) Nucleic Acids Res. 5, r15-r27.

Sprinzl, M., Kucharzewski, M., Hobbs, J. B., and Cramer, F. (1977) Eur. J. Biochem. 78, 55-61.

Tanada, S., Kawakami, M., Yoneda, T., and Takemura, S. (1981) J. Biochem. (Tokyo) 89, 1565-1572.

Tanada, S., Kawakami, M., Nishio, K., and Takemura, S. (1982) J. Biochem. (Tokyo) 91, 291-299.

Thompson, R. C., and Stone, P. J. (1977) Proc. Natl. Acad. Sci. U.S.A. 74, 198-202.

Thompson, R. C., Dix, D. B., Gerson, R. B., and Karim, A. M. (1981) J. Biol. Chem. 256, 81-86.

Travers, A. (1976) Nature 263, 641-646.

van der Meide, P. H., Vijgenboom, E., Dicke, M., and Bosch, L. (1982) FEBS Lett. 139, 325-330.

van der Meide, P. H., Vijgenboom, E., Talens, A., and Bosch, L. (1983) Eur. J. Biochem. 130, 397-407.

Wagner, T., and Sprinzl, M. (1980) Eur. J. Biochem. 108, 213-221.

Wagner, T., Jelenc, P. C., Ehrenberg, M., and Kurland, C. G. (1982) Eur. J. Biochem. 122, 193-197.

Wikman, F. P., Siboska, G. E., Petersen, H. U., and Clark, B. F. C. (1982) EMBO Journal 1, 1095-1100.

Wittinghofer, A., Frank, R., Gast, W. H., and Leberman, R. (1979) J. Mol. Biol. 132, 253-256.

Yamane, T., Miller, D. L., and Hopfield, J. J. (1981) Biochemistry 21, 7059-7063.

APPENDIX A

This is an example of the programs used to obtain ternary complex dissociation constants from titrations of fluorescent aa-tRNAs with EF-Tu*GTP using a nonlinear least squares analysis. The statistical package available on the IBM 3081 which is capable of this type of analysis, among others, is "SAS", a product of the Statistical Analysis System (SAS Institute, Inc., Cary, NC). There are no line numbers here because SAS does not require numbered lines. An asterisk in front of a line indicates a comment statement, one which is to be ignored by SAS. The semicolon is the delimiter for ends of statements in SAS. The first section, all lines beginning with //, contains the job control language (JCL) required to run the program on the IBM 3081.

Each section which begins with DATA is called a "data step". This is where the data are read into the program from disk files, using INPUT statements. The first set of input values and their assigned variable names are (in order):

Date	DATE
Descriptive header 1	HDR1
Descriptive header 2	HDR2
Number of titration points	NPTS
Initial sample volume	VO
Sample volume after assay removal	V

Concentration of the aa-tRNA-F stock (A_{260}/mL)	CR
Volume of aa-tRNA-F added to sample (mL)	VR
Concentration of the EF-Tu*GDP stock solution (mg/mL)	CT
Volume to which EF-Tu is diluted to use as titrant (uL)	VU
Volume of EF-Tu diluted (uL)	VT
F_o integrated fluorescence intensity of Na_2Fluorescein sample	FF
F_o integrated fluorescence intensity for aa-tRNA-F sample	FS
Integrated fluorescence of blank	B

The next INPUT statement reads the values of the addition volume (uL), aa-tRNA-F sample integrated fluorescence, Na_2Fluorescein integrated fluorescence, and time from the previous scan (min). Values for the various concentrations and the fluorescence for each point in a titration are calculated in the data step, using the input values from the data file, other measured quantities (e.g. $F/F_{o(max)}$, acid-insoluble radioactivity), an estimate for K_d, and the deacylation rate. The calculated values are then stored with the input values in temporary SAS data sets (called INx, where x is the number of the input data file) to be used in NLIN. Although the equations in each data step are the same, SAS requires the use of one data step for each input data file.

After the last data step, the data sets (IN1, IN2, etc.) are merged into a larger data set (ENTIRE) using the SET statement. Only the data sets specified in the SET statement will be used in the procedure (PROC) NLIN. For each point in a titration, this procedure calculates a value for the fluorescence (F) based on the computed concentrations (from the data steps) and on the estimated parameter(s) value(s) The PARMS statement lists the parameter(s) to be varied by NLIN to fit the data to the equation in the MODEL. NLIN fits the data using an iterative method

to converge on values for the parameter(s) which minimize the sum of the squares of the residuals (also called the residual sum of squares or SSE), where the residual = [actual value of F] - [predicted value of F]. When the convergence criterion are met, the converged value is output, along with a 95% asymtotic confidence interval, and a table of correlation coefficients for the parameters.

The next section in the program uses other SAS procedures to aid in the analysis of the goodness-of-fit. PROC GLM (general linear model) fits the residuals to polynomials to the third degree in T_t and F. The last procedure, PROC PLOT, plots the actual data overlaid with the calculated values, and the residuals both as a function of T_t and F.

```
//LOGONIDK JOB NOlNOZIT,'JA:NL-BND',CLASS=J,TIME=(1,Ø),
//      PASSWORD=XXXXXX,NOTIFY=LOGONID,
//      MSGCLASS=C
/*JOBPARM D=R3
/*JOBPARM C=2ØØØØ,L=1Ø
/*ROUTE   PUNCH PHSC
//NLINBND EXEC SAS
//FT2ØFØØ1 DD DSN=AB13ØØ.GRIDBIG.DATA,
//       UNIT=TSODISK,DISP=OLD,
//       DCB=(RECFM=FB,LRECL=133,BLKSIZE=133Ø)
//INDATA1 DD DSN=AB3248.TUØ4Ø283.DATA,
//       UNIT=TSODISK,DISP=SHR,
//       DCB=(RECFM=FB,LRECL=8Ø,BLKSIZE=32ØØ)
//INDATA2 DD DSN=AB3248.TUØ31483.DATA,
//       UNIT=TSODISK,DISP=SHR,
//       DCB=(RECFM=FB,LRECL=8Ø,BLKSIZE=32ØØ)
//INDATA3 DD DSN=AB3248.TU122Ø82.DATA,
//       UNIT=TSODISK,DISP=SHR,
//       DCB=(RECFM=FB,LRECL=8Ø,BLKSIZE=32ØØ)
//INDATA4 DD DSN=AB3248.TU11Ø382.DATA,
//       UNIT=TSODISK,DISP=SHR,
//       DCB=(RECFM=FB,LRECL=8Ø,BLKSIZE=32ØØ)
//SYSIN DD *
 TITLE PHE HEPES PH 7.6 DK=1.1ØE-3 KD=Ø.84NM;
  DATA IN1;
       INFILE INDATA1;
         INPUT DATE $1-7Ø #2 HDR1 $1-7Ø #3 HDR2 $1-7Ø #4 NPTS 2.
               #5 VØ #6 V #7 CR #8 VR #9 CT #1Ø VU #11 VT #12 FF
               #13 FS #14 B @;
            FI=Ø.998 ;
```

```
          NDSN=1;
          KDEST=Ø.84E-9; K2EST=1.1E-3;
          Y=873/16ØØ; Y1=791/16ØØ;
          Z=1.Ø;
          FMAX=1.176;
          V=V*1E-6;VØ=VØ*1E-6; CT=Z*CT*2.31E-5; T=CT*VT/VU;
          RT=CR*1.6E-9*VR/VØ; RAØ=RT*Y;
         TT=Ø; VC=1.Ø; FØ=FS-B; ADDT=Ø;VT=V;TIME=Ø;RA=RAØ;VPREV=V;
        DO I = 1 TO NPTS  ;
            INPUT / ADDN 1-8 / TRNA  1-8 / NA2F 1-8  DTIME 11-2Ø @;
              TIME=TIME+DTIME;
              TEMP=(TT+RA+KDEST);
              RB=(TEMP-SQRT(TEMP*TEMP-4*RA*TT))/2;
              RA=(RB+(RA-RB)*EXP(-K2EST*DTIME));
              ADDN=ADDN*1E-6;
              ADDT=ADDT+ADDN;
              VPREV=VT;
              VT=VT+ADDN;
              TT=ADDT*T/VT;
              VCTOT=VT/V; VC=VT/VPREV;
              RT=RT/VC;
              RA=RA/VC;
              RB=RB/VC;
              RE=RT*Y1;
              F=(TRNA*VCTOT-B)/FØ;
            OUTPUT;
        END;
            INPUT;
DATA IN2;
     INFILE INDATA2;
       INPUT DATE $1-7Ø #2 HDR1 $1-7Ø #3 HDR2 $1-7Ø #4 NPTS 2.
             #5 VØ #6 V #7 CR #8 VR #9 CT #1Ø VU #11 VT #12 FF
             #13 FS #14 B @;
         FI=1.ØØØ1;
         NDSN=2;
         KDEST=Ø.84E-9; K2EST=1.1E-3;
         Y=885/16ØØ; Y1=836/16ØØ;
         Z=1.Ø;
         FMAX=1.221;
         V=V*1E-6;VØ=VØ*1E-6; CT=Z*CT*2.31E-5; T=CT*VT/VU;
         RT=CR*1.6E-9*VR/VØ; RAØ=RT*Y;
         TT=Ø; VC=1.Ø; VPREV=V;FØ=FS-B; ADDT=Ø;VT=V;TIME=Ø;RA=RAØ;
        DO I = 1 TO NPTS  ;
            INPUT / ADDN 1-8 / TRNA  1-8 / NA2F 1-8  DTIME 11-2Ø @;
              TIME=TIME+DTIME;
              TEMP=(TT+RA+KDEST);
              RB=(TEMP-SQRT(TEMP*TEMP-4*RA*TT))/2;
              RA=(RB+(RA-RB)*EXP(-K2EST*DTIME));
              ADDN=ADDN*1E-6;
              ADDT=ADDT+ADDN;
              VPREV=VT;
              VT=VT+ADDN;
              TT=ADDT*T/VT;
```

```
            VCTOT=VT/V; VC=VT/VPREV;
            RT=RT/VC;
            RA=RA/VC;
            RB=RB/VC;
            RE=RT*Y1;
            F=(TRNA*VCTOT-B)/FØ;
          OUTPUT;
      END;
          INPUT;
DATA IN3;
     INFILE INDATA3;
       INPUT DATE $1-7Ø #2 HDR1 $1-7Ø #3 HDR2 $1-7Ø #4 NPTS 2.
             #5 VØ #6 V #7 CR #8 VR #9 CT #1Ø VU #11 VT #12 FF
             #13 FS #14 B @;
         FI=Ø.994;
         NDSN=3;
         KDEST=Ø.84E-9; K2EST=1.1E-3;
         Y=941/16ØØ; Y1=824/16ØØ;
         Z=1.Ø;
         FMAX=1.214;
         V=V*1E-6;VØ=VØ*1E-6; CT=Z*CT*2.31E-5; T=CT*VT/VU;
         RT=CR*1.6E-9*VR/VØ; RAØ=RT*Y;
         TT=Ø; VC=1.Ø; VPREV=V;FØ=FS-B; ADDT=Ø;VT=V;TIME=Ø;RA=RAØ;
       DO I = 1 TO NPTS  ;
           INPUT / ADDN 1-8 / TRNA  1-8 / NA2F 1-8  DTIME 11-2Ø @;
             TIME=TIME+DTIME;
             TEMP=(TT+RA+KDEST);
             RB=(TEMP-SQRT(TEMP*TEMP-4*RA*TT))/2;
             RA=(RB+(RA-RB)*EXP(-K2EST*DTIME));
             ADDN=ADDN*1E-6;
             ADDT=ADDT+ADDN;VPREV=VT;
             VT=VT+ADDN;
             TT=ADDT*T/VT;
             VCTOT=VT/V; VC=VT/VPREV;
             RT=RT/VC;
             RA=RA/VC;
             RB=RB/VC;
             RE=RT*Y1;
             F=(TRNA*VCTOT-B)/FØ;
           OUTPUT;
       END;
           INPUT;
DATA IN4;
     INFILE INDATA4;
       INPUT DATE $1-7Ø #2 HDR1 $1-7Ø #3 HDR2 $1-7Ø #4 NPTS 2.
             #5 VØ #6 V #7 CR #8 VR #9 CT #1Ø VU #11 VT #12 FF
             #13 FS #14 B @;
         FI=Ø.998;
         NDSN=4;
         KDEST=Ø.84E-9; K2EST=1.1E-3;
         Y=78Ø/16ØØ; Y1=679/16ØØ;
         Z=1.Ø;
         FMAX=1.124;
```

```
          V=V*1E-6;VØ=VØ*1E-6; CT=Z*CT*2.31E-5; T=CT*VT/VU;
          RT=CR*1.6E-9*VR/VØ; RAØ=RT*Y;
          TT=Ø; VC=1.Ø; FØ=FS-B; ADDT=Ø;VT=V;TIME=Ø;RA=RAØ; VPREV=V;
        DO I = 1 TO NPTS  ;
            INPUT / ADDN 1-8 / TRNA  1-8 / NA2F 1-8  DTIME 11-2Ø @;
              TIME=TIME+DTIME;
              TEMP=(TT+RA+KDEST);
              RB=(TEMP-SQRT(TEMP*TEMP-4*RA*TT))/2;
              RA=(RB+(RA-RB)*EXP(-K2EST*DTIME));
              ADDN=ADDN*1E-6;
              ADDT=ADDT+ADDN;
              VPREV=VT;
              VT=VT+ADDN;
              TT=ADDT*T/VT;
              VCTOT=VT/V; VC=VT/VPREV;
              RT=RT/VC;
              RA=RA/VC;
              RB=RB/VC;
              RE=RT*Y1;
              F=(TRNA*VCTOT-B)/FØ;
            OUTPUT;
        END;
            INPUT;
 DATA ENTIRE;
    SET IN1 IN2 IN3 IN4 ;
   PROC PRINT;
   VAR NDSN TT RA RE RB RAØ;
 DATA ;
    SET ENTIRE;
    KEEP F FMAX Y1 RA RT TT;
PROC SORT;
   BY TT;
*PROC PRINTTO UNIT=2Ø NEW;
* OPTIONS NOCENTER ;
PROC NLIN METHOD=DUD EFORMAT ;
* PARMS KD=1E-11 TO 1ØØE-11 BY 2E-11 FI=Ø.98 TO 1.Ø2 BY Ø.ØØ1;
 PARMS KD=1E-1Ø FI=1.Ø ;
    BOUNDS KD>1E-15 ;
              D=(FMAX+Y1-1)/Y1;
              S1=(D-1)/(2*RT);
              S2=(RA+TT+KD);
   MODEL F=FI+(S1*(S2-SQRT(S2*S2-4*RA*TT)));
   OUTPUT OUT=E1 P=FHAT R=RESID PARMS=KD ;
PROC GLM ;
   MODEL RESID=TT TT*TT TT*TT*TT;
PROC GLM ;
   MODEL RESID=F F*F F*F*F;
PROC PLOT ;
   PLOT F*TT='+' FHAT*TT='X' / OVERLAY ;
   PLOT RESID*TT / VREF=Ø.Ø;
   PLOT RESID*F / VREF=Ø.Ø;
  /*
```

APPENDIX B

This is the BASIC program which was written for use on an Apple II Plus microcomputer to obtain estimates for the ternary complex K_d from titrations of fluorescent aa-tRNAs with EF-Tu*GTP. Unlike the NLIN procedure in SAS which can analyze data from several combined data sets (see Appendices A and D), this program only evaluates data from one experiment. The first lines (20 to 90) define abbreviations for commands to the printer (NEC model PC-8023A-C). The next lines (through 360) are used select, open, read, and close the text file which contains the data. The input values are the same as in Appendix A (and in the same order), except that no times are entered for the individual titration points. When the program is run, the user enters values for the acid-insoluble radioactivity at the beginning and end of the experiment, the fractional activity of the EF-Tu (=1, in all of my analyses), and the $F/F_{o(max)}$, in the INPUT statements. The input values are used to calculate a K_d at each titration point using the relationships in equations 1 through 5 (see Chapter II). An average K_d is calculated for the specified number of points in the titration.

```
2Ø UL$(Ø) = CHR$ (27) + CHR$ (88): REM UNDERLINE ON
3Ø UL$(1) = CHR$ (27) + CHR$ (89): REM UNDERLINE OFF
4Ø GC$ = CHR$ (27) + CHR$ (38): REM SELECT GREEK CHARACTER SET
5Ø AS$ = CHR$ (27) + CHR$ (36): REM ASCII ON
6Ø FF$ = CHR$ (12): REM FORM FEED
7Ø LF$ = CHR$ (1Ø): REM LINE FEED
```

```
8Ø LM$ = CHR$ (27) + "LØ1Ø": REM LEFT MARGIN SET TO 1Ø
9Ø CR$ = CHR$ (13)
1ØØ PRINT LM$
         DISK DRIVE
13Ø REM ************************
14Ø REM ***** TULIP ************
15Ø REM ************************
16Ø DIM A(3Ø,99)
17Ø REM DATA FILE READ IN HERE
18Ø D$ = CHR$ (4)
19Ø INPUT "FILE TO BE USED: ";A$
2ØØ INPUT "DRIVE LOCATION OF FILE:";DR%
21Ø IF DR% < 1 OR DR% > 2 GOTO 2ØØ
22Ø PRINT LF$
23Ø POKE 33,4Ø: HOME : POKE 33,33
24Ø PRINT D$;"OPEN ";A$;",D";DR%
25Ø PRINT D$;"READ ";A$
26Ø ONERR GOTO 1Ø5Ø
27Ø INPUT B$(1),B$(2),B$(3),DP
28Ø INPUT VØ,V,CR,VR,CT,VU,VT,FF,FS,B
29Ø REM FF IS FØ(NA2F) ** FS IS FØ(SAMPLE)
3ØØ FOR J = 1 TO DP
31Ø FOR I = 1 TO 3
32Ø INPUT A(I,J)
33Ø NEXT
34Ø NEXT
35Ø PRINT D$"CLOSE"A$
36Ø PRINT "# DATA PTS. IN FILE: ";DP
37Ø PRINT UL$(Ø);B$(1);" ";B$(2);" ";B$(3);UL$(1)
38Ø INPUT "TCA AT FØ (PMOL/A26Ø) = ";Y
39Ø INPUT "TCA AT PLATEAU = ";Y1
4ØØ INPUT "FRACTION OF ACTIVE EF-TU = ";Z
41Ø INPUT "FMAX (MUST BE >1.Ø) = ";FM
42Ø INPUT "# DATA POINTS = ";P
43Ø IF P = Ø THEN GOTO 99Ø
44Ø HTAB 1: PRINT UL$(Ø);"TRNA";
45Ø HTAB 8: PRINT "TU";
46Ø HTAB 14: PRINT "F/FØ";
47Ø HTAB 22: PRINT "KD (E-9 M)";
48Ø HTAB 34: PRINT GC$"B";
49Ø HTAB 39: PRINT AS$"(Z*TU-TC)";UL$(1)
5ØØ AV = Ø:CYC = Ø:A1 = Ø
51Ø Y = Y / 16ØØ:Y1 = Y1 / 16ØØ
52Ø V = V * 1.ØE - 6:VØ = VØ * 1.ØE - 6:VU = VU * 1.ØE - 6:VT =
      VT * 1.ØE - 6
53Ø CT = CT * 2.31E - 5: REM CONC'N OF TU STOCK (M)
54Ø T = VT * CT / VU: REM T IS CONC'N OF TU IN 'T' (M)
55Ø TR = CR * 1.6E - 9 * VR / VØ: REM CONC'N OF TRNA IN SOL'N
      (M)
56Ø V1 = V: REM V IS VOL OF SOLN AT FØ
57Ø FØ = FS - B: REM SAMPLE FØ
58Ø F2 = (FM - 1 + Y1) / Y1
59Ø FOR J = 1 TO P
```

```
600 FOR I = 1 TO 3
610 A = A(1,J):F = A(2,J):G = A(3,J)
620 REM F =  SAMPLE FL; G = NA2F FL
630 A = A * 1.ØE - 6
640 A1 = A + A1: REM  A1 = TOTAL AMT OF 'T' IN SOL'N (TO HERE)
650 V1 = V1 + A: REM V1 = TOTAL VOL OF SOL'N
660 TU = A1 * T / V1: REM TU IS TU CONC'N IN SOL'N
670 VC = V1 / V: REM VC IS VOL CORRXN FACTOR
680 T1 = TR * Y / VC: REM T1 IS AA-TRNA CONC'N (TO HERE)
690 G = G / FF: REM G IS CORRXN FOR SIGNAL FLUXES
700 F = ((F * VC) / G - B) / FØ
710 FB = (F - 1) / (Y * F2 - Y)
720 TC = FB * T1
730 Z1 = Z * TU - TC
740 KD = (T1 * (1 - FB)) * Z1 / TC
750 AV = AV + KD:CYC = CYC + 1
760 KD = KD * 1.ØE9
770 TU = TU * 1.ØE9
780 T1 = T1 * 1.ØE9
790 T1$ = STR$ (T1):TU$ = STR$ (TU)
800 F$ = STR$ (F):KD$ = STR$ (KD)
810 HTAB 1: PRINT LEFT$ (T1$,4);
820 HTAB 7: PRINT LEFT$ (TU$,4);
830 HTAB 13: PRINT LEFT$ (F$,6);
840 HTAB 21: PRINT LEFT$ (KD$,6) + RIGHT$ (KD$,4);
850 N = 33: HTAB N
860 IF J = 1 GOTO 900
870 IF (K - KD) < = Ø THEN PRINT GC$"'";
880 IF (K - KD) > Ø THEN PRINT GC$")";
890 N = N + 1
900 ZZ$ = STR$ (Z1)
910 N = N + 3
920 HTAB N: PRINT AS$ LEFT$ (ZZ$,4) + RIGHT$ (ZZ$,4)
930 K = KD
940 NEXT J
950 F2$ = STR$ (F2)
960 PRINT UL$(Ø);"F2= "; LEFT$ (F2$,6);UL$(1)
970 AV = AV / CYC:AV$ = STR$ (AV)
980 PRINT UL$(Ø);"KD(AVG) = "; LEFT$ (AV$,6) + RIGHT$
       (AV$,4);UL$(1);" CYCLES = ";CYC
990 PRINT "ANOTHER RUN, SAME DATA? (FILE IS NOW ";A$;") (Y/N)": GET
       Z$
1000 IF Z$ = "Y" THEN GOTO 220
1010 PRINT "ANOTHER RUN, DIFFERENT DATA? (Y/N)": GET W$
1020 IF W$ = "Y" THEN GOTO 170
1030 POKE 33,40
1040 END
1050 PRINT "THIS FILE MAY NOT EXIST. DO YOU WISH TO DELETE '";A$  ;"'
       ? (Y/N)": INPUT Q$
1060 IF Q$ = "N" THEN GOTO 990
1070 PRINT "ARE YOU SURE YOU WANT TO DELETE THIS FILE? (Y/N)":
       INPUT R$
1080 IF R$ = "N" THEN GOTO 990
```

```
1Ø9Ø PRINT
11ØØ PRINT D$;"DELETE"A$
111Ø GOTO 1Ø1Ø
```

APPENDIX C

The determination of the 67% confidence intervals for the K_d values obtained from NLIN is a multistep procedure. First, the NLIN program, such as the ones given in Appendices A and D, is run with a few changes. (i) The best estimates of the parameter value(s) is inserted in each of the data steps. (ii) The asterisks preceding the PROC PRINTTO and OPTIONS statements (immediately before the PROC NLIN statement) are removed. The PROC PRINTTO tells SAS to send the output, i.e. everything normally output by PROC NLIN, to a specified file. (iii) The PARMS statement under PROC NLIN is changed to specify the grid of values of the parameter(s) which is to be examined. (iv) The procedures for analyzing the residuals of the fit are removed or converted to comments (with *). (v) Often the time allowed for running the NLIN program as a background job must be extended to permit it to be run, because it requires more computer time than when NLIN is run without a parameter grid to be evaluated.

The next step requires the modification of the output from NLIN to make it compatible with the program which determines the confidence interval. This involves deleting everything from the file containing the output from NLIN except a title, the converged values of the parameters, the number of degrees of freedom, the residual sum of squares at the converged minimum (in that order), and the listing of the

individual points in the grid with their corresponding residual sums of squares. The first few lines of one output data file in its modified form is given below:

```
 P VS P HEPES KD1=Ø.85NM KD2=9.6E-11M DK1=1.1E-3 DK2=1.1E-3
1.ØØ667549E+ØØ 9.58688265E-11 43 3.52223960E-Ø3
 1.ØØØØE-11 9.95ØØE-Ø1 1.54446995E-Ø2
 1.ØØØØE-11 9.97ØØE-Ø1 1.29267575E-Ø2
 1.ØØØØE-11 9.99ØØE-Ø1 1.Ø7688156E-Ø2
 1.ØØØØE-11 1.ØØ1ØE+ØØ 8.97Ø87361E-Ø3
 1.ØØØØE-11 1.ØØ3ØE+ØØ 7.53293164E-Ø3
 1.ØØØØE-11 1.ØØ5ØE+ØØ 6.45498968E-Ø3
 1.ØØØØE-11 1.ØØ7ØE+ØØ 5.737Ø4772E-Ø3
 1.ØØØØE-11 1.ØØ9ØE+ØØ 5.37910576E-Ø3
```

Once the file with the NLIN output file is modified, it is used as the input data for the program listed below. Here, after the file has been read (INPUT), the ratio of the residual sum of squares (SSE) for each value of the parameter(s) to the residual sum of the squares at the converged minimum (SSEMIN) is evaluated. The level of significance of this ratio is determined using a probability function (PROBF) and the number of degrees of freedom (DF). Those values of the parameter(s) which yield a ratio of the sums of the squares of the errors of the residuals with a significance level between Ø.3Ø and Ø.35 are included in the output from this program (by the IF ... THEN statement). The values to be output are sorted by increasing value of the parameter(s) before the output is printed. The list of the significance levels for the parameter value(s) is examined to find the minimum and maximum values of the parameter which yield a significance level of Ø.33 (or greater) to give the 67% confidence interval. If the lower or upper limit of the confidence interval is the same as the limit of the values of the parameter which were tested, the range (or increment) of the grid

must be adjusted in the NLIN procedure to reevaluate the confidence interval.

```
//LOGONIDE JOB NO1NOZIT,'JA:NL-BND',CLASS=J,TIME=(Ø,3Ø),
//      REGION=3338K,PASSWORD=XXXXXX,NOTIFY=LOGONID,
//      MSGCLASS=C
/*JOBPARM D=R3
/*JOBPARM C=2ØØØØ,L=2Ø
/*ROUTE    PUNCH PHSC
//FSTAT    EXEC SAS
//INDATA   DD DSN=AB13ØØ.GRIDBIG.DATA,
//       UNIT=TSODISK,DISP=SHR,
//       DCB=(RECFM=FB,LRECL=133,BLKSIZE=133Ø)
//SYSIN DD *
DATA;
         INFILE INDATA END=LASTOBS;
   INPUT HDR $ 1-8Ø / FIMIN KDMIN DF SSEMIN @;
      DO UNTIL(LASTOBS=1);
           INPUT / KDEST FIEST SSE @;
              X=SSE/SSEMIN;
              SIGL=2*(1-PROBF(X,DF,DF));
                 IF SIGL<Ø.35 AND SIGL>Ø.3Ø THEN OUTPUT;
*             OUTPUT;
      END;
     INPUT;
     CALL SYMPUT('KMIN',KDMIN);
     CALL SYMPUT('FMIN',FIMIN);
     CALL SYMPUT('XXX',HDR);
PROC SORT;
    BY KDEST ;
*PROC PRINTTO UNIT=2Ø NEW;
TITLE &XXX;
TITLE2 CONVERGED FI=&FMIN;
TITLE3 CONVERGED KD=&KMIN ;
PROC PRINT;
    VAR SIGL KDEST FIEST ;
PROC SORT;
  BY FIEST;
PROC PRINT;
    VAR SIGL KDEST FIEST ;
/*
```

APPENDIX D

This is an example of the programs used to obtain dissociation constants for the ternary complex of an unmodified non-fluorescent aa-tRNA using a nonlinear least squares analysis. This type analysis procedure was used for experiments in which a mixture of the unmodified and a fluorescent aa-tRNA were titrated with EF-Tu*GTP. The form of this program is very similar to that of the program listed in Appendix A. The differences in this particular program arise in the equations which calculate values for concentrations pertaining to the unmodified aa-tRNA. Thus within each data step, the additional values in the first INPUT statement, CS and VS, are the concentration of the unmodified aa-tRNA stock (A_{260}/mL) and the volume of the unmodified aa-tRNA added to the sample, respectively. After the second INPUT statement in a data step, a series of equations (from DEACYL to RETURN) are required to calculate the concentration of the bound aa-tRNA-F using the relationships in equations 9, 10, and 11 (see Chapter II), and to correct for the deacylation of both aa-tRNAs. As noted in Appendix A, although the equations in each data step are the same, SAS requires a separate data step for each set of data input from a file.

In the NLIN procedure, the data are fit to a model based on equation 8. This expression requires the calculation of the concentration of the bound aa-tRNA-F, and hence a series of equations

similar to those in the individual data steps.

```
//LOGONIDP JOB NOINOZIT,'JA:NL-BND',CLASS=J,TIME=(1,00),
//      REGION=3338K,PASSWORD=XXXXXX,NOTIFY=LOGONID,
//      MSGCLASS=C
/*JOBPARM D=R3
/*JOBPARM C=20000
/*ROUTE   PUNCH PHSC
//NLINBND EXEC SAS,REGION=3338K
//VECTR2  DD DSN=&VECTR2,SPACE=(CYL,(60,3)),UNIT=SYSDA
//FT20F001 DD DSN=AB1300.GRIDBIG.DATA,
//       UNIT=TSODISK,DISP=OLD,
//       DCB=(RECFM=FB,LRECL=133,BLKSIZE=1330)
//INDATA1 DD DSN=AB3248.CRP61683.DATA,
//       UNIT=TSODISK,DISP=SHR,
//       DCB=(RECFM=FB,LRECL=80,BLKSIZE=3200)
//INDATA2 DD DSN=AB3248.CR062283.DATA,
//       UNIT=TSODISK,DISP=SHR,
//       DCB=(RECFM=FB,LRECL=80,BLKSIZE=3200)
//INDATA3 DD DSN=AB3248.CR111283.DATA,
//       UNIT=TSODISK,DISP=SHR,
//       DCB=(RECFM=FB,LRECL=80,BLKSIZE=3200)
//INDATA4 DD DSN=AB3248.CR051384.DATA,
//       UNIT=TSODISK,DISP=SHR,
//       DCB=(RECFM=FB,LRECL=80,BLKSIZE=3200)
//SYSIN DD *
TITLE'P VS P HEPES KD1=0.85NM KD2=9.6E-11M DK1=1.1E-3 DK2=1.1E-3';
TITLE2 '4 DATA SETS COMBINED '    ;
*****************************************************************;
***       READ IN DATA FROM DD STMT LISTED IN INFILE          ****;
*****************************************************************;
 DATA IN1;
      INFILE INDATA1;
*****************************************************************;
***     INPUT VARIABLES THAT DESCRIBE INITIAL CONDITIONS      ****;
*****************************************************************;
      INPUT DATE $1-70 / HDR1 $1-70 / HDR2 $1-70 / NPTS 2. / V0 / V
                / CR / VR / CT / VU / VT / FF / FS / BL/ CS / VS @;
*****************************************************************;
***                VARIABLE DEFINITIONS                       ****
*****************************************************************
  NPTS=# OF DATA PTS.                  V0=INITIAL VOLUME
  V=VOLUME AT T=0 (AFTER TCA ASSAY) CR=CONCENTRATION OF TRNA1
  VR=VOLUME OF TRNA1                CT=CONCENTRATION OF TU STOCK
  VU=VOLUME OF TU STOCK              VT=VOLUME OF EACH TU ALIQUOT
  FF=INITIAL FLUORESCEIN SIGNAL      FS=INITIAL SAMPLE FLUORESCENCE
  BL=BLANK FLUORESCENCE               CS=AA-TRNA2 CONCENTRATION
  VS=AA-TRNA2 VOLUME
*****************************************************************;
**                   INSERT ESTIMATES HERE                     ****;
*****************************************************************;
          FI=1.05;          *INITIAL FLUORESCENCE;
```

```
        NDSN=1;            *DATA SET# (USED BY SOME SORTING PROCEDURES
                                WHEN THERE ARE MULTIPLE DATA SETS);
        KD1EST=0.85E-9; *ESTIMATED TU-TRNA1 KD;
            DK1=1.1E-3; *ESTIMATED DEACYLATION RATE FOR TRNA1;
        KD2EST=9.6E-11; *ESTIMATED TU-TRNA2 KD;
            DK2=1.1E-3; *ESTIMATED DEACYLATION RATE FOR TRNA2;
        Y=826/1600; *Y=FRACTION TRNA1 AMINO-ACYLATED AT T=0;
            Y1=748/1600; *Y1=FRACTION TRNA1 AMINO-ACYLATED AT END;
        Y2=840/1600; *Y2=FRACTION TRNA2 AMINO-ACYLATED AT T=0;
            Y3=756/1600; *Y3=FRACTION TRNA2 AMINO-ACYLATED AT END;
             Z=1;          *FRACTION OF TU THAT IS ACTIVE;
             FMAX=1.168; *MAXIMUM FLUORESCENCE CHANGE (I.E. THE
                                SPECIFIC FL-BOUND/FL-FREE;
*****************************************************************;
**          NORMALIZE UNITS OF VOLUME & CONCENTRATION          **;
**                  TO LITERS AND MOLAR                        **;
*****************************************************************;
        V=V*1E-6;V0=V0*1E-6; CT=Z*CT*2.31E-5; T=CT*VT/VU;
        RT=CR*1.6E-9*VR/V0; RA0=RT*Y;
        ST=CS*1.6E-9*VS/V0; SA0=ST*Y2;
        TT=0; VC=1.0;
        VPREV=V; F0=FS-BL; ADDT=0;VT=V;TIME=0;RA=RA0; SA=SA0;
*****************************************************************;
***            INPUT 3 'CARDS' PER DATA POINT:                 **;
***                1=VOLUME OF TU ADDITION                     **;
***                2=FLUORESCENCE OF TRNA SOLUTION             **;
***                3=FLUORESCENCE OF FLUORESCEIN STANDARD      **;
***                     & TIME INCREMENT FROM LAST SET         **;
***                     OF SCANS                               **;
*****************************************************************;
 DO I = 1 TO NPTS  ;
          INPUT / ADDN 1-8 / TRNA  1-8 / NA2F 1-8  DTIME 11-20 @;
            TIME=TIME+DTIME; *TOTAL TIME                        ;
    LINK DEACYL ;
            ADDN=ADDN*1E-6;    *TU VOLUME INCREMENT IN LITERS ;
            ADDT=ADDT+ADDN;    *TOTAL VOLUME OF TU ADDED      ;
            VPREV=VT;          *TOTAL VOL. AT PREV. POINT  ;
            VT=VT+ADDN;        *TOTAL SOLUTION VOLUME         ;
            TT=ADDT*T/VT;      *TOTAL CONCENTRATION TU        ;
            VC=VT/VPREV;       *VOLUME CORRECTION FACTOR      ;
            VCTOT=VT/V;        *OVERALL CORRXN FACTOR  ;
            RT=RT/VC;          *TRNA1 CONCENTRATION           ;
            RA=RA/VC;
            SA=SA/VC;
            SB=SB/VC;
            ST=ST/VC;          *TRNA2 CONCENTRATION           ;
            RE=RT*Y1;          *TRNA1 CONCENTRATION @ EXPT END;
            SE=ST*Y3;          *TRNA2 CONCENTRATION @ EXPT END;
            F=(TRNA*VCTOT-BL)/F0; *VOL-CONC CORRECTED FLUORESCENCE;
        OUTPUT;                *OUTPUT VALUES CALCULATED FOR
                                      THIS RECORD;
     END;
*****************************************************************;
```

```
**           INPUT FINAL CARD AND RELEASE DATA SET                **;
*****************************************************************;
         INPUT / COM $1-70; *COMMENT IS LAST RECORD OF FILE;
      STOP;                          *END EXECUTION OF THIS DATA STEP;
DEACYL:*********************************************************;
**             ESTIMATE RBEST IN PRESENCE OF DEACYLATION       **;
*****************************************************************;
**   CALCULATE COEFFICIENTS OF CUBIC EQUATION FOR TRNA1         **;
**               BOUND AT EACH DATA POINT                      **;
**     BASED ON VALUES FOR TU, AATRNA1, AATRNA2 AND KD1        **;
**FORM OF EQUATION   D*RBEST**3 + A*RBEST**2 + B*RBEST + C = 0**;
*****************************************************************;
*************D=COEFFICIENT*FOR*CUBIC*TERM**********************;
       D=(KD1EST-KD2EST);
*************A=COEFFICIENT*FOR*QUADRATIC*TERM*******************;
       A=(TT*KD2EST + 2*RA*KD2EST + KD1EST*KD2EST - RA*KD1EST +
       SA*KD1EST - TT*KD1EST - KD1EST**2);
*************B=COEFFICIENT*FOR*LINEAR*TERM**********************;
       B=-1*(RA*SA*KD1EST - RA*TT*KD1EST + 2*RA*TT*KD2EST
       + KD2EST*RA**2 + RA*KD1EST*KD2EST);
*******C=CONSTANT*TERM*******************************************;
       C=(KD2EST*TT*RA**2);
*****************************************************************;
**            DIVIDE COEFFICIENTS THROUGH BY D                 **;
**    RECAST AS RBEST**3 + P*RBEST**2 + Q*RBEST + R = 0        **;
*****************************************************************;
       P=A/D;     Q=B/D;     R=C/D;
*****************************************************************;
**          & SUBSTITUTE IN X=RBEST+P/3                        **;
**       TO GET FORM X**3 + AA*X + BB = 0, WHERE               **;
*****************************************************************;
       AA=(1/3)*(3*Q - P**2);
       BB=(1/27)*(2*P**3 - 9*P*Q + 27*R);
*****************************************************************;
**       FIND ROOTS TRIGONOMETRICALLY OF THIS EQUATION         **;
**       FROM ARCCOS(PHI) OF -BB/(2*SQRT(-1*AA**3/2))          **;
*****************************************************************;
       PHI = ARCOS(-BB/(2*SQRT(-1*AA**3/2)));
       PI=3.14159282;
*****************************************************************;
**       ROOT OF X IS 2*SQRT(-AA/3)*COS(PHI/3+2*PI/3)          **;
**             WHEN KD1EST < KD2EST                            **;
*****************************************************************;
    IF KD1EST<KD2EST THEN X= 2*SQRT(-AA/3)*COS(PHI/3+2*PI/3) ;
*****************************************************************;
**       ROOT OF X IS 2*SQRT(-AA/3)*COS(PHI/3+4*PI/3)          **;
**             WHEN KD1EST > KD2EST                            **;
*****************************************************************;
    IF KD1EST>KD2EST THEN X= 2*SQRT(-AA/3)*COS(PHI/3+4*PI/3) ;
*****************************************************************;
**               SET RBEST = X - P/3                           **;
*****************************************************************;
       RBEST= X - P/3 ;
```

```
*****************************************************************;
**        USE RBEST TO CALCULATE ESTIMATE OF RA                  **;
*****************************************************************;
      RA=(RBEST+(RA-RBEST)*EXP(-DK1*DTIME));
*****************************************************************;
**        USE RBEST TO CALCULATE ESTIMATE OF SA                  **;
*****************************************************************;
      TEMP=(TT-RBEST+SA+KD2EST);
      SB=(TEMP-SQRT(TEMP*TEMP-4*SA*(TT-RBEST)))/2;
      SA=(SB+(SA-SB)*EXP(-DK2*DTIME));
RETURN;
*****************************************************************;
***       READ IN DATA FROM DD STMT LISTED IN INFILE          ****;
*****************************************************************;
 DATA IN2;
      INFILE INDATA2;
*****************************************************************;
***    INPUT VARIABLES THAT DESCRIBE INITIAL CONDITIONS       ****;
*****************************************************************;
      INPUT DATE $1-7Ø / HDR1 $1-7Ø / HDR2 $1-7Ø / NPTS 2. / VØ / V
                / CR / VR / CT / VU / VT / FF / FS / BL/ CS / VS @;
*****************************************************************;
***              VARIABLE DEFINITIONS                         ****
*****************************************************************
  NPTS=# OF DATA PTS.                  VØ=INITIAL VOLUME
  V=VOLUME AT T=Ø (AFTER TCA ASSAY) CR=CONCENTRATION OF TRNA1
  VR=VOLUME OF TRNA1                  CT=CONCENTRATION OF TU STOCK
  VU=VOLUME OF TU STOCK                VT=VOLUME OF EACH TU ALIQUOT
  FF=INITIAL FLUORESCEIN SIGNAL        FS=INITIAL SAMPLE FLUORESCENCE
  BL=BLANK FLUORESCENCE                 CS=AA-TRNA2 CONCENTRATION
  VS=AA-TRNA2 VOLUME
*****************************************************************;
**                   INSERT ESTIMATES HERE                     ****;
*****************************************************************;
      FI=1.Ø6;         *INITIAL FLUORESCENCE;
      NDSN=2;            *DATA SET# (USED BY SOME SORTING PROCEDURES
                              WHEN THERE ARE MULTIPLE DATA SETS);
      KD1EST=Ø.85E-9; *ESTIMATED TU-TRNA1 KD;
          DK1=1.1E-3; *ESTIMATED DEACYLATION RATE FOR TRNA1;
      KD2EST=9.6E-11; *ESTIMATED TU-TRNA2 KD;
          DK2=1.1E-3; *ESTIMATED DEACYLATION RATE FOR TRNA2;
      Y=752/16ØØ; *Y=FRACTION TRNA1 AMINO-ACYLATED AT T=Ø;
          Y1=6/Ø/16ØØ; *Y1=FRACTION TRNA1 AMINO-ACYLATED AT END;
      Y2=79Ø/16ØØ; *Y2=FRACTION TRNA2 AMINO-ACYLATED AT T=Ø;
          Y3=7Ø9/16ØØ; *Y3=FRACTION TRNA2 AMINO-ACYLATED AT END;
           Z=1;          *FRACTION OF TU THAT IS ACTIVE;
           FMAX=1.151; *MAXIMUM FLUORESCENCE CHANGE (I.E. THE
                              SPECIFIC FL-BOUND/FL-FREE;
*****************************************************************;
****         NORMALIZE UNITS OF VOLUME & CONCENTRATION          **;
****                    TO LITERS AND MOLAR                     **;
*****************************************************************;
           V=V*1E-6;VØ=VØ*1E-6; CT=Z*CT*2.31E-5; T=CT*VT/VU;
```

```
          RT=CR*1.6E-9*VR/VØ; RAØ=RT*Y;
          ST=CS*1.6E-9*VS/VØ; SAØ=ST*Y2;
          TT=Ø; VC=1.Ø;
          VPREV=V; FØ=FS-BL; ADDT=Ø;VT=V;TIME=Ø;RA=RAØ; SA=SAØ;
*****************************************************************;
*****              INPUT 3 'CARDS' PER DATA POINT:              **;
*****                  1=VOLUME OF TU ADDITION                  **;
*****                  2=FLUORESCENCE OF TRNA SOLUTION          **;
*****                  3=FLUORESCENCE OF FLUORESCEIN STANDARD   **;
*****                       & TIME INCREMENT FROM LAST SET      **;
*****                       OF SCANS                            **;
*****************************************************************;
 DO I = 1 TO NPTS  ;
          INPUT / ADDN 1-8 / TRNA  1-8 / NA2F 1-8  DTIME 11-2Ø @;
            TIME=TIME+DTIME; *TOTAL TIME                         ;
    LINK DEACYL ;
            ADDN=ADDN*1E-6;    *TU VOLUME INCREMENT IN LITERS ;
            ADDT=ADDT+ADDN;    *TOTAL VOLUME OF TU ADDED      ;
            VPREV=VT;          *TOTAL VOL. AT PREV. POINT  ;
            VT=VT+ADDN;        *TOTAL SOLUTION VOLUME         ;
            TT=ADDT*T/VT;      *TOTAL CONCENTRATION TU        ;
            VC=VT/VPREV;       *VOLUME CORRECTION FACTOR      ;
            VCTOT=VT/V;        *OVERALL CORRXN FACTOR    ;
            RT=RT/VC;          *TRNA1 CONCENTRATION           ;
            RA=RA/VC;
            SA=SA/VC;
            SB=SB/VC;
            ST=ST/VC;          *TRNA2 CONCENTRATION           ;
            RE=RT*Y1;          *TRNA1 CONCENTRATION @ EXPT END;
            SE=ST*Y3;          *TRNA2 CONCENTRATION @ EXPT END;
            F=(TRNA*VCTOT-BL)/FØ; *VOL-CONC CORRECTED FLUORESCENCE;
        OUTPUT;                *OUTPUT VALUES CALCULATED FOR
                                    THIS RECORD;
     END;
*****************************************************************;
****           INPUT FINAL CARD AND RELEASE DATA SET           **;
*****************************************************************;
         INPUT / COM $1-7Ø; *COMMENT IS LAST RECORD OF FILE;
     STOP;                      *END EXECUTION OF THIS DATA STEP;
DEACYL:*******************************************************;
**            ESTIMATE RBEST IN PRESENCE OF DEACYLATION      **;
*******************************************************;
**   CALCULATE COEFFICIENTS OF CUBIC EQUATION FOR TRNA1      **;
**              BOUND AT EACH DATA POINT                     **;
**     BASED ON VALUES FOR TU, AATRNA1, AATRNA2 AND KD1      **;
**FORM OF EQUATION   D*RBEST**3 + A*RBEST**2 + B*RBEST + C = Ø**;
*******************************************************;
*******D=COEFFICIENT*FOR*CUBIC*TERM*************************;
        D=(KD1EST-KD2EST);
**********A=COEFFICIENT*FOR*QUADRATIC*TERM*******************;
        A=(TT*KD2EST + 2*RA*KD2EST + KD1EST*KD2EST - RA*KD1EST +
        SA*KD1EST - TT*KD1EST - KD1EST**2);
**********B=COEFFICIENT*FOR*LINEAR*TERM**********************;
```

```
        B=-1*(RA*SA*KD1EST - RA*TT*KD1EST + 2*RA*TT*KD2EST
        + KD2EST*RA**2 + RA*KD1EST*KD2EST);
**********C=CONSTANT*TERM*****************************************;
        C=(KD2EST*TT*RA**2);
*****************************************************************;
**            DIVIDE COEFFICIENTS THROUGH BY D                   **;
**    RECAST AS RBEST**3 + P*RBEST**2 + Q*RBEST + R = 0          **;
*****************************************************************;
      P=A/D;    Q=B/D;    R=C/D;
*****************************************************************;
**         & SUBSTITUTE IN X=RBEST+P/3                           **;
**      TO GET FORM X**3 + AA*X + BB = 0, WHERE                  **;
*****************************************************************;
      AA=(1/3)*(3*Q - P**2);
      BB=(1/27)*(2*P**3 - 9*P*Q + 27*R);
*****************************************************************;
**      FIND ROOTS TRIGONOMETRICALLY OF THIS EQUATION            **;
**      FROM ARCCOS(PHI) OF -BB/(2*SQRT(-1*AA**3/2/))            **;
*****************************************************************;
      PHI = ARCOS(-BB/(2*SQRT(-1*AA**3/2/)));
      PI=3.14159282;
*****************************************************************;
**      ROOT OF X IS 2*SQRT(-AA/3)*COS(PHI/3+2*PI/3)             **;
**            WHEN KD1EST < KD2EST                               **;
*****************************************************************;
    IF KD1EST<KD2EST THEN X= 2*SQRT(-AA/3)*COS(PHI/3+2*PI/3) ;
*****************************************************************;
**      ROOT OF X IS 2*SQRT(-AA/3)*COS(PHI/3+4*PI/3)             **;
**            WHEN KD1EST > KD2EST                               **;
*****************************************************************;
    IF KD1EST>KD2EST THEN X= 2*SQRT(-AA/3)*COS(PHI/3+4*PI/3) ;
*****************************************************************;
**              SET RBEST = X - P/3                              **;
*****************************************************************;
      RBEST= X - P/3 ;
*****************************************************************;
**        USE RBEST TO CALCULATE ESTIMATE OF RA                  **;
*****************************************************************;
      RA=(RBEST+(RA-RBEST)*EXP(-DK1*DTIME));
*****************************************************************;
**        USE RBEST TO CALCULATE ESTIMATE OF SA                  **;
*****************************************************************;
      TEMP=(TT-RBEST+SA+KD2EST);
      SB=(TEMP-SQRT(TEMP*TEMP-4*SA*(TT-RBEST)))/2;
      SA=(SB+(SA-SB)*EXP(-DK2*DTIME));
RETURN;
*****************************************************************;
***       READ IN DATA FROM DD STMT LISTED IN INFILE          ****;
*****************************************************************;
 DATA IN3;
     INFILE INDATA3;
 *****************************************************************;
 **    INPUT VARIABLES THAT DESCRIBE INITIAL CONDITIONS       ****;
```

```
*****************************************************************;
   INPUT DATE $1-7Ø / HDR1 $1-7Ø / HDR2 $1-7Ø / NPTS 2. / VØ / V
           / CR / VR / CT / VU / VT / FF / FS / BL / CS / VS @;
*****************************************************************
***              VARIABLE DEFINITIONS                         ****
*****************************************************************
  NPTS=# OF DATA PTS.                VØ=INITIAL VOLUME
  V=VOLUME AT T=Ø (AFTER TCA ASSAY) CR=CONCENTRATION OF TRNA1
  VR=VOLUME OF TRNA1                CT=CONCENTRATION OF TU STOCK
  VU=VOLUME OF TU STOCK              VT=VOLUME OF EACH TU ALIQUOT
  FF=INITIAL FLUORESCEIN SIGNAL      FS=INITIAL SAMPLE FLUORESCENCE
  BL=BLANK FLUORESCENCE               CS=AA-TRNA2 CONCENTRATION
  VS=AA-TRNA2 VOLUME
*****************************************************************
**                  INSERT ESTIMATES HERE                      ****
*****************************************************************
       FI=1.Ø6;          *INITIAL FLUORESCENCE;
       NDSN=3;             *DATA SET# (USED BY SOME SORTING PROCEDURES
                                WHEN THERE ARE MULTIPLE DATA SETS);
       KD1EST=Ø.85E-9; *ESTIMATED TU-TRNA1 KD;
           DK1=1.1E-3; *ESTIMATED DEACYLATION RATE FOR TRNA1;
       KD2EST=9.6E-11; *ESTIMATED TU-TRNA2 KD;
           DK2=1.1E-3; *ESTIMATED DEACYLATION RATE FOR TRNA2;
       Y=698/16ØØ; *Y=FRACTION TRNA1 AMINO-ACYLATED AT T=Ø;
           Y1=6/8/16ØØ; *Y1=FRACTION TRNA1 AMINO-ACYLATED AT END;
       Y2=816/16ØØ; *Y2=FRACTION TRNA2 AMINO-ACYLATED AT T=Ø;
           Y3=782/16ØØ; *Y3=FRACTION TRNA2 AMINO-ACYLATED AT END;
            Z=1;          *FRACTION OF TU THAT IS ACTIVE;
            FMAX=1.147; *MAXIMUM FLUORESCENCE (I.E. THE F/FØ MAX);
*****************************************************************
**          NORMALIZE UNITS OF VOLUME & CONCENTRATION          **
**                    TO LITERS AND MOLAR                      **
*****************************************************************
          V=V*1E-6;VØ=VØ*1E-6; CT=Z*CT*2.31E-5; T=CT*VT/VU;
          RT=CR*1.6E-9*VR/VØ; RAØ=RT*Y;
          ST=CS*1.6E-9*VS/VØ; SAØ=ST*Y2;
          TT=Ø; VC=1.Ø ;
          VPREV=V; FØ=FS-BL; ADDT=Ø;VT=V;TIME=Ø;RA=RAØ; SA=SAØ;
*****************************************************************
***              INPUT 3 'CARDS' PER DATA POINT:              **
***                  1=VOLUME OF TU ADDITION                  **
***                  2=FLUORESCENCE OF TRNA SOLUTION          **
***                  3=FLUORESCENCE OF FLUORESCEIN STANDARD   **
***                       & TIME INCREMENT FROM LAST SET      **
***                       OF SCANS                            **
*****************************************************************
 DO I = 1 TO NPTS  ;
         INPUT / ADDN 1-8 / TRNA  1-8 / NA2F 1-8  DTIME 11-2Ø @;
             TIME=TIME+DTIME; *TOTAL TIME                      ;
     LINK DEACYL;
             ADDN=ADDN*1E-6;     *TU VOLUME INCREMENT IN LITERS ;
             ADDT=ADDT+ADDN;     *TOTAL VOLUME OF TU ADDED      ;
             VPREV=VT;           *TOTAL VOL. AT PREV. POINT     ;
```

```
            VT=VT+ADDN;          *TOTAL SOLUTION VOLUME          ;
            TT=ADDT*T/VT;        *TOTAL CONCENTRATION TU         ;
            VC=VT/VPREV;         *VOLUME CORRECTION FACTOR       ;
            VCTOT=VT/V;          *OVERALL CORRXN FACTOR          ;
            RT=RT/VC;            *TRNA1 CONCENTRATION            ;
            RA=RA/VC;
            SA=SA/VC;
            SB=SB/VC;
            ST=ST/VC;            *TRNA2 CONCENTRATION            ;
            RE=RT*Y1;            *TRNA1 CONCENTRATION @ EXPT END;
            SE=ST*Y3;            *TRNA2 CONCENTRATION @ EXPT END;
            F=(TRNA*VCTOT-BL)/F0; *VOL-CONC CORRECTED FLUORESCENCE;
         OUTPUT;                 *OUTPUT VALUES CALCULATED FOR
                                        THIS RECORD;
      END;
*****************************************************************
**           INPUT FINAL CARD AND RELEASE DATA SET             **
*****************************************************************
         INPUT / COM $1-70; *COMMENT IS LAST RECORD OF FILE;
      STOP;                      *END EXECUTION OF THIS DATA STEP;
DEACYL:*********************************************************
**             ESTIMATE RBEST IN PRESENCE OF DEACYLATION       **
*****************************************************************
**   CALCULATE COEFFICIENTS OF CUBIC EQUATION FOR TRNA1         **
**               BOUND AT EACH DATA POINT                      **
**     BASED ON VALUES FOR TU, AATRNA1, AATRNA2 AND KD1        **
**FORM OF EQUATION   D*RBEST**3 + A*RBEST**2 + B*RBEST + C = 0**
*****************************************************************
**********D=COEFFICIENT*FOR*CUBIC*TERM*************************
       D=(KD1EST-KD2EST);
**********A=COEFFICIENT*FOR*QUADRATIC*TERM*********************
       A=(TT*KD2EST + 2*RA*KD2EST + KD1EST*KD2EST - RA*KD1EST +
       SA*KD1EST - TT*KD1EST - KD1EST**2);
**********B=COEFFICIENT*FOR*LINEAR*TERM***********************
       B=-1*(RA*SA*KD1EST - RA*TT*KD1EST + 2*RA*TT*KD2EST
       + KD2EST*RA**2 + RA*KD1EST*KD2EST);
**********C=CONSTANT*TERM***************************************
       C=(KD2EST*TT*RA**2);
*****************************************************************
**             DIVIDE COEFFICIENTS THROUGH BY D                **
**    RECAST AS RBEST**3 + P*RBEST**2 + Q*RBEST + R = 0        **
*****************************************************************
       P=A/D;     Q=B/D;     R=C/D;
*****************************************************************
**          & SUBSTITUTE IN X=RBEST+P/3                        **
**       TO GET FORM X**3 + AA*X + BB = 0, WHERE               **
*****************************************************************
       AA=(1/3)*(3*Q - P**2);
       BB=(1/27)*(2*P**3 - 9*P*Q + 2/*R);
*****************************************************************
**       FIND ROOTS TRIGONOMETRICALLY OF THIS EQUATION         **
**       FROM ARCCOS(PHI) OF -BB/(2*SQRT(-1*AA**3/2/))         **
*****************************************************************
```

```
      PHI = ARCOS(-BB/(2*SQRT(-1*AA**3/27)));
      PI=3.14159282;
*****************************************************************
**       ROOT OF X IS 2*SQRT(-AA/3)*COS(PHI/3+2*PI/3)          **
**            WHEN KD1EST < KD2EST                             **
*****************************************************************
    IF KD1EST<KD2EST THEN X= 2*SQRT(-AA/3)*COS(PHI/3+2*PI/3) ;
*****************************************************************
**       ROOT OF X IS 2*SQRT(-AA/3)*COS(PHI/3+4*PI/3)          **
**            WHEN KD1EST > KD2EST                             **
*****************************************************************
    IF KD1EST>KD2EST THEN X= 2*SQRT(-AA/3)*COS(PHI/3+4*PI/3) ;
*****************************************************************
**              SET RBEST = X - P/3                            **
*****************************************************************
      RBEST= X - P/3 ;
*****************************************************************
**        USE RBEST TO CALCULATE ESTIMATE OF RA                **
*****************************************************************
      RA=(RBEST+(RA-RBEST)*EXP(-DK1*DTIME));
*****************************************************************
**        USE RBEST TO CALCULATE ESTIMATE OF SA                **
*****************************************************************
      TEMP=(TT-RBEST+SA+KD2EST);
      SB=(TEMP-SQRT(TEMP*TEMP-4*SA*(TT-RBEST)))/2;
      SA=(SB+(SA-SB)*EXP(-DK2*DTIME));
RETURN;
*****************************************************************
***       READ IN DATA FROM DD STMT LISTED IN INFILE         ****
*****************************************************************
DATA IN4;
     INFILE INDATA4;
*****************************************************************
***    INPUT VARIABLES THAT DESCRIBE INITIAL CONDITIONS       ****
*****************************************************************
    INPUT DATE $1-7Ø / HDR1 $1-7Ø / HDR2 $1-7Ø / NPTS 2. / VØ / V
        / CR / VR / CT / TU1 / TU2 / FF / FS / BL / CS / VS @;
            %LET MTIT1=;
            %LET MTIT2=;
*****************************************************************
***              VARIABLE DEFINITIONS                         ****
*****************************************************************
  NPTS=# OF DATA PTS.                VØ=INITIAL VOLUME
  V=VOLUME AT T=Ø (AFTER TCA ASSAY) CR=CONCENTRATION OF TRNA1
  VR=VOLUME OF TRNA1                 CT=CONCENTRATION OF TU STOCK
  TU1=CONCN OF TU TITRANT#1          TU2=CONCN OF TU TITRANT#2
  FF=INITIAL FLUORESCEIN SIGNAL      FS=INITIAL SAMPLE FLUORESCENCE
  BL=BLANK FLUORESCENCE              CS=AA-TRNA2 CONCENTRATION
  VS=AA-TRNA2 VOLUME
*****************************************************************
**                  INSERT ESTIMATES HERE                      ****
*****************************************************************
      FI=1.Ø6;        *INITIAL FLUORESCENCE;
```

```
      NDSN=4;            *DATA SET# (USED BY SOME SORTING PROCEDURES
                              WHEN THERE ARE MULTIPLE DATA SETS);
      KD1EST=0.85E-9; *ESTIMATED TU-TRNA1 KD;
          DK1=1.1E-3; *ESTIMATED DEACYLATION RATE FOR TRNA1;
      KD2EST=9.6E-11; *ESTIMATED TU-TRNA2 KD;
          DK2=1.1E-3; *ESTIMATED DEACYLATION RATE FOR TRNA2;
      Y=952/1600; *Y=FRACTION TRNA1 AMINO-ACYLATED AT T=0;
          Y1=818/1600; *Y1=FRACTION TRNA1 AMINO-ACYLATED AT END;
      Y2=857/1600; *Y2=FRACTION TRNA2 AMINO-ACYLATED AT T=0;
          Y3=716/1600; *Y3=FRACTION TRNA2 AMINO-ACYLATED AT END;
           Z=1;          *FRACTION OF TU THAT IS ACTIVE;
           FMAX=1.170; *MAXIMUM FLUORESCENCE (I.E. THE F/F0MAX);
*****************************************************************
**         NORMALIZE UNITS OF VOLUME & CONCENTRATION           **
**                  TO LITERS AND MOLAR                        **
*****************************************************************
         V=V*1E-6;V0=V0*1E-6;
         RT=CR*1.6E-9*VR/V0; RA0=RT*Y;
         ST=CS*1.6E-9*VS/V0; SA0=ST*Y2;
         TT=0; VC=1.0;
         VPREV=V; F0=FS-BL; ADDT=0;VT=V;TIME=0;RA=RA0; SA=SA0;
*****************************************************************
***             INPUT 3 'CARDS' PER DATA POINT:               **
***                 1=VOLUME OF TU ADDITION                   **
***                 2=FLUORESCENCE OF TRNA SOLUTION           **
***                 3=FLUORESCENCE OF FLUORESCEIN STANDARD    **
***                      & TIME INCREMENT FROM LAST SET       **
***                      OF SCANS                             **
*****************************************************************
 DO I = 1 TO NPTS  ;
           INPUT / ADDN  TRNA  NA2F  DTIME INDEX  @;
             TIME=TIME+DTIME; *TOTAL TIME                      ;
      LINK DEACYL ;
             ADDN=ADDN*1E-6;    *TU VOLUME INCREMENT IN LITERS ;
             IF INDEX=1 THEN ADDT=ADDT+ADDN*TU1;
               ELSE ADDT=ADDT+ADDN*TU2; *TOTAL MOLES OF TU ADDED;
             VPREV=VT;          *TOTAL VOL. AT PREV. POINT ;
             VT=VT+ADDN;        *TOTAL SOLUTION VOLUME         ;
             TT=ADDT/VT;        *TOTAL CONCENTRATION TU        ;
             VC=VT/VPREV;       *VOLUME CORRECTION FACTOR      ;
             VCTOT=VT/V;        *OVERALL CORRXN FACTOR ;
             RT=RT/VC;          *TRNA1 CONCENTRATION           ;
             RA=RA/VC;
             SA=SA/VC;
             SB=SB/VC;
             ST=ST/VC;          *TRNA2 CONCENTRATION           ;
             RE=RT*Y1;          *TRNA1 CONCENTRATION @ EXPT END;
             SE=ST*Y3;          *TRNA2 CONCENTRATION @ EXPT END;
             F=(TRNA*VCTOT-BL)/F0; *VOL-CONC CORRECTED FLUORESCENCE;
         OUTPUT;                *OUTPUT VALUES CALCULATED FOR
                                       THIS RECORD;
      END;
*****************************************************************
```

```
**            INPUT FINAL CARD AND RELEASE DATA SET                **
*****************************************************************
          INPUT / COM $1-7Ø; *COMMENT IS LAST RECORD OF FILE;
      STOP;                          *END EXECUTION OF THIS DATA STEP;
DEACYL:*********************************************************
**              ESTIMATE RBEST IN PRESENCE OF DEACYLATION       **
*****************************************************************
**    CALCULATE COEFFICIENTS OF CUBIC EQUATION FOR TRNA1        **
**                 BOUND AT EACH DATA POINT                     **
**      BASED ON VALUES FOR TU, AATRNA1, AATRNA2 AND KD1        **
**FORM OF EQUATION   D*RBEST**3 + A*RBEST**2 + B*RBEST + C = Ø**
*****************************************************************
**********D=COEFFICIENT*FOR*CUBIC*TERM*************************
       D=(KD1EST-KD2EST);
**********A=COEFFICIENT*FOR*QUADRATIC*TERM*********************
       A=(TT*KD2EST + 2*RA*KD2EST + KD1EST*KD2EST - RA*KD1EST +
       SA*KD1EST - TT*KD1EST - KD1EST**2);
**********B=COEFFICIENT*FOR*LINEAR*TERM************************
       B=-1*(RA*SA*KD1EST - RA*TT*KD1EST + 2*RA*TT*KD2EST
       + KD2EST*RA**2 + RA*KD1EST*KD2EST);
**********C=CONSTANT*TERM***************************************
       C=(KD2EST*TT*RA**2);
*****************************************************************
**              DIVIDE COEFFICIENTS THROUGH BY D                **
**     RECAST AS RBEST**3 + P*RBEST**2 + Q*RBEST + R = Ø        **
*****************************************************************
       P=A/D;     Q=B/D;     R=C/D;
*****************************************************************
**          & SUBSTITUTE IN X=RBEST+P/3                         **
**       TO GET FORM X**3 + AA*X + BB = Ø, WHERE                **
*****************************************************************
       AA=(1/3)*(3*Q - P**2);
       BB=(1/27)*(2*P**3 - 9*P*Q + 27*R);
*****************************************************************
**       FIND ROOTS TRIGONOMETRICALLY OF THIS EQUATION          **
**       FROM ARCCOS(PHI) OF -BB/(2*SQRT(-1*AA**3/27))          **
*****************************************************************
       PHI = ARCOS(-BB/(2*SQRT(-1*AA**3/27)));
       PI=3.14159282;
*****************************************************************
**       ROOT OF X IS 2*SQRT(-AA/3)*COS(PHI/3+2*PI/3)           **
**              WHEN KD1EST < KD2EST                            **
*****************************************************************
    IF KD1EST<KD2EST THEN X= 2*SQRT(-AA/3)*COS(PHI/3+2*PI/3) ;
*****************************************************************
**       ROOT OF X IS 2*SQRT(-AA/3)*COS(PHI/3+4*PI/3)           **
**              WHEN KD1EST > KD2EST                            **
*****************************************************************
    IF KD1EST>KD2EST THEN X= 2*SQRT(-AA/3)*COS(PHI/3+4*PI/3) ;
*****************************************************************
**                 SET RBEST = X - P/3                          **
*****************************************************************
       RBEST= X - P/3 ;
```

```
*****************************************************************
**        USE RBEST TO CALCULATE ESTIMATE OF kA                **
*****************************************************************
       RA=(RBEST+(RA-RBEST)*EXP(-DK1*DTIME));
*****************************************************************
**        USE RBEST TO CALCULATE ESTIMATE OF SA                **
*****************************************************************
       TEMP=(TT-RBEST+SA+KD2EST);
       SB=(TEMP-SQRT(TEMP*TEMP-4*SA*(TT-RBEST)))/2;
       SA=(SB+(SA-SB)*EXP(-DK2*DTIME));
RETURN;
***********END*OF*INDIVIDUAL*DATA*SET*INPUT*********************
*****************************************************************
** COMBINE DATA & REDUCE NUMBER OF VARIABLES IN SAS DATASET   **
*****************************************************************
DATA ENTRE;
   SET IN1 IN2 IN3 IN4 ;
PROC PRINT ;
   VAR NDSN TT RA RE RB RT RA0 SA SE SB ST SA0 VC VCTOT;
   BY NDSN;
   ID NDSN;
   PAGEBY NDSN;
DATA ENTIRE;
   SET ENTRE;
    IF TT <> 0 THEN LTT=LOG10(TT) ;
      KEEP  RA SA KD1EST TT LTT FMAX Y1 RT F;
*****************************************************************
**                SORT OBSERVATIONS BY TT                      **
*****************************************************************
PROC SORT DATA=ENTIRE OUT=SENTIRE ;
         BY TT;
*****************************************************************
**              PERFORM NONLINEAR LEAST SQUARES                **
**              ANALYSIS WITH CONVERGENCE ON KD2               **
*****************************************************************
*PROC PRINTTO UNIT=20 NEW;
*    OPTIONS NOCENTER ;
PROC NLIN DATA=SENTIRE METHOD=DUD EFORMAT ;
*    PARMS KD2=1.0E-11 TO 3.5E-10 BY 3E-12 FI=0.995 TO 1.015 BY .002 ;
   PARMS KD2=1.0E-10 FI=1.0 ;
         BOUNDS KD2>1E-15  ;
*****************************************************************
**   CALCULATE COEFFICIENTS OF CUBIC EQUATION FOR TRNA1        *****
**              BOUND AT EACH DATA POINT                       *****
**     BASED ON VALUES FOR TU, AATRNA1, AATRNA2 AND KD1        *****
**     FORM OF EQUATION   D*RB**3 + A*RB**2 + B*RB + C = 0 ****;
*****************************************************************
**********D=COEFFICIENT*FOR*CUBIC*TERM**************************
       D=(KD1EST-KD2);
**********A=COEFFICIENT*FOR*QUADRATIC*TERM**********************
       A=(TT*KD2 + 2*RA*KD2 + KD1EST*KD2 - RA*KD1EST + SA*KD1EST -
          TT*KD1EST - KD1EST**2);
**********B=COEFFICIENT*FOR*LINEAR*TERM*************************
```

```
      B=-1*(RA*SA*KD1EST - RA*TT*KD1EST + 2*RA*TT*KD2 + KD2*RA**2 +
         RA*KD1EST*KD2);
**********C=CONSTANT*TERM*****************************************
      C=(KD2*TT*RA**2);
*****************************************************************
**            DIVIDE COEFFICIENTS THROUGH BY D                  **
**        RECAST AS RB**3 + P*RB**2 + Q*RB + R = 0              **
*****************************************************************
      P=A/D;     Q=B/D;     R=C/D;
*****************************************************************
**          & SUBSTITUTE IN X=RB+P/3                            **
**       TO GET FORM X**3 + AA*X + BB = 0, WHERE                **
*****************************************************************
      AA=(1/3)*(3*Q - P**2);
      BB=(1/27)*(2*P**3 - 9*P*Q + 27*R);
*****************************************************************
**       FIND ROOTS TRIGONOMETRICALLY OF THIS EQUATION          **
**       FROM ARCCOS(PHI) OF -BB/(2*SQRT(-1*AA**3/27))          **
*****************************************************************
      PHI = ARCOS(-BB/(2*SQRT(-1*AA**3/27)));
      PI=3.14159282;
*****************************************************************
**       ROOT OF X IS 2*SQRT(-AA/3)*COS(PHI/3+2*PI/3)           **
**             WHEN KD1 < KD2                                   **
*****************************************************************
   IF KD1EST<KD2  THEN  X= 2*SQRT(-AA/3)*COS(PHI/3+2*PI/3) ;
*****************************************************************
**       ROOT OF X IS 2*SQRT(-AA/3)*COS(PHI/3+4*PI/3)           **
**             WHEN KD1 > KD2                                   **
*****************************************************************
   IF KD1EST>KD2  THEN  X= 2*SQRT(-AA/3)*COS(PHI/3+4*PI/3) ;
*****************************************************************
**             & SET RB = X - P/3                               **
*****************************************************************
      RB= X - P/3 ;
      RB_RT=RB/RT ; *FRACTION OF TRNA1 THAT IS BOUND;
*****************************************************************
**       DETERMINE MOLAR FLUORESCENCE GAIN ON BINDING           **
**                      AS GG                                    **
*****************************************************************
            GG=(FMAX+Y1-1)/Y1;
*****************************************************************
**             MODEL FLUORESCENCE F/F0                          **
**              IN TERMS OF GG AND RB                           **
*****************************************************************
   MODEL F= FI + (GG-1)*RB/RT ;
*****************************************************************
**          AND OUTPUT THE RESULTING DATA IN                    **
**              A SASDATA SET NAMED FIT                         **
*****************************************************************
  OUTPUT OUT=FIT P=FHAT R=RESID PARMS=KD2 SSE=SSEMIN;
*****************************************************************
**     USE PROC PLOT TO GRAPH DATA WITH FITTED POINTS           **
```

```
          OVERLAYED AND TO EXAMINE THE RESIDUALS                    **
**              AS FUNCTIONS OF F AND TT                              **
*****************************************************************
PROC GLM ;
   MODEL RESID=TT TT*TT TT*TT*TT;
PROC GLM ;
   MODEL RESID=F F*F F*F*F;
PROC PLOT;
  PLOT F*LTT='+  FHAT*LTT='X'/OVERLAY;
  PLOT RESID*LTT/VREF=0.0;
  PLOT RESID*TT/VREF=0.0;
  PLOT RESID*F/VREF=0.0;
/*
```

APPENDIX E

This is the BASIC program written for use on an Apple II Plus microcomputer to calculate dissociation constants for the ternary complex of an unmodified tRNA with EF-Tu*GTP from experiments where Phe-tRNA^{Phe}-F^{8}*EF-Tu*GTP was titrated with the competing tRNA. This program reads data in from text files, and asks the user to input six experimentally determined values, as in the program in Appendix B. The concentration of the ternary complex-bound Phe-tRNA^{Phe}-F^{8} in the presence of added EF-Tu*GTP is obtained from the fluorescence, using an expression derived from equation 8 (see Chapter II). A correction for the effects of deacylation on the concentration of the Phe-tRNA^{Phe}-F^{8} is included in this calculation. The next segment of the program calculates the concentration of the bound Phe-tRNA^{Phe}-F^{8} from the fluorescence after the addition of each aliquot of the competing tRNA. This calculation uses the fluorescence change per bound aa-tRNA-F (E_b/E_f) and the K_d value for the aa-tRNA-F as previously determined (see Table II). The K_d value for the ternary complex with the competing tRNA is determined from the relationships expressed in equations 8, 9, and 10 (see Chapter II, Section J).

```
30 UL$(0) = CHR$ (27) + CHR$ (88): REM UNDERLINE ON
40 UL$(1) = CHR$ (27) + CHR$ (89): REM UNDERLINE OFF
50 GC$ = CHR$ (27) + CHR$ (38): REM SELECT GREEK CHARACTER SET
60 AS$ = CHR$ (27) + CHR$ (36): REM ASCII ON
```

```
7Ø FF$ = CHR$ (12): REM FORM FEED
8Ø LF$ = CHR$ (1Ø): REM LINE FEED
9Ø LM$ = CHR$ (27) + "LØ1Ø": REM LEFT MARGIN SET TO 1Ø
1ØØ CR$ = CHR$ (13)
11Ø PRINT LM$
12Ø REM ************************
13Ø REM ****** COMPETE *********
14Ø REM ************************
15Ø REM THIS PROGRAM CALCULATES A KD FOR A SECOND SPECIES AS IT IS
        TITRATED INTO THE COMPLEX
16Ø REM OF THE FIRST SPECIES, REVERSING THE FLUORESCENCE
        CHANGE.
17Ø DIM A(3Ø,3Ø)
18Ø REM DATA FILE READ IN HERE
19Ø D$ = CHR$ (4)
2ØØ INPUT "FILE TO BE USED: ";A$
21Ø INPUT "DRIVE LOCATION OF FILE:";DR%
22Ø IF DR% < 1 OR DR% > 2 GOTO 21Ø
23Ø PRINT LF$
24Ø PRINT D$"OPEN";A$;",D";DR%
25Ø PRINT D$"READ"A$
26Ø INPUT B$(1),B$(2),B$(3),DP
27Ø INPUT VØ,V,CR,VR,CT,VU,VT,FF,FS,B,CS,VS
28Ø FOR J = 1 TO DP
29Ø FOR I = 1 TO 3
3ØØ INPUT A(I,J)
31Ø NEXT
32Ø NEXT
33Ø INPUT CO$
34Ø PRINT D$"CLOSE"A$
35Ø POKE 33,4Ø: HOME : POKE 33,33
36Ø PRINT CO$
37Ø PRINT "# DATA PTS. IN FILE: ";DP
38Ø PRINT UL$(Ø);B$(1);" ";B$(2);" ";B$(3);UL$(1)
39Ø INPUT "TCA AT FØ (PMOL/A26Ø) FOR AA-TRNA-F = ";Y
4ØØ INPUT "TCA AT FØ FOR TRNA-2 = ";W
41Ø INPUT "FRACTION OF ACTIVE EF-TU = ";Z
42Ø INPUT "F(BOUND)/F(FREE) = ";F2
43Ø INPUT "KD FOR AA-TRNA-F (E-9 M) = ";K1
44Ø INPUT "DEACYLATION RATE (PER MIN) = ";DK
45Ø INPUT "# DATA POINTS = ";P
46Ø IF P = Ø THEN GOTO 1Ø/Ø
47Ø HTAB 1: PRINT UL$(Ø);"TRNAF";
48Ø HTAB 8: PRINT "TU";
49Ø HTAB 14: PRINT "F/FØ";
5ØØ HTAB 22: PRINT "BOUND TU (NM)";UL$(1)
51Ø A1 = Ø:TB = Ø:WC = 1.Ø
52Ø Y2 = Y / 16ØØ
53Ø W1 = W / 16ØØ
54Ø V4 = V * 1.ØE - 6:VO = VØ * 1.ØE - 6:V2 = VU * 1.ØE - 6:V3 = VT
* 1.ØE - 6
55Ø K1 = K1 * 1.ØE - 9
56Ø C1 = CT * 2.31E - 5: REM CONC N OF TU STOCK (M)
```

```
570 T = V3 * C1 / V2: REM CONC N OF TU IN TITRANT (M)
580 RT = CR * 1.6E - 9 * VR / VO: REM CONC N OF TRNA-F IN SOL'N (M)
590 TJ = Y2 * RT: REM CONC N OF AA-TRNA-F IN SOL'N AT START (M)
600 V1 = V4
610 F0 = FC - B
620 FOR J = 1 TO 3
630 GOSUB 1210
640 TU = A1 * T / V1: REM TOTAL TU CONC'N TO HERE
650 TU = TU * Z
660 TB = RT * (F - 1) / (F2 - 1): REM CONC N OF TU BOUND TO
      AA-TRNA-F
670 TJ = TI - TB
680 TF = TU - TB
690 TP = TB * 1.0E9
700 TY = TU * 1.0E9
710 T1 = TI * 1.0E9
720 T1$ = STR$ (T1):TU$ = STR$ (TY)
730 F$ = STR$ (F):TP$ = STR$ (TP)
740 HTAB 1: PRINT LEFT$ (T1$,4);
750 HTAB 7: PRINT LEFT$ (TU$,4);
760 HTAB 13: PRINT LEFT$ (F$,6);
770 HTAB 24: PRINT LEFT$ (TP$,6)
780 NEXT J
790 REM SECOND PART OF THE EXPERIMENT ** DIFFERENT TITRANT
800 HTAB 1: PRINT UL$(0);"TRNA";
810 HTAB 10: PRINT "TB";
820 HTAB 16: PRINT "F/F0";
830 HTAB 24: PRINT "K2     ";UL$(1)
840 AV = 0:CYC = 0:A1 = 0
850 FOR J = 4 TO P
860 GOSUB 1210
870 TU = TU / VC
880 TB = RT * (F - 1) / (F2 - 1): REM CONC N OF TU BOUND TO
       AA-TRNA-F
890 TJ = TI - TB: REM CONC N OF AA-TRNA-F (FREE)
900 TF = K1 * TB / TJ: REM CONC N OF FREE TU
910 TS = A1 * W1 * CS * 1.6E - 6 / V1: REM TOTAL CONC'N OF TRNA2 IN
       SOL'N
920 TX = TB + TF
930 TC = TU - (TB + TF): REM CONC N OF TU BOUND TO TRNA2
940 T2 = TS - TC: REM CONC N OF FREE TRNA2
950 K2 = TF * T2 / TC: REM KD FOR TRNA2
960 AV = AV + K2:CYC = CYC + 1
970 TQ = TS * 1.0E6:TP = TB * 1.0E9
980 TQ$ = STR$ (TQ):TP$ = STR$ (TP)
990 F$ = STR$ (F):K2$ = STR$ (K2)
1000 HTAB 1: PRINT LEFT$ (TQ$,4);
1010 HTAB 9: PRINT LEFT$ (TP$,4);
1020 HTAB 15: PRINT LEFT$ (F$,6);
1030 HTAB 23: PRINT LEFT$ (K2$,6) + RIGHT$ (K2$,4)
1040 NEXT J
1050 AV = AV / CYC:AV$ = STR$ (AV)
1060 PRINT UL$(0);"K2(AVG) = "; LEFT$ (AV$,6) + RIGHT$
```

```
          (AV$,4);UL$(1);" CYCLES = ";CYC
1070 PRINT "ANOTHER RUN, SAME DATA? (FILE NOW IS ";A$;") (Y/N)":
          GET Z$
1080 IF Z$ = "Y" THEN GOTO 350
1090 PRINT "ANOTHER RUN, DIFFERENT DATA? (Y/N)": GET W$
1100 IF W$ = "Y" THEN GOTO 180
1110 POKE 33,40
1120 END
1130 PRINT "THIS FILE MAY NOT EXIST"
1140 PRINT "DO YOU WISH TO DELETE '";A$;"' ? (Y/N)": INPUT Q$
1150 IF Q$ = "N" THEN GOTO 1070
1160 PRINT "ARE YOU SURE YOU WANT TO DELETE THIS FILE ? (Y/N)":
          INPUT R$
1170 IF R$ = "N" THEN GOTO 1070
1180 PRINT
1190 PRINT D$;"DELETE"A$
1200 GOTO 1090
1210 REM CALCULATE VOLUME CHANGES, CONC NS, ETC.
1220 A = A(1,J):F = A(2,J):DT = A(3,J)
1230 A = A * 1.0E - 6: REM ADDED TITRANT IN LITERS
1240 A1 = A + A1: REM COUNTER FOR VOL. ADDED
1250 VP = V1: REM VOL. AT PREV. POINT
1260 V1 = V1 + A: REM COUNTER FOR TOTAL VOL.
1270 WC = V1 / VP: REM INCREMENTAL VOL. CORRXN
1280 VC = V1 / V4: REM VC IS VOL. CORRXN FACTOR (TOTAL)
1290 TI = (TB + TJ * EXP ( - DK * DT)) / WC: REM CONC N OF
           AA-TRNA-F JUST BEFORE ADDITION
1300 F = ((F * VC) - B) / F0
1310 RETURN
```